Determination of autumn senescence in subtropical sourveld grasslands, KwaZulu-Natal, South Africa, based on remote sensing techniques: an approach towards forage quality and quantity assessment

Lwando Royimani

Submitted in fulfilment of the academic requirements of Doctor of Philosophy (PhD) in Environmental Science: (Specialization: GIS and Remote Sensing)

School of Agricultural, Earth and Environmental Sciences

College of Agriculture, Engineering and Science

University of KwaZulu-Natal

Pietermaritzburg

South Africa

January 2023

Preface

The research contained in this thesis was completed by the candidate while based in the Discipline of Geography, School of Agricultural, Earth and Environmental Sciences, of the Collage of Agriculture, Engineering and Science, University of KwaZulu-Natal, Pietermaritzburg Campus, South Africa. The research was financially supported by the National Research Foundation (NRF) of South Africa, Research Chair initiative in Land Use Planning and Management ((SARChI) (Grant Numbers: 84157).

The contents of this work have not been submitted in any form to another university and, except where the work of others is acknowledged in the text, the results reported are due to investigations by the candidate.

Lwando Royimani Signed: [redacted] Date: 23/01/2023

As the candidate′s supervisors, we certify the aforementioned statement and have approved this thesis for submission.

Supervisor:

Prof. Onisimo Mutanga Signed: [redacted] ate: 23/01/2023

Co-supervisors:

Prof. Rob Slotow Signed_____ Date_____

Dr. Sindiso Chamane Signed_____ Date_____

Declaration I: Plagiarism

I, Lwando Royimani, declare that:

i. The research reported in this thesis, except where otherwise indicated or acknowledged, is my original work;
ii. This thesis has not been submitted in full or in part for any degree or examination to any other university;
iii. This thesis does not contain other persons' data, pictures, graphs, or other information, unless specifically acknowledged as being sourced from other persons;
iv. This thesis does not contain other persons' writing, unless specifically acknowledged as being sourced from other researchers. Where other written sources have been quoted, then:
    a. Their original words have been paraphrased, but the general information attributed to them has been referenced.
    b. Where their exact words have been used, then their writing has been placed inside quotation marks, and referenced.
v. Where I have used material for which publications followed, I have indicated in detail my role in the work;
vi. This dissertation is primarily a collection of material, prepared by myself, published as journal articles or presented as a poster and oral presentations at conferences. In some cases, additional material has been included;
vii. This thesis does not contain text, graphics or tables copied and pasted from the Internet, unless specifically acknowledged, and the source being detailed in the dissertation and in the References sections.

Signed: Lwando Royimani

23 January 2023

Declaration II: Manuscripts and publications

1) Royimani, L., Mutanga, O. & Dube, T. 2021. Progress in remote sensing of plant senescence: a review on the challenges and opportunities. *IEEE Journal of Selected Topics in Applied Earth Observations and Remote Sensing*, 14, 7714-7723.

2) Royimani L., Mutanga, O., Sibanda, M., Dube, T. & Slotow, R. Assessing the effect of senescence on mesic sub-tropical grass quality and quantity using *in-situ* and Sentinel-2 data. (**Submitted to a Journal**).

3) Royimani, L., Mutanga, O., Odindi, J., Sibanda, M. & Chamane, S. 2022. Determining the onset of autumn grass senescence in subtropical sour-veld grasslands using remote sensing proxies and the breakpoint approach. *Ecological Informatics,* 69, 101651.

4) Royimani, L., Mutanga, O., Odindi, J. & Slotow, R. Multi-temporal assessment of remotely sensed autumn grass senescence across climatic and topographic gradients. *Land*, 12, 183.

5) Royimani, L., Mutanga, O. & Odindi, J. Identifying the optimal waveband positions for mapping the autumn grassland senescence using the broadband multispectral remotely sensed dataset. (**Submitted to a Journal**).

Signed: Lwando Royimani

23 January 2023

Abstract

Autumn grass senescence is considered a key driver of quality and quantity in grassland ecosystems – hence foraging resource productivity – particularly in communal rangelands that are situated in sourveld. This is primarily the case because sourveld grasses significantly lose nutrients during senescence, thereby, reducing the condition of the subsequent forage. More importantly, in rangeland settings the autumn grassland senescence impact on fodder banks and this has serious implications on forage distribution and allocation particularly during dry seasons. Popular methods for assessing plant senescence have previously been dominated by visual scoring of leaf coloration and fall. However, the latter is often not applicable in grassland senescence assessments due to, among others, the tiny size and large number of grass leaves. Often the "big-leaf-hypothesis", which treats the entire plant canopy as a leaf, is recommended in estimation of autumn grassland senescence. Besides, several challenges have been reported with the adoption of the aforementioned techniques and they include, among others, subjectivity, time lag effect, small scale applications and non-repeatability, particularly at landscape scale. By contrast, the advent of remote sensing has overcome similar challenges in other circumstances, and offered great prospects to effective monitoring of dynamics around plant phenology, including senescence. Taking the advantage of these techniques, the present study assessed the impact of autumn grass senescence on forage quality and quantity in subtropical sourveld grasslands of the KwaZulu-Natal's (KZN) Midlands, South Africa, based on the modern generation broadband multispectral remotely sensed data with improved sensing characteristics.

This was achieved by investigating the following objectives: 1) to provide an overview on the progress of remote sensing applications in characterizing grass senescence with possible challenges and opportunities, 2) to quantify the magnitude of decline in nGongoni (*Aristida junciformis*) grass quality and quantity owing to senescence using *in-situ* and Sentinel-2 data, 3) to characterize the onset of autumn senescence in mesic subtropical sourveld grasslands using remotely sensed data, 4) to evaluate the relationship between remotely sensed autumn grass senescence and climatic factors plus topography and 5) to test the potential of the modern multispectral remote sensing dataset (i.e., Sentinel 2 and Landsat) in mapping grass senescence, and to identify the optimal waveband positions that are suitable for separating between senescent and non-senescent grass.

The findings indicated that successful assessment of grass senescence based on remote sensing techniques is a function of monitoring the changes in its chlorophyll, biomass and Leaf Area

Index (LAI). Furthermore, the use of remote sensing data in concert with Random Forest analysis could predict grass quality and quantity at pre-senescence and senescence phases. In addition, there was a significant decrease in foraging resource quality from 24.52 µg Chl/cm^2 to 7.34 µg Chl/cm^2 and quantity from 2.11 kg/m^2 to 1.22 kg/m^2 due to senescence. The onset of autumn grassland senescence in the study area was successfully determined with an inflection point on day number ± 102 of the year. The key environmental drivers of autumn grassland senescence in the study area were determined to be; the minimum (T_{min}) and maximum (T_{max}) air temperatures, together with soil moisture. The findings emphasised the value of using modern broadband multispectral remote sensing sensors with improved sensing properties in detecting autumn grassland senescence, highlighting the Red-Edge Position (REP) jointly with the Visible green and red bands as the most sensitive regions of the spectrum for mapping grassland senescence.

The findings obtained in this study underscore the importance of the modern broadband multispectral remote sensing sensors like Sentinel 2 in reliable assessment of the dynamics around the occurrence of autumn grassland ecosystem senescence. This is vital to optimize our projections on potential onset of autumn grass senescence, hence, determination of possible duration of quality forage provision in the rangelands. Such information is required to improve planning, policy and decision-making pertaining to grazing patterns, the livestock numbers to be sustained as well as to signal appropriate times of livestock harvesting. This is more beneficial to small-holder farmers as they are often vulnerable to challenges arising from climate changes and poor rangeland management practices, among others.

Keywords: Autumn senescence, communal rangelands, grasslands, remote sensing, sourveld.

Dedication

This work is dedicated to Amahle Royimani and my late junior brother Sanele Royimani. You passed on very early before you could witness this wonderful achievement. You'll forever be in my heart my lovely brother and your presence and kind smile will forever be missed in the family.

To my parents, (Mr. Gcinabantu Royimani and Mrs. Nofirst Royimani), as well as the rest of the family, *ivuthiwe masiyophule, yeyethu sonke Mancotshe*!

Acknowledgements

Who would have known? Who would have thought that a young man from the dusty streets of eNgcobo, eDeberha, KwaDala could one day earn himself a prestigious achievement like a PhD? As a product of the so-called "rural schools" and with no recognizable formal educational history in the family, attaining this milestone accomplishment was never an easy task for me, however I made it anyway. This is a proof to any black child, particularly those from previously disadvantaged families that, "black child it's possible, it only takes courage, focus, determination and commitment". However, it has all come to reality because of the presence of *uSombawo namaNyange ephela, OoNdala, Mncotshe kaMomane*.

"The best way to eat an elephant in your path is to cut him up into little pieces" with this African proverb, I would like to express my kind words of appreciation for the unweaving support that I received from various individuals and organization for the duration of my studies – advising me to take it bit by bit and one step at a time – I say *nenze njalo nakwabanye*! My appreciation extends to the School of Agricultural, Earth and Environmental Sciences (SAEES), University of KwaZulu-Natal (UKZN) for allowing me a great opportunity to read for a PhD degree. More importantly, I would like to thank the National Research Foundation (NRF) of South Africa, Research Chair initiative in Land Use Planning and Management (Grant Numbers: 84157) for funding my PhD studies. I am grateful to the South African Weather Services for their assistance with climate data required to complete my story in this study.

Also, I would like to extend my gratitude to my supervisor and academic promoter, Professor Onisimo Mutanga for believing in me and granting me the opportunity to do my PhD studies under his supervision. Prof! I remember, when I first approached you in 2015 requesting to be your honours student. You gave me no difficulties in approving my request, but I was scared and always nervous, anyway, whenever I had to come for consultations. One of the reasons for that though was knowing the knowledge you possess – judging by your published contributions – in the field of Geographic Information System (GIS) and Remote Sensing. To my surprise, time proved me otherwise and now I can confidently say that "working under your supervision was the greatest thing to ever happen to me during my study-times at UKZN as you patiently nurtured and taught me the scientific way of thinking and the art of writing. In the same light, I would like to thank my co-supervisors, Professor Rob Slotow and Dr. Sindiso Chamane for their critical thinking and knowledge imparted in me during our consultation sessions. You guys pushed me far and taught me to think out of the box. It would be unkind of me not to

make mention of the funding administrators, Ms. Andile Mshengu and Ms. Precious Ncilliba, for their assistance with organizing vehicles for fieldwork and administering subsistence funds.

I am grateful to my academic advisors and co-authors, Professor John Odindi, Professor Timothy Dube and Dr. Mbulisi Sibanda. You guided me from the beginning through the end, you helped me improve my style of writing, I thank you for your efforts, sacrifices, patience and assistance. I also salute the entire staff of the Geography Department at UKZN, Pietermaritzburg campus particularly Mr. Brice Gijsbertsen, Mrs. Shanitha Ramroop and Mr. Donavan De Vos for their kindness and valuable administrative support. To my friends, family and colleagues in the Geography Department and beyond, I say thank you guys, it's done now. Specific mention is made to Dr. Trylee Nyasha Matongera, Dr. Omosalewa Odebiri, Mr. Mngadi Mthembeni, Miss Siphiwokuhle Buthelezi, Miss Snethemba Ndlovu, Mr. Asekho Mantsintsilili, Miss Xolile Zuma, Miss Anita Masenyama, Miss Thembelihle Ngiba, Ms Mbaweni Manqela, Miss Kimara Moodley, Mr. Pedzisayi Kowe and Mr. Collins Matiza, the long sleepless nights in those LANs have paid off. Thank you guys for your moral and brotherly/sisterly love and support.

A word of thanks also goes to Mr. Thandilizwe Bengeza, our friendship has been in existence for long man and through time we have undoubtedly formed a formidable amity against many challenges, whether its social, economic and scientific. That's what friendship is all about. To my elder sister, Mrs. Ncumisa Noxhanti Nkomo/Royimani, *mntase* you know everything, thank you very much. Again, my word of appreciation goes to Mrs. Nolindo Cetywayo for your moral support, *ndithi qhubeka njalo nentliziyo yakho entle Jola*. Last but not least, I would like to thank my immediate (parents and siblings) and extended family for your support.

Table of content

Preface....i

Declaration I: Plagiarism....ii

Declaration II: Manuscripts and publications....iii

Abstract....iv

Dedication....vi

Acknowledgements....vii

Table of content....ix

List of tables....xiv

List of figures....xv

Chapter One:....1

General introduction and overview....1

1. Introduction....2

1.1 Autumn senescence in grassland ecosystems....2

1.2 The socio-economic and ecological impact of autumn grass senescence....3

1.3 The impact of grass senescence on the livestock in the context of veld type and rangeland management system....4

1.4 Conventional and remote sensing methods for assessing plant senescence....6

1.5 Aim....7

1.6 Objectives of the study....7

1.7 Study site description....8

1.8 Scope of the study....10

1.9 Thesis outline....11

Chapter Two....**Error! Bookmark not defined.**

2 Progress in remote sensing of grass senescence: a review on the challenges and opportunities....14

Abstract....15

2.1 Introduction....15

2.2 Literature search and selection of source articles 18
2.3 Grass senescence and its impact on forage quality and quantity across various veld types 18
2.4 Spectral properties of green versus senescent grass 21
2.5 Remote sensing techniques and common vegetation indices for assessing grass senescence 23
2.6 Challenges in remote sensing of grass senescence 27
2.7 Possible directions for future research endeavors 29
2.8 Conclusion 31
Chapter Three 32
3 Assessing the effect of senescence on mesic sub-tropical grass quality and quantity using in-situ and Sentinel-2 data 33
Abstract 34
3.1 Introduction 34
3.2 Methods and materials 37
3.2.1 Sampling design and field data collection 37
3.2.2 Image acquisition 38
3.2.3 Vegetation indices 39
3.2.4 Statistical analysis 39
3.2.5 Random Forest model establishment and optimization 40
3.2.6 Forage availability status from the pre-senescent and senescent nGongoni grasses 42
3.3 Results 43
3.3.1 Descriptive statistics 43
3.3.2 Correlation between field-measured and spectral variables 45
3.3.3 Pre-senescent and senescent grass quality and quantity estimation using Sentinel 2 data 43

3.3.4 Decline in grass quality and quantity due to senescence and forage availability status 48
3.4 Discussion 49
3.4.1 Estimation of grass quality and quantity decline through senescence using Sentinel 2 data 49
3.4.2 Implications of the observed findings on rangeland's resource management 52
3.5 Conclusion 52
Chapter Four 54
4 Determining the onset of autumn grass senescence in subtropical sourveld grasslands using remote sensing proxies and the breakpoint approach 55
Abstract 56
4.1 Introduction 56
4.2 Methods and materials 58
4.2.1 Sampling strategy 58
4.2.2 Remote sensing proxies 61
4.2.3 Statistical analysis 62
4.2.4 Optimal remote sensing proxies for estimating autumn grass senescence 63
4.2.5 Detecting the inflection point in grass chlorophyll during autumn senescence 64
4.3 Results 65
4.3.1 Descriptive statistics 65
4.3.2 Optimal remote sensing proxy for detecting the autumn grass senescence 66
4.3.3 Onset of autumn grass senescence 70
4.4 Discussion 71
4.5 Conclusion 74
Chapter Five 75
5 Multi-temporal assessments of remotely sensed autumn grass senescence across climatic and topographic gradients 76
Abstract 77

5.1 Introduction 77
5.2 Materials and Methods 80
5.2.1 Field data collection 80
5.2.2 Remotely sensed autumn grass senescence 80
5.2.3 Climatic and topographic variables 80
5.2.4 Data processing and statistical analysis 81
5.2.5 Model optimization and identification of key environmental determinants of autumn grass senescence 82
5.3 Results 83
5.3.1 Descriptive statistics 83
5.3.2 Remotely sensed autumn grass senescence with climatic and topographic variables 83
5.3.3 Climatic and topographic drivers of the autumn grass senescence 87
5.4 Discussion 92
5.6 Conclusion 94
Chapter Six 95
6 Identifying the optimal waveband positions for mapping the autumn grassland senescence using the broadband multispectral remotely sensed dataset 96
Abstract 97
6.1 Introduction 97
6.2 Methods and materials 100
6.2.1 Field data collection 100
6.2.2 Broadband multispectral remotely sensed data acquisition 101
6.2.3 Classification algorithm and identification of optimal wavebands 102
6.2.4 Accuracy assessment 103
6.3 Results 103
6.3.1 Landsat 8 and Sentinel 2 classification performance 103

6.3.2 Spectral sensitive regions of the spectrum for discriminating between senescent and non-senescent grass 104
6.3.3 Optimal wavebands for mapping senescent grass 105
6.4 Discussion 106
6.5 Conclusion 109
Chapter Seven 110
7 Remote sensing of grassland autumn senescence for foraging resource quality and quantity: a synthesis, conclusion and recommendations for future 111
7.1 Introduction 111
7.2 Exploration of remote sensing techniques and associated plant properties for detection of autumn senescence 113
7.3 Quantifying the decrease in foraging resource quality and quantify due to senescence using Sentinel 2 and in-situ data 114
7.4 Characterization of autumn senescence onset in sourveld grassland ecosystems based on remote sensing dataset 114
7.5 Evaluating the influence of climate and topography on autumn grassland senescence 115
7.6 Testing the potential of the modern multispectral remote sensing in mapping grassland senescence and identifying the associated optimal wavebands for spectrally discriminating between senescent and non-senescent grass 115
7.7 Conclusion 116
7.8 Recommendations and the future 117
Reference: 119

List of tables

Table 2.1 Summary of commonly used vegetation indices in estimating plant phenology and senescence.....24
Table 3.1 Vegetation indices that were calculated in the present study.....40
Table 3.2 Pre-senescent and senescent chlorophyll content and biomass of the nGongoni grass. 43
Table 3.3 Correlations between the Sentinel 2 variables and biomass as well as chlorophyll content of the nGongoni grass. 44
Table 3.4 Estimation accuracies of the nGongoni grass quality and quantity and the associated ntree and mtry values.....45
Table 3.5 Dry Matter and Moisture contents of the nGongoni grass for the pre-senescent and senescent stages. 48
Table 4.1 Field data collection dates and the variables collected, frequency, and sampling scale. 59
Table 4.2 Field captured visuals of the grass between March and June 2021 to illustrate the condition of the grass from pre-senescent through to senescent phase. 60
Table 4.3 Sentinel 2 image acquisition dates and the cloud cover proportions. 61
Table 4.4 Chosen vegetation indices in the present study.....63
Table 4.5 Descriptive statistics of the field-measured grass chlorophyll content.....65
Table 4.6 Correlation coefficients between the chlorophyll content of the grass and the remote sensing proxies. Values in bold are insignificant at $p > 0.001$. 67
Table 4.7 Chlorophyll content slopes and intercepts before and after the breakpoint. 70
Table 5.1 Topographic plus climatic variables used in this study. 80
Table 5.2 Descriptive statistics of the data collected and extracted for analysis. 83
Table 5.3 Performance of the adopted algorithms based on the R^2, MEA and the RMSE. 84
Table 5.4 Optimal RFR results for the relationships between remotely sensed grass senescence and climatic factors and topography. 86
Table 5.5 Correlations between remotely sensed grass senescence and climatic factors and topography. Influential variables are shown in bold.....88
Table 6.1 Summary of the field collected data for each class.....99
Table 6.2 Description of waveband positions and resolutions for the Landsat 8 and Sentinel 2 spectral bands used in the current study. 100
Table 6.3 Classification accuracies from the Landsat 8 and Sentinel 2 images.....101

List of figures

Figure 1.1 The location of Vulindlela communal area, KwaZulu-Natal, South Africa. 9

Figure 2.1 Schematic representation of the process of leaf senescence as a result of, both, internal and external factors. **(**Adapted from Lim et al. 2007). 19

Figure 2.2 Seasonal dynamics in percentage nitrogen (N) concentration in sweet, mixed, and sour veld grasses. (Source: Zacharias 1995). 21

Figure 2.3 Averaged spectral reflectance of green versus senescent *Aristida junciformis* grasses extracted from the visible, NIR and SWIR bands of the Landsat 8. 22

Figure 3.1 Photos of the nGongoni grass taken on the 22nd of March and 3rd of September 2020 in the study site to illustrate the conditions of pre-senescent (a) and senescent (b) grass, respectively. 38

Figure 3.2 Data analysis framework adopted in estimating the quality and quantity of the nGongoni grass at pre-senescent and senescent stages. 42

Figure 3.3 Relationship between measured and predicted nGongoni grass quality during (a) pre-senescent and (b) senescent stages as well as quantity over (c) pre-senescent and (d) senescent periods. 45

Figure 3.4 Variable importance ranking for the estimation of the nGongoni grass quality during (a) pre-senescent and (b) senescent stages and quantity during (c) pre-senescent and (d) senescent periods. 46

Figure 3.5 Decline in mean (a) chlorophyll content and (b) mean biomass of the nGongoni grass following senescence. 48

Figure 3.6 Spatial distribution of predicted grass quality at (a) pre-senescent and (b) senescent stages as well as the quantity during (c) pre-senescent and (d) senescent periods. 49

Figure 4.1 Schematic representation of the mean monthly grass chlorophylls with extrapolated values for day number ± 27 and 55 to represent the January and February months, respectively. The black dotted rectangle at the centre of the figure illustrates the four dates used to determine the best breakpoint. 65

Figure 4.2 Distribution of field-collected chlorophyll content of the grass. 66

Figure 4.3 Relationship between field-measured (SPAD-502 values) and predicted grass chlorophyll based on optimal remote sensing proxies for all the months of data collection. The top row illustrates the correlation between grass chlorophyll and the $NDVI_{705}$ for (a) March, (b) April, (c) May, and (d) June, while the bottom row shows the grass chlorophyll against the CHL-RED-EDGE for (e) March, (f) April, (g) May and (j) June. 68

Figure 4.4 Four chosen breakpoints to estimate the onset of autumn grass senescence and their prediction accuracy in terms of the Mean Square Error (MSE). 69
Figure 4.5 Estimated onset of autumn grass senescence based on the (a) $NDVI_{705}$ and the (b) CHL-RED-EDGE remote sensing proxies. 70
Figure 5.1 Algorithm's performances based on the (a) RMSE, (b) MAE and the (c) R^2**.**.....85
Figure 5.2 RFR model's variable importance for assessing the response of remotely sensed autumn grass senescence against the climatic and topographic factors in (a) March, (b) April, (c) May, and (d) June. 87
Figure 5.3 The responses of the (a-c) $NDVI_{705}$-based autumn grass senescence to (a) T_{min}, (b) T_{max} and (c) soil moisture together with that of the (d-f) CHL-RED-EDGE based autumn grass senescence to (d) T_{min}, (e) T_{max} and (f) soil moisture through time. 98
Figure 6.1 Important variables as ranked by the random forest model for separating between the senescent and the non-senescent grass using the (a) Sentinel 2 and (b) Landsat 8. 102
Figure 6.2 Mean spectral reflectance values for the senescent (dotted red) and non-senescent (solid black) grass from the (a) Sentinel 2 and (b) Landsat 8 multispectral datasets. The dotted blue boxes show areas with distinctive spectral variations. 103
Figure 6.3 Significant bands for classifying the senescent from the non-senescent grass based on the (a) Sentinel 2 and (b) Landsat 8 multispectral sensors. 104
Figure 6.4 Typical spectral reflectance of the vegetation showing the sensitive waveband positions for discriminating between the senescent and non-senescent grass based on the broadband multispectral remote sensing dataset. The blue highlighted corresponds to the Sentinel 2 while the red dotted boxes indicates the Landsat 8 sensitive bands. 106

Chapter One:

General introduction and overview

1. Introduction

1.1 Autumn senescence in grassland ecosystems

Grass phenology can be defined as the study of periodic changes in the life cycle of the grass as a result of varying topographic and seasonal climatic conditions (Bertin, 2008). Broadly, in temperate regions such as the Midlands mist belt grasslands, these periodic changes comprise of the growing, maturity, senescence and dormancy stages and they are respectively associated with spring, summer, autumn and winter conditions (Volaire *et al*., 2009). The most common form of senescence in the grass is leaf senescence and is described as a decaying phase in the phenology of the grass (Corbane *et al.* 2008; Gregersen *et al.* 2008; Buchanan-Wollaston *et al.* 2003). Leaf senescence is characterized by gradually programmed cell deaths and is often indicative of the end of a growth cycle, while equally signifying the beginning of the new one (Royimani *et al.* 2021; Munné-Bosch and Alegre 2004; Gepstein *et al.* 2003). According to Munné-Bosch and Alegre (2004), this process is highly regulated at the cellular, physiological, molecular and biochemical levels of the plant, and is marked by three distinct phases, i.e., the onset, degeneration, and the terminal stages. During senescence, several changes are noted in the gene expression, physiology and metabolism of the grass leaves (Michelson *et al.* 2018; Guo *et al.* 2004). The occurrence of grassland leaf senescence can be detected by the combined observation of these signs. The first visual sign of grass leaf senescence is yellowing or leaf coloration which is the change in the color of the leaves from green to yellow due to chlorophyll degradation and carotenoid dominance (Buchanan-Wollaston *et al.* 2003). Also senescing plant leaves can appear red because of increased anthocyanins content (Munné-Bosch and Alegre 2004). Unlike other programmed cell death in vegetation, senescence is distinguishable by its gradual progression, and the association with nutrient translocation, from the photosynthetic parts like the leaves to the storage organs such as the roots (Buchanan-Wollaston *et al.* 2003).

Like any other physiologically programmed cell death process, leaf senescence is largely controlled by intrinsic biological processes and ecological factors, otherwise known as internal and external factors (Lim *et al.* 2007). These external drivers include, among others, waterlogging, drought, extreme temperatures, high or low incoming solar radiation, insufficient soil nutrients, excessive salinity, pathogens, or physical damage, while the internal factors include hormonal imbalances, age, reproductive development, ill-health etc. (Michelson *et al.* 2018; Munné-Bosch and Alegre 2004; Guo *et al.* 2004). Both, these internal and external factors contribute to the initiation and progression of senescence in the grass, and may individually or collectively accelerate or delay the occurrence of senescence (Smart 1994).

Consequent to the pressure exerted by the aforementioned factors in each grass leaf and the subsequent leaf response, grass leaves may senesce separately or together and the latter is always uniformly detected at the canopy level (Royimani *et al.* 2021). However, from a forage quality and quantity perspectives in grassland ecosystems, the senescence of individual grass leaves is unworthy due to its disjointed nature of occurrence (Royimani *et al.* 2022). Instead, autumn grassland senescence, which is described as the seasonal grass wilting due to old age and the climatic conditions associated with autumn (Mariën *et al.* 2019), has generated interest due to its relative uniformity across the landscape. Therefore, in order to understand the impact of senescence on foraging resource quality and quantity as well as the potential implications on the livestock and livelihood mechanisms, the need to assess the dynamics around autumn grassland senescence is critical due to uniformity in occurrence.

1.2 The socio-economic and ecological impact of autumn grass senescence

The importance of monitoring autumn grassland senescence in rangeland settings including the opportunity to gain knowledge on the distribution, allocation, condition and availability status of forage, particularly during dry seasons (Asner *et al.* 2004). This is necessary for improved planning and decision-making pertaining to the livestock production systems, stocking rates, livestock harvesting as well as potential food shortages. During senescence, grass nutrients are withdrawn from the foliar to the rooting systems, thus, affect the conditions of the subsequent forage (Purdy *et al.* 2015). More importantly, senescence degrades plant enzymes such as chlorophyll and macromolecules like lipids, nuclei acids and proteins, and, thus, generally decreasing the photosynthetic activities in the leaves (Guo *et al.* 2004). Likewise, the effect of leaf detachment – as a result of dead grass leaves – at later stages of senescence (Gepstein *et al.* 2003), may significantly decrease the amount of biomass, hence foraging resource quantity. Considering the increasing rainfall variability and drought activities associated with the changing climatic conditions, especially in southern Africa (Van der Walt and Fitchett 2020), the impact of autumn senescence on grasslands is expected to rise. Meanwhile, knowledge on the dynamics around autumn grassland senescence is essential for the understanding of fodder bank capacities and the potential impact on the livestock and livelihood mechanisms of small-holder farmers.

Besides, grassland senescence is an important process not only for its ecological relevance but also in terms of persistence of the individual grass plants (Royimani *et al.* 2021). For instance, the reserved nutrients (from the leaves to the roots) during senescence help to reactivate growth and development of new, and often nutrient content rich, grasses in the next season (Buchanan-

Wollaston *et al.* 2003) and this is beneficial to quality forage production in rangelands. Also, ecologically, senescence is considered an adaptive mechanism of the plants, particularly during dry periods, as it helps to reduce the plant-water demand (Munné-Bosch and Alegre 2004). Specifically, senescence leads to stomatal closure and this reduces the amount of water lost by the grass through evapotranspiration, hence, the low grass-water demand (Anderegg *et al.* 2020). In addition, the fallen grass leaves due to leaf detachment at later stages of senescence contributes to the decomposable waste material, which helps to increase the organic matter and nutrient content of the soil, and, thus, promoting primary productivity (Gepstein *et al.* 2003). Also, the high organic matter content as a result of increased decomposed waste material helps to improve the structure and water holding capacity of the soil, thereby, reducing soil erosion (Royimani *et al.* 2021). The accumulated waste material from the senescent fallen grass leaves may also act as a buffer to protect the soil surface by intercepting the incoming rainfall droplets, which decreases their intensity, soil splash and erosion. Similarly, the accumulated waste material often increases the fuel load, and, thus, promotes the occurrence of fires (Royimani *et al.* 2021), a key veld management process and practice in grassland ecosystems (O'Connor *et al.* 2020). Despite the above-mentioned socio-economic and ecological impact of senescence, there is a limited knowledge on the implications of autumn grassland senescence in the context of veld type and adopted rangeland management practices. This is critical considering the remarkable decline reported in sourveld grass quality because of senescence (Zacharias 1995), as well as the poor management practices that characterizes communal rangelands (Selemani 2014).

1.3 The impact of grass senescence on the livestock in the context of veld type and rangeland management system

The impact of autumn grassland senescence on foraging resource quality and quantity is mainly experienced in sourveld as opposed to sweetveld (Royimani *et al.* 2021). In contextualizing the characterization of grasslands as either sweet or sour, this is a southern African concept and is used to distinct between grasslands that are found in high rainfall areas of soils with a low base status (sourveld) and those occurring in low rainfall areas of soils with a high base status (sweetveld) (Ellery *et al.* 1995). The high rainfall that characterizes sourveld (Ellery *et al.* 1995) often promotes the leaching of grass nutrients. Using nitrogen content as a proxy for grass quality across sweet, mixed and sourveld, Zacharias (1995) discovered that, although sweet and mixed-veld grasses lose quality during senescence, the amount of decline in grass quality is remarkable in sourveld. With high nutrient loss in sourveld grasses, there is a greater

risk of quality forage shortages, hence, livestock starvation. Additional evidence suggests that, there is a general loss in body weights of animals that are feeding on sourveld during dry periods due to decrease in forage quality below the required level to sustain growth (Ellery *et al.* 1995). This discussion emphasizes the need to prioritize sourveld grazing lands in efforts aimed at monitoring the dynamics around autumn senescence as well as the associated impact on forage quality and quantity.

With regards to management regimes, the impact of autumn grass senescence on forage quality and quantity is expected to be significant on communal rangelands compared to private grazing areas. Broadly, this could be due to either poor or lack of management practices in communal rangelands (Kiguli *et al.* 1999), together with absence of infrastructural facilities such as fencing (Bennett *et al.* 2010) to support the adoption of effective livestock and grazing management efforts. With issues emanating from resource constraints (Cousins 1999), communal farmers can barely afford the cost to fund the infrastructure of their rangelands and that can lead to poor protection or unsustainable utilization of available free-ranging natural forage. Communal rangelands can be defined as the veld whereby grazing areas and the subsequent resources, through the custodianship of traditional authorities, are managed and shared communally (Cousins 1999). This management approach often increases pressure on foraging resources, hence, the common perception that communal rangelands are either degraded or unproductive (Selemani 2014).

In addition, the autumn grass senescence may, therefore, further increase the pressure on the quality and availability status of forage in communal rangelands. The pressure on communal rangelands forage could be further intensified owing to the lack of common commercial forage quality enhancement measures such as fertilizer applications, irrigation systems and supplementary feed (Brown and Shrestha 2000). Some of these measures like the irrigation and fertilizers can directly reduce the impact of autumn grass senescence by delaying its onset (Fataftah *et al.* 2021; ZHU *et al.* 2012), while supplements could contribute indirectly by lowering the amount of livestock reliance on natural pastures. Considering the importance of communal rangelands as the primary source of free-ranging feed for the livestock (Cousins 1999) – a key livelihood mechanism for small-holder farmers, particularly in poor rural communities (Herrero *et al.* 2013) – the impact of autumn grassland senescence may threaten rural livestock and increase the vulnerability of small-holder farmers to poverty. In light of this background, the comprehensive examination of autumn grassland senescence is critical, particularly when viewed in the angle of addressing global Sustainable Development Goals

(SDGs) number 1, 2 and 10, which talks to no poverty, zero hunger and reduced inequality, respectively.

1.4 Conventional and remote sensing methods for assessing plant senescence

Traditional methods for assessing plant leaf senescence are dominated by field surveys, which are dependent on visual scoring of leaf coloration and fall (Anderegg *et al.* 2020). However, the main shortcomings of using such approaches in monitoring plant phenology are well documented in literature, and they include, among others, subjectivity, limitation to plot-scale, and effect of time lag (i.e., they can only occur beyond a given decline in chlorophyll threshold) (Mariën *et al.* 2019). Similar studies have also stressed the challenges of using manual methods like field surveys in gathering data on vegetation properties, highlighting the associated high cost, the intensive time and labour required, as well as the difficulty in accessing remote areas (Royimani *et al.* 2019b). In contrast, earth observation instruments such as remote sensing have been a reliable primary source of data supporting the characterization of earth surface features such as vegetation in a spatially and temporally explicit manner (Sibanda *et al.* 2017a). Such approaches could be effective for continual broad-scale monitoring of autumn grass senescence at the landscape scale. However, few studies have been done to fully understand the role of remote sensing in autumn grassland senescence assessment (Liu *et al.* 2013; Asner *et al.* 2004; Bork *et al.* 1999). By far, these studies have been dominated by either the use of Analytical Spectral Devices (ASD) field spectroradiometer, which are limited to plot-scale, or the coarse resolution data like the Landsat 5 Thematic Mapper (TM) and 7 Enhanced Thematic Mapper Plus (ETM+) (Asner *et al.* 2004; Qi *et al.* 2002). Besides the averaging sensing properties, the Landsat 7 is known to suffer from the scan line error which compromises the quality of its data (Trigg *et al.* 2006; Storey *et al.* 2005). Furthermore, the course spatial resolution provided by instruments such as the Moderate Resolution Imaging Spectroradiometer (MODIS) (Kuenzer *et al*., 2015), although often recommended for large-scale applications, may not be suitable for estimating autumn grass senescence due to the high species diversity that characterizes grasslands (Collinge *et al*. 2003). Equally, the high spatial resolution (e.g., RapidEye, Quickbird, WorldView-2/3, etc.) and hyperspectral (e.g., Hyperion EO-1, Global Imager (GLI), etc.) datasets which are often commended for their improved quality are generally inappropriate for wall-to-wall and ongoing assessments required for autumn grassland senescence monitoring at the landscape scale. This is the case because of the expensive acquisition costs that characterizes these datasets *vis-à-vis* the small area coverage (Timothy *et al.* 2016).

Based on the above given background, it is evident that the application of remote sensing in grass senescence remains shallowly explored, and this has limited our potential to accurately, timely and reliably assess autumn senescence in grassland ecosystem, especially from a forage quality and quantity perspectives. Meanwhile, the launch of modern generation multispectral remote sensing sensors such as the Landsat 8 and Sentinel 2, with better spatial, spectral and temporal resolutions, offers prospects for the ongoing and large-scale monitoring of autumn grass senescence in a spatially and temporally explicit manner. The Landsat 8 provides readily available optical data captured at a spatial resolution of 30 m across the Visible, Near Infrared and Shortwave Infrared regions over an area coverage of 185 km. The Sentinel 2, on the other hand, allows for a free provision of the information collected at a spatial scale of 10 – 60 m through the Visible, Red Edge Position (REP) and the Shortwave Infrared (SWIR) sections of the spectrum across a geographical extent of 290 km. The high revisit time (i.e., 5 and 16 days for Sentinel 2 and Landsat 8) coupled with better spectral and spatial properties of these sensors will promote effective characterization of autumn grassland senescence even in resource constrained countries. In addition, these instruments are generally characterized by refined and strategically located spectral bands to optimize the assessment of autumn grassland senescence.

1.5 Aim

The aim of the current study was, therefore, to assess the impact of autumn grass senescence on foraging resource quality and quantity in subtropical sourveld grasslands of KwaZulu-Natal (KZN), South Africa, based on the modern generation broadband multispectral remotely acquired data. The focus was on a case study in the KZN Midlands communal rangelands.

1.6 Objectives of the study

The specific objectives were:

1. To provide a detailed overview on the progress of remote sensing applications in characterizing grass senescence and the possible challenges and opportunities.
2. To quantify the amount of decline in nGongoni (*Aristida junciformis*) grass, a dominant sourveld species, quality and quantity because of senescence, using *in-situ* and Sentinel-2 data. Also, to assess forage availability status at pre-senescence and senescence stages based on the Dry Matter content (DM) of the grass.
3. To characterize the onset of autumn senescence in mesic subtropical sourveld grasslands using remotely sensed data.

4. To evaluate the climatic and topographic drivers of remotely sensed autumn grassland senescence.
5. To test the potential of the modern multispectral remote sensing dataset (i.e., Sentinel 2 and Landsat 8) in mapping grass senescence, and to identify the optimal waveband positions that are suitable for discriminating between senescent and non-senescent grass.

1.7 Study site description

This research was carried out at Vulindlela communal land, west of Pietermaritzburg, KwaZulu-Natal, South Africa (Figure 1.1) with central geographic coordinates 29°.40'37.3584''S and 30°.8'13.6572''E. Broadly, this area is situated in the sourveld of the Midlands mist belt grassland region (Mucina *et al.* 2006). The area has subtropical climates, which include hot and wet summers and cold and dry frosty winters (Sibanda *et al.* 2021). The frost conditions generally start in mid-April through to end of August (Royimani *et al.* 2022). The frosty conditions associated with winter may promote grass senescence, and thereby increase the susceptibility of the grass to wildfires. The mean annual rainfall is around 950 mm (Singh *et al.* 2018; Sibanda *et al.* 2021), with most and least rainfall experienced during summer and winter, respectively. The average annual minimum and maximum temperatures are 6°C and 22°C in winter and summer, respectively (Royimani *et al.* 2023). Although not pronounced, the topography is defined by hilly and valley landscapes and an altitude ranging between 1273 to 1412 m.a.s.l. The soils at Vulindlela are predominantly loam with random rocky surfaces (Royimani *et al.* 2023).

Historically, Vulindlela was dominated by forb-rich and sour *Themeda triandra* type grass species, however, has since been severely transformed owing to, among others, the nGongoni (*Aristida junciformis*) grass invasion (Scott-Shaw and Escott 2011). Consequently, the current vegetation at Vulindlela is strongly defined by the nGongoni and other mesic subtropical grass types of the sourveld along with patches of shrubs and pine (*Pinus*) and gum (*Eucalyptus*) plantations (Royimani *et al.* 2022). According to Sibanda *et al.* (2021) and Fynn *et al.* (2011), these mesic subtropical grasses comprises of, among others, *Alloteropsis semialata*, *Aristida junciformis*, *Tristachya leucothrix*, *Themeda triandra*, *Panicum maximum*, *Eragrostis tenuifolia*, *Paspalum urvillei*, *Setaria sphacelata* and *Sorghum bicolour*. Furthermore, Royimani *et al.* (2021) noted that sourveld grasses are generally known for their high degree of nutrient loss – hence decline in grazing value – particularly during the winter season and

that makes them a perfect choice of investigation in efforts aimed at understanding the impact of senescence on foraging resource quality and quantity.

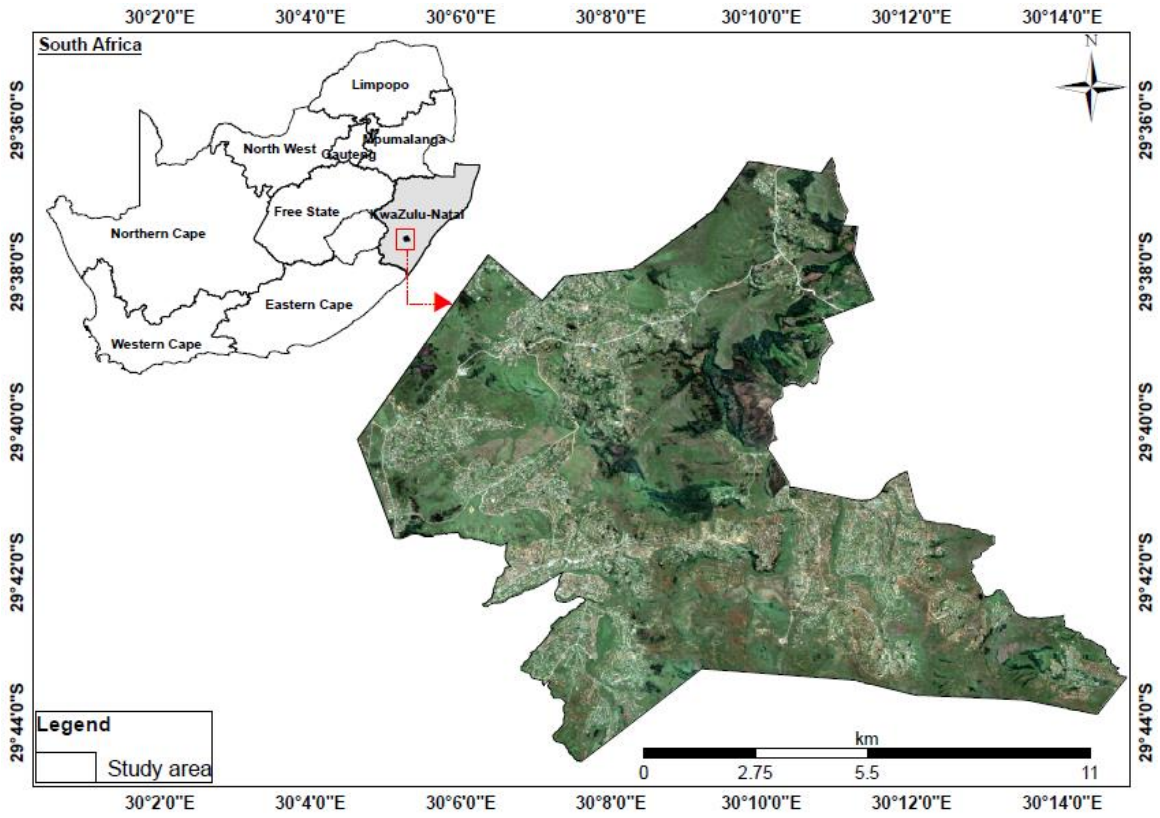

Figure 1.1 The location of Vulindlela communal area, KwaZulu-Natal, South Africa.

In addition, observational evidence suggested that grasses at Vulindlela are largely exposed to continuous and uncontrolled grazing patterns. This is due to the lack of infrastructural facilities such as fencing to regulate the movement, grazing patterns as well as the numbers of the livestock or stocking densities. In contrast to rotational grazing, which is a common practice in commercial rangelands, continuous grazing is known to increase the pressure on grazing resources and often prevent grass growth (Teague *et al*., 2008). This may have negative implications on fodder bank capacities and further increase the risk of fodder deficiency, particularly during dry seasons. Moreover, uncontrolled fires were observed to be a common practice, especially over the dry winter period when the grass is dormant because of senescence, in turn affecting forage availability. Livestock farming has been identified as one of the key agricultural land use practice in the area, with a main focus on communal livestock production systems (Sibanda *et al.* 2021). However, evidence suggest that the management of

natural resources like pastures and the grazing patterns adopted in communal grazing lands are either not sustainable or ineffective (Ayantunde *et al.* 2014).

With regards to household headships and socioeconomic activities, Vulindlela – a former homeland of KwaZulu – is typical of a South African rural community which is characterized by female-headed households and high levels of poverty and unemployment (Darbes *et al*., 2014). Nonetheless, research shows that, by far, rural women constitute the greatest portion of the most vulnerable and marginalized population groups in underdeveloped rural communities like Vulindlela (Govender and Qwabe, 2022). The limited access to economic opportunities coupled with high levels of unemployment in Vulindlela suggest that the only means thorough which local populations can sustain their survival is by farming. However, observational evidence indicated that agriculture at Vulindlela is largely dominated by smallholder farming which include subsistence livestock and small household gardens. According to reports, the rise in demand for land to support developmental projects such as housing has led to increased loss of productive agricultural land at Vulindlela (Isikhungusethu Environmental Services (Pty) Ltd, 2016), thus, putting more pressure on limited productive agricultural land. Notable from this discussion is the importance of the livestock as a key household livelihood mechanism.

1.8 Scope of the study

In optimizing the assessment of grass senescence for the knowledge on foraging resource quality and quantity in communal rangelands that are situated in sourveld, the focus of this work was on exploring the role of the modern generation multispectral remote sensing dataset in monitoring the dynamics around the occurrence of autumn grassland senescence. Using the broadband multispectral remote sensing instruments in concert with robust and advanced algorithms like the Random Forest, this study assessed spectral, spatial and temporal windows for optimal detection of autumn grassland senescence. Specially, this work investigated the optimal remote sensing techniques, jointly with *in-situ* measurements of plant parameters, for reliable assessment of the onset and impact of autumn grass senescence on foraging resource quality and quantity. It further examined the climatic and topographic drivers of autumn grassland senescence, as well as the spatial scale required for effective discrimination between senescent and non-senescent grasses. Overall, the study revealed the importance of the Random Forest in extracting useful information for understanding the remotely sensed autumn grassland senescence. Equally, the study has identified the required period of time, spatial scale as well as spectral regions for reliable estimation of grassland autumn senescence together with key environmental drivers of this phenological stage.

1.9 Thesis outline

This thesis comprises of seven chapters, of which five are stand-alone papers either published or submitted for publication in appropriate international journals, while the other two are this introduction and the final synthesis sections. The five chapters sent for publication addresses each of the research objective stipulated in section 1.6. There may be some overlap and repetition across chapters because of the need for each to stand alone as a separate published paper.

1.9.1 General introduction and contextualization

1.9.1.1 Chapter One

This serves as an introductory chapter and provides the overview and contextualization of the study. More importantly, it highlights the main aim, scope and the outline of the work done together with specific research objectives to be addressed. It further illustrates the relevance of understanding the dynamics around, and the impact of, autumn grassland senescence on foraging resource quality and quantity, the chosen study area (communal sourveld grassland), as well as the adopted remote sensing-based methodology to address the stipulated research objectives.

1.9.1.2 Chapter Two

This chapter gives a detailed overview on the progress of remote sensing applications in characterizing grass senescence. It further elaborates on the challenges and possible opportunities presented by these techniques in assessing plant senescence. The chapter also presents the biophysical and biochemical properties of the plant, including chlorophyll content, biomass, LAI and the leaf coloration and fall, commonly used in remote sensing studies of plant senescence. It also highlighted the gaps together with the need for adoption of more objective ways of assessing grass senescence.

1.9.2 Operational scale assessment of grassland autumn senescence

1.9.2.1 Chapter Three

Using the nGongoni (*Aristida junciformis*) grass as an example, this chapter estimated the magnitude of decline in the quality and quantity of foraging resources because of senescence, using *in-situ* and Sentinel-2 data, and the random forest regression model. It further assessed forage availability status at pre-senescence and senescence phenological stages of the nGongoni grass using the Dry Matter content (DM) as a surrogate.

1.9.2.2 Chapter Four

Owing to the understanding of the degree of decline in foraging resource quality and quantity following senescence (chapter three), this chapter sought to characterize the onset of autumn senescence in mesic subtropical sourveld grasslands using remotely sensed data. Taking advantage of the high temporal resolution of the Sentinel 2 remotely sensed datasets, specifically, this chapter developed monthly vegetation indices from January through June to meaningfully understand the grass senescence onset (i.e., inflection point in chlorophyll content). This was necessary to ascertain the potential duration of quality forage provision in rangeland ecosystems through the dry season.

1.9.2.3 Chapter Five

Having successfully determined the onset of autumn grassland senescence in the study area, chapter five focused on understanding the key remote sensing-derived environmental drivers of autumn grass senescence. Therefore, this chapter examined the spatial correlation between remotely sensed autumn grass senescence *vis-a-vis* climatic and topographic variables in the mesic subtropical grasslands. This was not only essential to understand the occurrence of senescence and its impact on foraging resources, but also to assist in developing effective rangeland management practices.

1.9.2.4 Chapter Six

In order to gain a conclusive understanding of the potential role of remote sensing techniques in the assessment of autumn grassland senescence, this chapter investigated the potential of the modern multispectral remote sensing dataset (i.e., Sentinel 2 and Landsat 8) in mapping grass senescence, and tested the optimal waveband positions that are suitable for discriminating between senescent and non-senescent grasses. This was necessary to gain knowledge on the possible scale of mapping required for detection of autumn grassland senescence.

1.9.3 Synthesis and conclusion

1.9.3.1 Chapter Seven

This is a final chapter and it gives a synthesis of the conclusions drawn from the findings of the five analysis chapters presented in this work. The study has clearly determined the spectral spatial, and temporal, windows for effective monitoring of autumn grassland senescence using remote sensing techniques. In concluding, the section outlined the direction for future research and made recommendations for the application of this knowledge in practice.

Chapter Two

2 Progress in remote sensing of grass senescence: a review on the challenges and opportunities

This chapter is based on:

Royimani, L., Mutanga, O. & Dube, T. 2021. Progress in remote sensing of plant senescence: a review on the challenges and opportunities. *IEEE Journal of Selected Topics in Applied Earth Observations and Remote Sensing*, 14, 7714-7723.

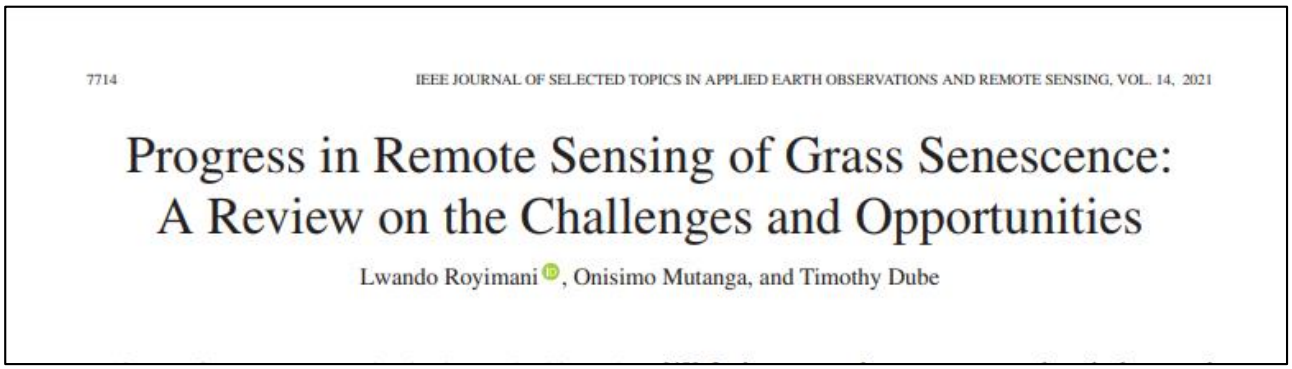

Abstract

Grass senescence estimation in rangeland environments is particularly important for monitoring the conditions of forage quality and quantity. During senescence, grasses lose their nutrients from the leaves to the root systems, and, thereby, affecting forage quality. Several remote sensing studies have been conducted on grasslands during the senescence phenological stage with a particular focus on detecting proportions of senescent grass leaves. Although the reported results from those studies were promising, our understanding of the role of remote sensing in estimating the autumn grassland senescence is still shallow. More so, the strengths and limitations presented by the newly developed remote sensing instruments in grass senescence estimation are not well documented. This work therefore provides a detailed overview on the progress of remote sensing applications in characterizing grass senescence. The review further highlights the challenges and possible opportunities presented by these techniques. Overall, the review indicated that the available studies on remotely sensed grass senescence applications are focused on understanding biophysical and biochemical properties and these studies identify the Leaf Area Index (LAI), biomass, chlorophyll content and leaf coloration and fall, among others, as key indicators of grass senescence. Nonetheless, recent scientific work highlights a mismatch between studies on vegetation phenology and the development in remote sensing technologies. The use of sophisticated and robust time-series analysis techniques like the piecewise linear regression with a breaking-point jointly with enhanced sensing properties from the modern generation sensors, presents novel prospects for the reliable estimation of grassland senescence at resolutions complementary to the spatial scale of the rangelands. It is, therefore, recommended that future studies close this research gap by adopting the recent satellite technologies together with advanced spatial data analytics to enhance rangeland resources monitoring.

Keywords: Forage resources, grass quality and quantity, senescence, rangelands, remote sensing.

2.1 Introduction

The understanding of grass senescence in rangeland environments is of great importance as it informs the knowledge on availability status, condition, distribution and allocation of forage (Xu *et al.* 2019; Fuhlendorf and Engle 2001; Pickup 1996). By definition, senescence is generally described as the last phase in the plant's lifespan (Lim and Nam 2007). In the process, plant components such as the leaves and stems individually or collectively deteriorates through time as a result of either internal or external factors (Gepstein *et al.* 2003; Lohman *et al.* 1994;

Smart 1994; Partridge and Barton 1996). Highlighting the impact of external factors in senescence, Castro and Sanchez-Azofeifa (2008), noted that the autumn senescence of deciduous vegetation in temperate regions is strongly influenced by the day-length of the region during this particular period. Buchanan-Wollaston *et al.* (2003), also noted that the process of grass senescence is invaluable for livestock production as it helps to promote the growth and development of new and often nutritious feed. Nonetheless, many other studies have also highlighted the ecological relevance of grass senescence (Asner *et al.* 2004; Bartlett *et al.* 1989). For instance, senescence reduces leaf area thereby minimizing the stomatal pores of the associated grass foliar and this in turn lowers the evapotranspiration fraction (Curran 1980). Also, the senescent grass leaves are known for their low absorptive capacity of the atmospheric carbon and thus decreasing the amount of sequestrated carbon (Asner *et al.* 2004; Bartlett *et al.* 1989). In addition to the common stressors of foraging resources like rangeland degradation (Pickup 1996), climate change (Adjorlolo *et al.* 2012), and the undesirable anthropogenic activities, grass senescence also presents extra pressure on ranch and forage quality and quantity. Therefore, this emphasizes the need to understand grass senescence, especially in developing countries where Gross Domestic Products (GDPs) are largely depended on livestock farming. Such information will not only provide insightful baseline knowledge on grass-production-budgets but also boost awareness on the value of livestock farming towards poverty alleviation which addresses Sustainable Development Goals number 1 (i.e., no poverty) and 2 (i.e., zero hunger).

Traditionally, grass senescence estimation has been achieved, largely, by means of visual inspections and handheld field spectrometers (Liu *et al.* 2013; McKean *et al.* 1991; Asrar *et al.* 1986a). However, the major drawbacks of such methods in vegetation assessment are well detailed in the literature and they include, among others, the limited spatial extents, compromised repeatability and excessive time and labour required (Royimani *et al.* 2019a; Royimani et al. 2019b). Contrastingly, remote sensing allows for reliable, cost-effective and repeated assessments of grass senescence at various landscape scales. Its ability to acquire spatial data repeatedly over the same locations provide the multi-temporal data required for detecting subtle changes in the physiology and phenology of grass canopies over time. In light of these benefits, scholars have explored the contributions of remote sensing techniques in estimating grass senescence using different sensing instruments, ranging from local (Asrar et al. 1986a) to regional (Asner et al. 2004; Qi et al. 2002) scales of application. Local scale assessment of grass senescence with remotely sensed data has often been done, using the

Analytical Spectral Devices (ASD) and other hyperspectral radiometers (Bork *et al.* 1999; Asrar *et al.* 1986a). Although these instruments produced adequate estimation accuracies, their limited coverage coupled with excessive acquisition cost often impede their adoption, especially for forage monitoring efforts at the landscape scale. Remote sensing multispectral sensors like the Landsat 5 Thematic Mapper (TM), Landsat 7, on the other hand, have dominated grass senescence monitoring at an operational scale (Guerini Filho *et al.* 2020; Liu *et al.* 2013; Asner *et al.* 2004; Qi *et al.* 2002; Bork *et al.* 1999). With improved spectral, spatial and temporal properties of these sensors, reasonable estimation accuracies of grass senescence in geographical scales that are complementary to the spatial extents of rangelands are achievable. Also, the free provision of data from these sensors is a huge advantage for rangeland resource monitoring, especially in resource limited regions like southern Africa. Nonetheless, the success of remote sensing techniques in characterizing grass senescence relies on the use of biochemical, physiological and phenological properties of the foliar as surrogates. Commonly used biophysical indicators that have aided the remote sensing of grass senescence include the Leaf Area Index (LAI) (Asrar *et al.* 1986a), fraction of absorbed photosynthetically active radiation (fAPAR) (Butterfield and Malmström 2009), chlorophyll content (Liu *et al.* 2013), aboveground grass biomass (Guerini Filho *et al.* 2020; Butterfield and Malmström 2009; Asner *et al.* 2004), among others.

Despite this knowledge, only a handful of studies have reviewed remote sensing applications on vegetation with an element of senescence in general. For instance, Bradley (2014) reviewed remote sensing techniques for detecting invasive plants using phenological, spectral and textural attributes. Moore *et al.* (2016), gave a synthesis of remote sensing approaches for monitoring changes in the phenology of the Australian vegetation. Although the potential of remote sensing in characterizing senescence has been noted, however, such studies have largely focused on croplands and woody vegetation instead of grass species. This highlights the need for the state of the art review in the literature to understand the contributions of remote sensing methods in estimating grass senescence. Also, this information will serve as a baseline for identifying critical knowledge gaps for future improvements. Such a synthesis is even more relevant owing to current developments in remote sensing technology. For instance, the recent introduction of broadband multispectral remote sensing instruments (e.g., Sentinel-2 and Landsat 8) with improved spatiotemporal and spectral properties provides new options for grass senescence assessment and estimation. Therefore, the current study provided an overview of remote sensing techniques and their applications in characterizing grass senescence with

associated challenges and opportunities. Primarily, the study gave a detailed discussion of the methodology followed in searching and identifying relevant literature for the review process. Further, the study explored the process of grass senescence jointly with the subsequent impact on forage quality and quantity across various veld types. In addition, the review examined the differences in spectral reflectance of green versus senescent grass species. The study also interrogated the commonly used remote sensing techniques and vegetation indices for characterizing grass senescence. Lastly, the study highlighted the common challenges in remote sensing of grass senescence together with possible directions for future studies in remote sensing of grass senescence.

2.2 Literature search and selection of source articles

To achieve the objective of the present study, relevant literature from selected peer-reviewed journals were gathered and reviewed. The selected articles were identified using key search words from the web of science, google scholar, and other revered scientific databases. These repositories are believed to be among popular databases, which are rich in terms of peer-reviewed scientific work of this nature. The key search words included: “remote sensing of grass senescence”, “remote sensing of dry grass biomass”, “grass senescence”, “sourveld grass development”, “livestock forage quality”, “remote sensing of grass phenology”, “autumn grassland senescence”, “pasture production”. Additional journal articles were found from the reference lists of included studies through a process known as backward reference list checking (Karlson and Ostwald 2016). Studies were, therefore, included or excluded on this work based on the above-mentioned criterion.

2.3 Grass senescence and its impact on forage quality and quantity across various veld types

Senescence is an important phenological stage in the life cycle of grasses which marks the end of the older life and paves a way for the beginning of a new one (Lim and Nam 2007; Dertinger *et al.* 2003). In the process, fundamental changes are notable in the gene expression, metabolism, and structure of various grass components such as the leaves and stem (Lim *et al.* 2007). The earliest and the most common form of senescence in grasses is leaf senescence, in which the individual green leaves of the grass gradually turn yellow to brown in colour as a result of breakdown and loss of chloroplast (Corbane *et al.* 2008; Gregersen *et al.* 2008; Buchanan-Wollaston *et al.* 2003). The progressive loss of green colour in grass foliage often coincides with the migration of nutrients from the tiller parts to the root systems (Das and Chaturvedi 2005). Broadly, the leaves can senesce as a result of either poor plant health status,

strenuous environmental conditions, and/or old age (Santos *et al.* 2010; Chaerle and Van Der Straeten 2000). The process whereby plant leaves uniformly go through senescence due to their old age, like the autumn senescence, at the landscape scale is called natural senescence (Gepstein *et al.* 2003), whereas induced senescence is consequent to actions of particular agents like diseases, extreme weather conditions or physical disturbances, among others (Figure 2.1).

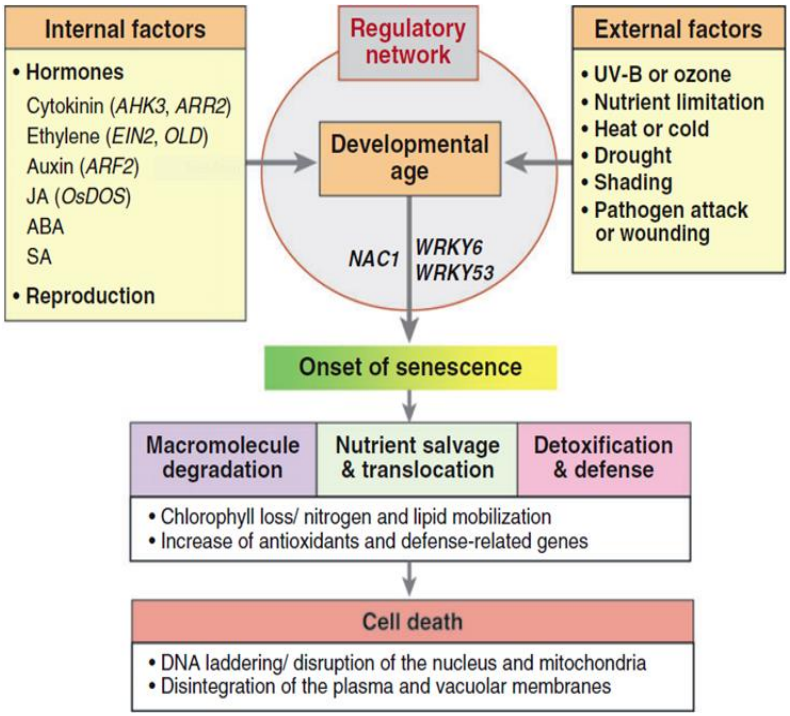

Figure 2.1 Schematic representation of leaf senescence as a result of internal and external factors. **(**Adapted from Lim *et al*. 2007).

Based on Lim *et al.* (2007), figure 2.1 illustrates the phenology of the vegetation with a particular focus on the senescent stage with internal and external casual factors, on the left and right hand sides, respectively. It can be seen that the internal factors are largely defined by the biochemical constituents of the plant itself while the external causes are more of an outside agent, like micro-climate and pathogens, etc. Under the influence of internal factors, grasses can senesce earlier than their natural expected time, mainly due to excess or shortage of particular hormones or ill health. However, in external factors, grasses senesce because of limited sunlight, water, and nutrients, among others (Buchanan-Wollaston *et al.* 2003). Research reveals that after senescence, the fallen grass material is decomposed to enhance the structure of the soil as well as water holding capacity, which also reduces soil erosion (Ackerly

1999; Kok *et al.* 1990). Likewise, the decomposed grass material activates soil nutrient turnover and primary productivity, which is necessary for livestock grazing purposes (Guo *et al.* 2004; Nagler *et al.* 2000). Clearly, grass senescence is not a completely undesirable process, especially for livestock production as it activates the development of new and mostly high nutrient forage (Buchanan-Wollaston *et al.* 2003). A detailed scientific report of this process is presented in the works of Woo *et al.* (2019), Lim and Nam (2007), Lim *et al.* (2007), and Gepstein *et al.* (2003), etc.

In addition, experimental studies showed that senescence is a major driver of grass quality and quantity (Hemminga *et al.* 1999; Lohman *et al.* 1994; Day 1983), especially for grazing purposes. This is particularly the case in sourveld grazing areas where grasses are subjected to a process of "leaf-to-root" nutrient translocation as a result of senescence (Smart 1994), and this significantly degrades grass leaf nutrients (Das and Chaturvedi 2005). A clear demonstration of this process has been made in Figure 2.2 using data extracted from Zacharias (1995). This author used nitrogen content as an indicator of grass quality to compare nutrient holding capacities between sweet-, mixed-, and sourveld grasses over different seasons. The results reveal that sweetveld grasses can hold nutrients constantly high throughout the year whereas the quality of mixed-veld grasses is highly variable mostly with seasons. On the other hand, sourveld grasses showed low nutritional content for most of the year, with the lowest (0.5%) nitrogen value reported in the transition from winter to spring. Evidently, sourveld grasses are mainly effective during summer as far as the livestock grazing purposes are concerned. Although grasses from the sweet- and mixed-veld are subjected to senescence, the ability of their leaves not to drastically lose nutrients makes them a better choice for the livestock production. It is also assumed that the yellow to brown leaves of sourveld grass, following senescence (Lim and Nam 2007) are not adequate nor even nutritious for the livestock consumption. Even though sourveld grazing areas are considered to be rich in terms of species diversity, Hardy *et al.* (1997) and Pickup (1996) maintain that not all the herbage produced in rangelands are palatable. This further perpetuates the selective grazing that has been reported in sourveld (Peddie 1995). Likewise, the selective grazing increases fuel loads (Little *et al.* 2015; Forsyth *et al.* 2010), and thereby promoting veld fires (Little *et al.* 2015). The remaining grass stems as a result of cold fires or senescence are often less likely to regrow their leaves until the next rainy season, mostly in spring, occur. This is precisely because grass production processes in sourveld are strongly influenced by seasonality and rainfall (Hardy *et al.* 1997). The subsequent impact, thereafter, is expected to be felt mostly by rural livestock

farmers who can barely afford the expensive supplementary forage (Rabumbulu and Badenhorst 2017). This argument shows the need for forage assessment studies that prioritize not only the investigation of grass senescence in general but rather in grasses that are situated in sourveld communal rangelands. Although previous experiences have proved that data collection for rangeland assessments can be laborious, resourceful, and time-consuming, remarkable progress has been made, using recent methods, which rely on spectral properties of the vegetation observed through remote sensing platforms.

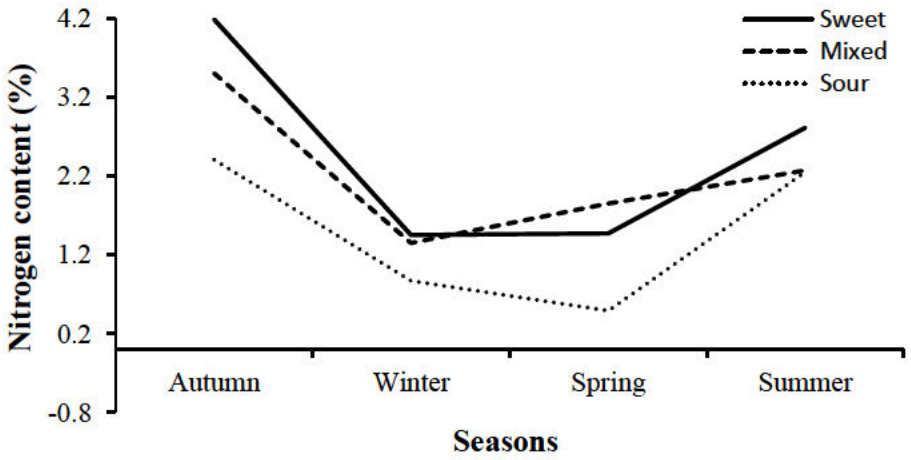

Figure 2.2 Seasonal dynamics in percentage nitrogen (N) concentration in sweet-, mixed-, and sourveld grasses. (Source: Zacharias 1995).

2.4 Spectral properties of green versus senescent grasses

A large body of evidence (Chemura *et al.* 2018; Adam *et al.* 2010; Clark *et al.* 1995b) suggests that the spectral signals of grasses, like any other vegetation, is governed by its internal and external features, including the structural and surface properties of the leaves along with distribution and concentration of pigments. Cole *et al.* (2014) and Clark *et al.* (1995b) indicated that these internal and external factors have measurable and known absorption and reflectance features in the electromagnetic spectrum. Certainly, variation in the distribution and quantities of these constituents among senescent and green grass leaves promote their spectral distinctiveness in different regions of the electromagnetic spectrum as shown in figure 2.3. Specifically, figure 2.3 shows the averaged spectral reflectance of green and senescent nGongoni (*Aristida junciformis*) grasses extracted from the Landsat 8 dataset to understand the behavior of the spectral response of the grass between these two phenological periods. In the process, two preprocessed Landsat 8 images covering the uMsunduzi Municipality of

KwaZulu-Natal, South Africa, were downloaded from Earth-Explorer, and each image corresponded to summer (i.e., 18 January 2020) and winter (i.e., 16 July 2020) to represent green versus senescent grasses, respectively.

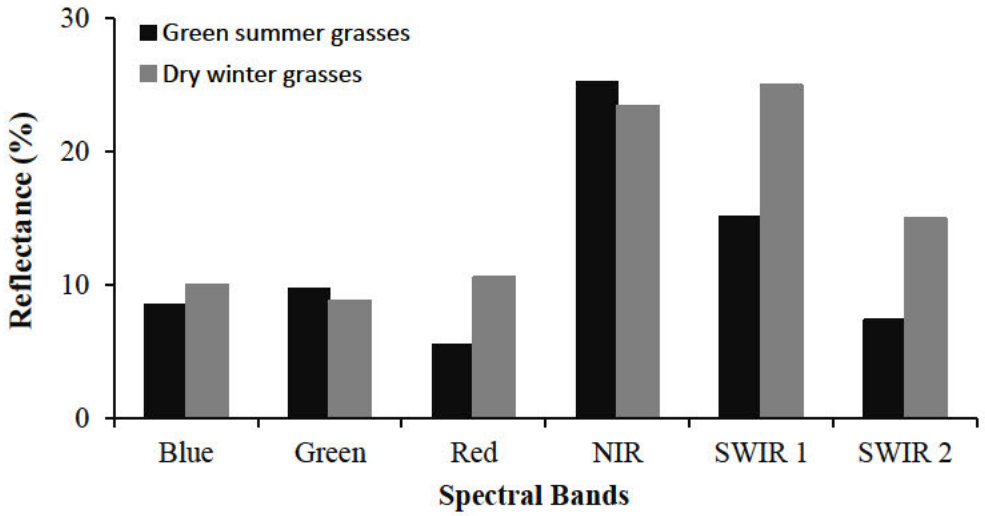

Figure 2.3 Averaged spectral reflectance of green versus senescent nGongoni grasses extracted from the Landsat 8 bands. There images were acquired on the 18 January and 16 July 2020 to represent summer and winter seasons, respectively.

It could be observed that the spectral signatures of green grass were dominant in the Visible green and the NIR regions whereas those of the senescent grass leaves were superior in the Visible blue, red and in the SWIR sections. Based on Peñuelas and Filella (1998), the high chlorophyll content in the leaves of green grass is responsible for the increased reflectance in the Visible green and the NIR while remaining low in the other regions because of increased absorption. These results are in agreement with findings by Adam *et al.* (2010), who noted that a typical spectrum of green leaves is characterized by increased reflected and absorbed spectra in the NIR and Mid Infrared (MIR) due to pigment concentration and water content, respectively. Other studies (Matongera *et al.* 2018; Asrar *et al.* 1986a) which have conducted a close comparison between green and dry plant spectra confirm the results presented in figure 2.3 that the spectral reflectance of senescent vegetation dominates the Visible and the SWIR regions of the spectrum. However, Elvidge (1990) emphasized that remote sensing works of vegetation assessment have predominantly been limited to green leaf spectra as opposed to the non-green canopies.

Contrary to the green leaves, the spectral properties of senescent vegetation are not easily discernable due to many factors including the soil background promoted by the decrease in foliar cover and LAI, among others. Similarly, spectral reflectance of senescing flora is often mixed and confused with fractions of adjacent green leaves and this is particularly the case when using measurements taken at the canopy level. However, with the understanding of the influential internal and external constituents, Asrar *et al.* (1986b) showed that the spectra of senescing leaves can also be detected from various regions of the spectrum. As opposed to the high chlorophyll content of green leaves, which induces the spectral signatures at 450 and 550 nm, the low chlorophyll content of senescent leaves increases the subsequent spectra at 675 nm wavelength (Peñuelas and Filella 1998). It is further noted that senescing leaves exhibit increased spectral reflectance in the red and SWIR regions of the spectrum due to decreased chlorophyll and water content (Matongera *et al*. 2018). The variation in water content between senescent and green leaves is further expected to induce their spectral distinctiveness in the MIR region of the electromagnetic spectrum (Adam *et al.* 2010).

2.5 Remote sensing techniques and common vegetation indices for assessing grass senescence

Globally, there is only a handful of remote sensing studies that have investigated the subject of grass senescence in rangeland ecosystems. For instance, Qi *et al.* (2002) tested the capabilities of the Landsat 5 and Landsat 7 images in estimating forage production based on combined fractional cover of the senescent and green leaves of the herbaceous vegetation in the Appleton Whittell Research Ranch, southeast of Arizona, United States of America (USA). The green canopy cover was assessed using the NDVI while the senescent components were characterized based on the Normalized Difference Senescence Vegetation Index (NDSVI) and the linear un-mixing analysis. The formula for NDSVI and other indices commonly used in estimating grass senescence are presented in Table 2.1. Optimal estimates of forage production were obtained with R^2 values of 0.91 and 0.93 and standard errors of 2% and 0.03(kg) for the senescent fractional cover and the total forage respectively. In addition, Qi *et al.* (2002) observed a poor correlation between the NDVI and the biomass of senescent grass, something that was also reported by Butterfield and Malmström (2009). The inability of the NDVI to successfully characterize grass senescence highlighted the need for an alternative technique like the NDSVI to optimize grass estimation during the senescent stage.

Table 2.1 Summary of commonly used vegetation indices in estimating plant phenology and senescence

Index name	Formula	Reference
Enhanced Vegetation Index (EVI)	2.5(NIR - Red)/(NIR + C1 * Red – C2 * Blue + L)	Gómez-Giráldez *et al.* (2020)
Simple Ratio (SR)	(NIR/red)	McKean *et al.* (1991)
Enhenced Vegetation Index 2 (EVI2)	2.5(NIR – Red)/(NIR + 2.4 * Red + 1)	Gómez-Giráldez *et al.* (2020)
Simple Ratio (SR)	(MIR/IR)	McKean *et al.* (1991)
Sentinel-2 Red Edge Position (S2REP)	705 + 35 * ((((NIR + R)/2) − RE1)/(RE2 − RE1))	Gómez-Giráldez *et al.* (2020)
Greenness Index	Karhunen-Loeve Transformation (KLT)	McKean *et al.* (1991)
Green Chromatic Coordinate (GCCs)	G/(R + G + B)	Gómez-Giráldez *et al.* (2020)
Meris Terrestrial Chlorophyll Index (MTCI)	(NIR − RE)/(RE − R)	Gómez-Giráldez *et al.* (2020)
Normalized Difference Vegetation Index (NDVI)	(NIR – R)/(NIR + R)	Butterfield and Malmström (2009); Di Bella *et al.* (2004)
Green Normalized Difference Vegetation Index (GNDVI)	(NIR - Red)/(NIR + Red)	Gómez-Giráldez *et al.* (2020)
Normalized Difference Senescence Vegetation Index (NDSVI)	$(R_{SWIR} - R_{red})/(R_{WSIR} + R_{red})$	Qi *et al.* (2002)
Inverted Red Edge Chlorophyll Index (IRECI)	(NIR − R)/(RE1/RE2)	Gómez-Giráldez *et al.* (2020)
Soil Adjusted Vegetation Index (SAVI)	1.5(NIR − Red)/(NIR + Red + 0.5)	Gómez-Giráldez *et al.* (2020)

Footnote: R = wavelength.

In another study, McKean *et al.* (1991) investigated the role of the multispectral Thematic Mapper Simulator NS001 (TMS-NS001) datasets and time-series analysis in explaining grass senescence as a result of landslide debris flow across an uneven terrain of the Marin County of California in the USA. The authors derived three vegetation indices from the four TMS-NS001 images acquired, of which two of those indices were based on the Simple Ratio (SR) calculated using band combinations from various regions of the spectrum (i.e., Near-Infrared/Red (Band 4/Band 3), Mid-Infrared/Infrared (Band 6/Band 4)) while the third being the greenness index

(i.e., greenness). Their findings pointed out that the greenness index was a crucial indicator of grass senescence estimation with an R^2 value of 0.60. Also, their results showed that the onset of senescence in grasses located in the valley areas was delayed and that could be attributed to the increased soil moisture content in those regions.

In addition, Asrar *et al.* (1986a) examined the capabilities of the Modular Multispectral (MMR) Model 15-1000 and the Model 100-A radiometers in spectrally separating soils, senescent and green grass leaves in the Konza Prairie Research Natural Area, Manhattan, USA, using the discriminant and canonical discriminant analysis procedures. Based on their findings, the senescent grass was spectrally discrete from the other land cover classes with classification accuracies of 99 and 82% for the MMR Model 15-1000 and the Model 100-A, respectively. The strength of remote sensing instruments such as radiometers in characterizing grass during senescence relies on their ability to detect subtle changes in pigment concentrations. For instance, Merzlyak *et al.* (1999) noted that the spectral signal of the vegetation increases around 550 and 740 nm due to senescence-induced chlorophyll degradation while remaining low at 400 and 500 nm because of carotenoid retention. Additional evidence highlighted that at 500 nm plant spectra are mainly controlled by both chlorophyll *a*/*b* as well as carotenoid, whereas at 680 nm it's determined by chlorophyll *a* (Cole *et al.* 2014; Castro and Sanchez-Azofeifa 2008; Merzlyak *et al.* 1999). Although, the problem of mixed pixels which is commonly reported in studies of dry vegetation and soils was also noted in the study by Asrar *et al.* (1986a) with an error rate of 3% and 20% for the MMR Model 15-1000 and the Model 100-A, respectively. Besides the superior spectral properties of the radiometers employed, the success of the results obtained by Asrar *et al.* (1986a) could be attributed to the fact that the analysis was done at early stage of senescence when the green elements were still evident in the grass as compared to later stages when all the grass was completely dry. Butterfield and Malmström (2009), also examined the impact of senescence on biomass of the *Avena fatua* L. *Bromus hordeaceus* L. and *Lolium multiflorum* Lam. grasses in Michigan, USA, using a hyperspectral radiometer. Three models, namely; the NDVI, fraction of absorbed photosynthetically active radiation (fAPAR) and the LAI, were used as indicators of grass biomass. The study further emphasized the poor correlation between the NDVI and grass biomass, particularly when the fraction of senescent grass canopy was more than 50%, and this showed that the NDVI is not a reliable indicator of senescent grass biomass. Instead, the significant relationships between grass biomass and the fAPAR ($R^2 = 0.82$, $p < 0.001$) and the LAI ($R2 = 0.80$, $p < 0.001$)

highlighted the suitability of these two indicators in characterizing grass senescence based on remotely sensed data.

Furthermore, Asner *et al.* (2004) evaluated the temporal dynamics in the biophysical and ecosystem biogeochemical features of meadow during the senescence stage in the south of Santarém, Brazil, using the Landsat 5 Thematic Mapper (TM) and spectral mixture analysis. Specifically, these authors tested the relationship between the aboveground biomass of the *Brachyaria brizantha* and *Pennesetum clandestinum* grasses and the soil organic carbon across two different soil types (clayey Oxisols and sandy Entisols) during the senescence stage and linked the resultant correlations to short and long-term signs of nutrients in the grass. Their findings exhibited a dual decrease in both the aboveground grass biomass and soil carbon storage with progress in senescence across the two soil types. Equally, the analysis of nutrients showed that phosphorus (P) concentration was low in all grasses situated in both soil types and it further decreased with advancements in the stage of senescence while nitrogen (N) content varied and correlated less with either the aboveground biomass or soil organic carbon. In a multi-temporal study, Bork *et al.* (1999) also examined the potential of simulated eight broadband Landsat 5 TM and 52 narrowband ASD spectral signals in characterizing rangeland cover components, including grasses, in the north of Dubois, Idaho, USA. The results showed that optimal estimation of grass cover was achieved during the later stage of summer (August) due to the effect of senescence with correlation coefficients (r) of 0.4 and 0.54 for the broadband (NIR) and narrowband ($AR_{green/blue}$) instruments, respectively. Guerini Filho *et al.* (2020) explored the robustness of the Sentinel 2 data jointly with subsequent vegetation indices and the multiple linear regression model in estimating green, senescent and the total biomass of the natural grasslands in the Federal University of Santa Maria in southern Brazil. Based on the findings obtained, an adjusted coefficient of determination ($R^2_{adjusted}$) and Root Mean Square Errors of 0.4, 0.3 and 0.42 as well as 0.13, 0.24 and 0.14 were, respectively, reported for the green, senescent and total biomass. The advantage of Sentinel 2 in detecting changes in grass pigments during senescence at a geographical scale adequate for rangelands monitoring was defined by its high spatial resolution (10 m) jointly with Red-Edge Position and large swath-width. Despite these promising results, overall observations suggest that the remote sensing of grass senescence remains a challenging undertaking, particularly at later stage of senescence. This is because of increased spectral mixing between the reflectance of the background soils and those of the senescent grass leaves.

Additionally, Di Bella *et al.* (2004) assessed the impact of senescence when estimating the fractional cover of photosynthetically active radiation based on green properties of ryegrass (*Lolium perenne* L. Manhattan) canopy measured with the NDVI. Findings showed that the impact of senescence on NDVI values was significant ($r^2 = 0.78$; $n = 16$ and $p < 0.001$). Likewise, Archibald and Scholes (2007) used time-series satellite data to identify environmental factors that influence green-up dates between different rangeland cover features like grass species. Their investigation showed that unlike in the high latitudes where temperature and photoperiod determine phenology, soil moisture was the major driving factor behind plant senescence in the tropical regions (Castro and Sanchez-Azofeifa 2008; Archibald and Scholes 2007). Liu *et al.* (2013) also evaluated the robustness of TIMESAT in monitoring grass phenology in Inner Mongolia, China, using the time-series analysis of the Moderate Resolution Spectrodiometer (MODIS) NDVIs and double logistic function-fitting algorithm. In operation, TIMESAT uses four transition dates, namely, the onset of green-up, maturity, senescence and dormancy phase of the grass phenology. The derived MODIS NDVIs were fitted in the model (TIMESAT) to construct smoothing time-series curves and to determine each of the transition dates (green-up, maturity, senescence and dormancy). The NDVI yielded satisfactory explanation in each of the four phenological stages under investigation. The high temporal resolution of MODIS (daily) along with its global coverage allowed for the comprehensive examination of the chronological changes in the distribution and concentration of grass pigments as a result of senescence. However, it could be observed from the evidence presented in this review that remote sensing of grass senescence has not been keeping up to speed with advancements in remote sensing technology. This is demonstrated by the lack of studies which have adequately explored the potential of modern remote sensing techniques like the Sentinel 2, Landsat 8, geostationary sensors (Meteostat of Europe, INSAT of India), unmanned aerial vehicles (UAVs) and phenocameras (PhenoCams) in grass senescence estimation. In this regard, the remote sensing of grass senescence is missing a great opportunity to benefit from high quality data which is acquired at suitable time intervals for optimum detection of grass phenology, including senescence.

2.6 Challenges in remote sensing of grass senescence

One of the major drawbacks in remote sensing of plant assessment is the difficulty of associating spectra at a given wavelength with individual pigment concentrations (Adam *et al.* 2010; Merzlyak *et al.* 1999; Blackburn 1998). Although it is known that grass spectral signature varies across the spectrum (Gómez-Giráldez *et al.* 2020; Asner *et al.* 2004), due to

phenology and changes in the biochemical components, the confidence of stating categorically that at this specific wavelength the spectra is changing because of a decrease or increase in concentrations of a particular pigment is still very low. For this reason, it has been difficult to highlight explicitly the regions of the electromagnetic spectrum that can characterize grass senescence with optimal accuracies. This is not only common with data from the averaging broadband multispectral remote sensing sensors, as previously reported, but also with hyperspectral remote sensing techniques. Again, the spectral signal of the grass correlate with that of other similar vegetation due to resemblance in either the phenological stages or biochemical components, and this is generally the case despite the sensor resolutions (Adam *et al.* 2010) though it is more pronounced in some sensors than others. On the other hand, the spectra of a given species can vary within a particular wavelength because of differences in the age and micro-climatic conditions (Adam *et al.* 2010). It is, therefore, logical to question the possibility of having a unique spectral reflectance for a particular grass species, especially at advanced stages of the senescence period. In addition, at advanced senescence stage , a lot of material like the exposed soil background and litter from non-grass plants, whose spectra resembles that of senescent grass leaves (Shoko and Mutanga 2017b), is dominant and this causes spectral confusion. This problem was also reported by Asrar *et al.* (1986b).

More so, the application scale of remote sensing techniques does not allow for the assessment of grass senescence at the plant of leaf level and this result in studies of this nature being conducted at the canopy level. Blackburn (1998), noted that the problems associated with the characterization of plant senescence at the canopy scale are not unusual in remote sensing of vegetation. They mainly stem from the uncertainty of whether the entire canopy is senescing or parts of it are going through senescence (Santos *et al.* 2010). Also, the adoption of the "big-leaf-hypothesis" which was proposed by Stylinski *et al.* (2002), would not always yield the intended outcomes when estimating grass senescence through remote sensing methods due to the possibility of having crucial information obscured. The "big-leaf-hypothesis" proposes that the entire canopy of the plant, including grasses, be treated as a single big leaf when analyzing its spectral reflectance (Stylinski *et al.* 2002). However, this approach assumes uniformity in the spectra of the canopy and overlooks the possibility of spectral variation because of differences in factors such as the age or health status of each individual grass plant or among different grass leaves. Consequently, remote sensing of plant senescence has predominantly been focused on crops (Gregersen *et al.* 2008; Chaerle and Van Der Straeten 2000; Merzlyak *et al.* 1999) than on other vegetation types such as grasses. This is the case because crop fields

are reasonable plots that can be sampled in totality, at the leaf or plant level, if need be, for the estimation of senescence, unlike rangelands which are largely extensive (Xu *et al.* 2019). Also, senescence is relatively uniform in crops because they are often grown as mono-species and at the same time.

2.7 Possible directions for future research endeavors

Although, research shows that remote sensing has a critical role to play in characterizing grass senescence by identifying spatial and spectral resolutions, wavelengths, and image processing techniques that are suitable for estimation at this phenological stage. During senescence, grass canopy cover decreases because of reduction in biomass and chlorophyll content (Adam *et al.* 2010) and this partly addresses the known problem of saturation which is common with remote sensing of green and dense covers (Mutanga and Skidmore 2004). Cole *et al.* (2014) also confirmed that the dry season offers a perfect time for discriminating between vegetation types. Using Sentinel 2 data, Mutanga and Shoko (2018) observed that the winter season, when vegetation was dry, was the best for discerning between C_3 and C_4 grasses. Also, previous studies have confirmed the possibility of successful assessment of plant senescence through remote sensing techniques (Cole *et al.* 2014; Santos *et al.* 2010; Chaerle and Van Der Straeten 2000). For these reasons, it is evident that remote sensing of grass senescence is an achievable task. However, for objective quantification of grass senescence through remote sensing techniques, this study suggests that in addition to the adoption of the "big-leaf-hypothesis" the time/period in which the analysis is conducted should be considered. It therefore proposes the use of the "big-leaf-hypothesis" jointly with autumn senescence. During autumn, grass senescence is driven by natural processes such as seasonality and the age of the plant and this helps to promote uniformity in the spectral reflectance at the canopy level.

Previous studies (Cole *et al.* 2014), have indicated that at the beginning of senescence, the spectra in the Red-Edge Position shift towards the shorter wavelengths due to alterations in the distribution and concentration of plant pigments. Likewise, Peñuelas and Filella (1998) state that the increasing concentration of carotenoid with respect to chlorophyll in senescing canopies serves as an indicator of the onset of senescence in the vegetation. With improved spatial and spectral properties and the availability of strategically located bands, current remote sensing sensors like Sentinel 2 are robust enough to detect these phenological changes in grass canopies. In another study, the concentrations of plant pigments (i.e., chlorophyll and carotenoid), based on an ASD field spectrometer data, were used successfully as pre-symptomatic indicators of senescence (Cole *et al.* 2014). This was possible because chlorophyll

generally degrades faster than carotenes during senescence while leaving the carotenoids dominant at the canopy. Again, research has discovered that most compounds such as starch, glucose, and nitrogen are reversed by the plant during senescence, and, thereby, leaving the lignin and cellulose dominant (Cole *et al.* 2014). It is, therefore, fulfilling to assume that the estimation of proportions between these pigments can serve as proxies for plant senescence from a remote sensing perspective.

Given that grass senescence is a process not a phenomenon, therefore, its effective characterization cannot be achieved through a single-date image acquisition but requires multi-date images to detect the chronological changes in the phenology and pigments of the grass. The success of this undertaking relies on the availability of sensors with high re-visit time. However, the current excessive acquisition cost associated with the high-spatial and hyperspectral data suggest that this technology is not suitable for multi-temporal and time-series analysis of grass senescence at the landscape scale. The provision of free quality data from optical remote sensing sensor, like the Landsat 8 and Sentinel 2, therefore, present new opportunities for objective estimation of grass senescence in a spatial scale complementary to the spatial extents of the rangelands. Besides the adequate resolutions and being readily available, the Sentinel 2 instrument also captures the Red-Edge Position of the spectrum (Sibanda *et al.* 2019), and this can benefit the characterization of rangeland resources even during senescence. It is believed that the availability of the Red-Edge Position in Sentinel 2 has contributed to its superior performance (96.18%) over Worldview 2 (94.44%) and Landsat 8 (91.67%) in separating *Festuca costata* and *Themeda triandra* grasses during the winter season (Shoko and Mutanga 2017b). Certainly, this will improve the monitoring of rangeland resources even by resource limited countries who can barely live up to the price of the high-spatial and hyperspectral sensors.

Furthermore, the recent launch of Sentinel 3 satellite instrument by the European Space Agency (ESA) is a great step towards achieving subcontinental monitoring of grass senescence. Despite the averaged spatial properties, Sentinel 3 data, with high temporal resolution, will promote time-series analysis which is required to detect grass senescence. Again, the utility of sophisticated and robust time-series modeling techniques such as TIMESAT and the piecewise regression with a breaking point (Liu *et al.* 2013) together with quality satellite data (e.g., Sentinel 2 and Landsat 8) can optimize the accuracy of grass senescence estimation at the landscape scale. However, for the sustainability of forage resource management efforts based on remote sensing, the current study expand on the proposal made by Dube *et al.* (2016) and

Dube *et al.* (2017), which seeks to accelerate the discussion on the issue of trade-offs between sensor type, resolution, data cost and the application scale. Future studies should try to close this scientific knowledge gap by testing the utility of time-series analysis techniques in modelling grass senescence based on spatial scales that are reasonable to the spatial extents of the rangelands. Other studies could also investigate the magnitude of decline in rangeland foraging resource quality and quantity because of senescence. Again, the role of environmental variables in influencing the occurrence of autumn senescence in grasslands is largely unknown. The findings of such studies will help contribute towards developing sound-based decision support systems for monitoring rangelands grazing resources in the face of global change and anthropogenic impacts.

2.8 Conclusion

The present study has provided an overview of remote sensing techniques for characterizing grass senescence with associated challenges and opportunities. Senescence is an important phenological stage in herbaceous vegetation that determines not only the availability and quality of forage but rather its distribution and allocation. Unlike the use of conventional methods, remote sensing provides non-destructive and cost-effective ways of estimating grass senescence at the landscape scale. Remote sensing efforts on grass senescence depend on monitoring the changes in biochemical and physiological components of the grass during this stage. However, remote sensing derivatives such as the NDVI have not always provided reliable means of characterizing grassland autumn senescence. More so, this review has revealed that grass senescence estimation efforts based on remote sensing approaches have not been up to speed with advancements in remote sensing sensor technology. On the other hand, the adoption of sophisticated and robust time-series analysis techniques like TIMESAT and the piecewise linear regression with a breaking point jointly with improved quality data from the Sentinel 2 and Landsat 8 sensing instruments could improve the estimation of grass senescence at the rangeland scale. The results presented in this study are particularly important to forage production and remote sensing community as they add value to efforts of foraging resource monitoring and management through remote sensing methods.

Chapter Three

3 Assessing the effect of senescence on mesic sub-tropical grass quality and quantity using *in-situ* and Sentinel-2 data

The chapter is based on:

Royimani L., Mutanga, O., Sibanda, M., Dube, T. & Slotow, R. Assessing the effect of senescence on mesic sub-tropical grass quality and quantity using *in-situ* and Sentinel-2 data. (**Submitted to a Journal**).

Abstract

Forage quality is one of the most important factors that determine the distribution and grazing patterns of the livestock. During senescence many herbaceous plants lose nutrients from the leaves to the roots, and, thus, making them unavailable for grazing. This study sought to quantify the amount of decline in nGongoni (*Aristida junciformis*) grass quality and quantity owing to senescence using *in-situ* and Sentinel 2 data and the Random Forest Regression. Also, it assessed forage availability status at pre-senescence and senescence stages based on the Dry Matter content (DM) of the grass. Chlorophyll content and biomass of the grass were used as surrogates for quality and quantity during pre-senescence and senescence stages, respectively, while averaged biomass values were used to determine DM contents. The adopted Random Forest yielded coefficients of determination (R^2) of 91.3 and 96.6% as well as Root-Mean-Square-Errors (RMSEs) of 2.12 and 0.55 µg Chl/cm^2 for grass quality during pre-senescence and senescence, respectively. Again, the model obtained an R^2 of 70.9 and 94.2% together with RMSEs of 0.34 and 0.02 kg/m^2 when predicting grass quantity at pre-senescence and senescence stages, respectively. Optimal predictions of grass quality and quantity, both, at pre-senescence and senescence stages were generally achieved with the Red-Edge and its associated indices jointly with the Near Infrared (NIR) and red band derivatives. There was a remarkable decrease in both quality (17.2 µg Chl/cm^2) and quantity (0.89 kg/m^2) of the grass because of senescence. A total of 68.5 and 78.2 %/m^2 DM content was reported for pre-senescent and senescent nGongoni grasses. These findings provide a novel, robust and cost-effective approach for understanding the quality and quantity of foraging resources during dry seasons using *in-situ* and Sentinel 2 data. This is vital to understand variability in forage quality and quantity through space and time, which is necessary to facilitate the adoption of appropriate livestock management measures, particularly by communal livestock farmers to sustain their livestock production systems with minimal additional production inputs.

Keyword: Forage quality and quantity, grazing, livestock, random forest, senescence, sentinel-2.

3.1 Introduction

Senescence is one of the most important processes that govern the quality and quantity of free-ranging livestock feed (Yang and Udvardi 2018). This is primarily the case in communal rangelands where common commercial forage quality enhancement inputs, such as fertilizer

applications, installation of irrigation systems, as well as the adoption of effective livestock control measures, are not available due to the husbandry model and resource constraints, among others (Brown and Shrestha 2000). Several studies have noted that during senescence, plants lose nutrients from the tiller parts to the roots (Gao and Li 2015; Guo and Gan 2014; Sarath *et al.* 2014). For instance, Cole *et al.* (2014), observed that during senescence, chemical properties like nitrogen, starch, and glucose are reversed from the leaves, and, thereby, leaving the cellulose and lignin dominating the canopy. Lignin and cellulose are indigestible structural parts of the leaves with minimal contributions to the plant nutrients and grazing requirements (Stichler 2002). Similarly, Yang and Udvardi (2018) noted a 61% decrease in nitrogen content from matured switchgrass (*Panicum virgatum*) leaves due to senescence. Rawnsley *et al.* (2002), also observed a significant decline in cocksfoot (*Dactylis glomerata* L.) grass quality because of senescence. According to Royimani *et al.* (2021), the impact of this phenomenon is dominant in sourveld grazing areas as opposed to the other veld types such as mixed- and sweetveld due to the year-round low grass nutrients associated with high rate of leaching. Given the widespread distribution of unpalatable grasses in sourveld grazing areas (Scott-Shaw and Escott 2011; Oudtshoorn 1999), partly because of selective grazing, this may create problems of forage deficiencies, particularly during the later stages of senescence. Certainly, there is a need for accurate measuring techniques to characterize the impact of autumn senescence on communal forage quality and availability. However, accurate, objective, and comprehensive means of estimating rangeland senescence in general, as well as the magnitude of decline in nutrients thereafter, are yet to be established.

Traditional methods for gathering data on plant senescence such as visual scoring of leaf coloration and Soil Plant Analysis Development (SPAD) chlorophyll meter are often regarded as laborious, time-consuming, and inappropriate for optimal rangeland assessments, due to compromised repeatability and limited areal extent (Laliberte *et al.* 2007; Adamsen *et al.* 1999). Alternatively, remote sensing allows for reliable and cost-effective means to monitor the dynamics in plant physiology and phenology in periods such as the senescence stage (Royimani, *et al*. 2022; Santos *et al.* 2010; Di Bella *et al.* 2004). In addition, remote sensing techniques provide repeated coverage (Royimani *et al.* 2019a), which is required to support time series analysis, hence, the opportunity to examine forage quality and quantity at various stages of senescence. Laliberte *et al.* (2007), successfully separated fractional cover components between senescent and green vegetation using high image resolution photography and the object-based image analysis techniques. Berdugo *et al.* (2013), also explained the

delays in wheat (*Triticum aestiuum* L.) senescence due to fungal infections using non-invasive sensing instruments (i.e., spectral reflectance, vegetation indices, chlorophyll fluorescence, and infrared thermography). Likewise, Santos *et al.* (2010) discriminated between pre-senescent, senescent, and dead tree leaves using hyperspectral remotely sensed data and univariate analysis of variance. Bremer *et al.* (2011) further demonstrated the contributions of the Normalised Difference Vegetation Index (NDVI) in explaining the visual quality of the turf-grasses. Their findings showed that the red band was superior to NDVI in describing turf-grass quality. More so, the recently launched broadband multispectral Sentinel 2 has yielded reasonable accuracies in estimating plant quality (i.e., fertilizer nutrients) and biomass (Sibanda *et al.* 2015). This can be attributed not only to their improved spatial and spectral properties, but also to the availability of the Red-Edge Position, which is sensitive to changes in plant vigor (Sibanda *et al.* 2015). The provision of readily available data from the broadband multispectral sensors like Sentinel 2 can, therefore, benefit the ongoing assessment of foraging resources at the landscape scale.

In addition, the adoption of non-parametric machine learning approaches like Random Forest, which are robust, has improved the characterization of vegetation traits like chlorophyll and biomass even on multispectral remote sensing datasets (Mutanga *et al.* 2012). These algorithms operate by creating subsets in the dataset to promote spectral distinctiveness of different features, hence, optimal prediction (Royimani *et al.* 2019a). For instance, the Random Forest uses the bagging (bootstrap) approach to create multiple decision trees from a given dataset, and averages the outcome based on the majority vote for classification while using the mean or median in regression (Odindi *et al.* 2016; Mutanga *et al.* 2012; Adelabu and Dube 2015). Several studies have demonstrated the strengths of the Random Forest technique in explaining plant foliar chlorophyll and biomass (Sonobe *et al.* 2020; Shah *et al.* 2019; Zhou *et al.* 2016; Mutanga *et al.* 2012). Again, unlike the parametric techniques such as the linear regression which assumes normality in the distribution of the data, the Random Forest is robust and does not suffer from the effect of overfitting (Odebiri *et al.* 2020). More so, Random Forest is fast, stable, and easy to implement (Abdel-Rahman *et al.* 2014; Odindi *et al.* 2014; Chan and Paelinckx 2008). Equally, many studies have used leaf chlorophyll, which is measurable through remote sensing means, as an indicator of plant health and quality (Ramoelo *et al.* 2015; Berdugo *et al.* 2013; Adamsen *et al.* 1999), while biomass has been used as a proxy for quantity (Sibanda *et al.* 2015 Skidmore *et al.* 2010; Mutanga and Skidmore 2004).

Despite this knowledge, the examination of grass nutrient decline following senescence, particularly to understand the quantity and quality of the last standing forage at later stages of senescence, using remote sensing methods, is still limited. Such information is required to provide a better understanding of resource availability and quality in a spatially and temporally explicit manner. This information is also critical for sustainable maintenance of livestock stocking rates and rangeland integrity during critical times of forage production. Furthermore, assessing forage quality across the senescence period is an important consideration for analyzing the behavior of the livestock feed (Molle *et al.* 2009). Therefore, the present study aimed at quantifying the magnitude of decline in nGongoni (*Aristida junciformis*) grass quality (i.e., chlorophyll) and quantity (i.e., biomass) owing to senescence, using *in-situ* and Sentinel-2 data and the Random Forest Regression model. To achieve this objective, the study estimated and compared the chlorophyll content and biomass of the nGongoni grass at pre-senescence and senescence stages. The study further examined the availability status of forage from the nGongoni grass in terms of Dry Matter (DM) during pre-senescence and senescence periods. The nGongoni grass was considered in this study because of its widespread distribution in the area (Scott-Shaw and Escott 2011), hence the main source of animal feed, especially during critical times of forage production when all the other patchy palatable grasses have been selectively grazed. It was, therefore, hypothesized, that the decline in nGongoni grass quality following senescence could be explained using the associated decrease in its leaf chlorophyll content, while quantity could be estimated based on its live-standing above-ground biomass.

3.2 Methods and materials

3.2.1 Sampling design and field data collection

A purposive sampling approach was employed, as detailed in Royimani *et al.* (2019b), to locate a total of 80 plots at 150 m distance apart. The centre coordinates of the plots were taken for traceability in future site visits. The size of each plot was 10m * 10m and these were located within larger homogenous grass patches of about 15m * 15m to cater for any possible pixel geo-location mismatch with the Sentinel 2 image. In each 10m * 10m plot, three quadrants of 50cm * 50cm in size were randomly established. Chlorophyll content readings and live-standing above-ground biomass of the nGongoni grass were measured in these 50cm * 50cm quadrants between the 20th and 23rd of March and 2nd and 7th of September 2020 to represent the pre-senescent (figure 2(a)) and senescent (figure 2(b)) grasses, respectively. During March, grass chlorophyll was believed to be at maximum due to maturity while at minimum in

September because of dormancy in the temperate regions of the study site (Figure 1.1). Chlorophyll content measurements were taken using the SPAD-502 Plus. To minimize possible errors in the values of pre-senescent chlorophyll content, measurements were only taken on grasses that were fully grown, while no specific considerations were made when sampling during senescence stage. All the grasses in the 50cm * 50cm quadrant were clipped and rapped using brown paper bags for estimation of wet and dry live-standing above-ground biomass. Both, the pre-senescent and senescent clipped grasses were separately measured for fresh weight, herein referred to as wet biomass, using a calibrated scale. Next, the clipped grass samples were oven-dried at 105^{o}C for 72 hours (Shreve *et al.* 2006) and weighed using the calibrated scale to determine the dry biomass and the outcomes were expressed as kilograms per square meter (kg/m^2).

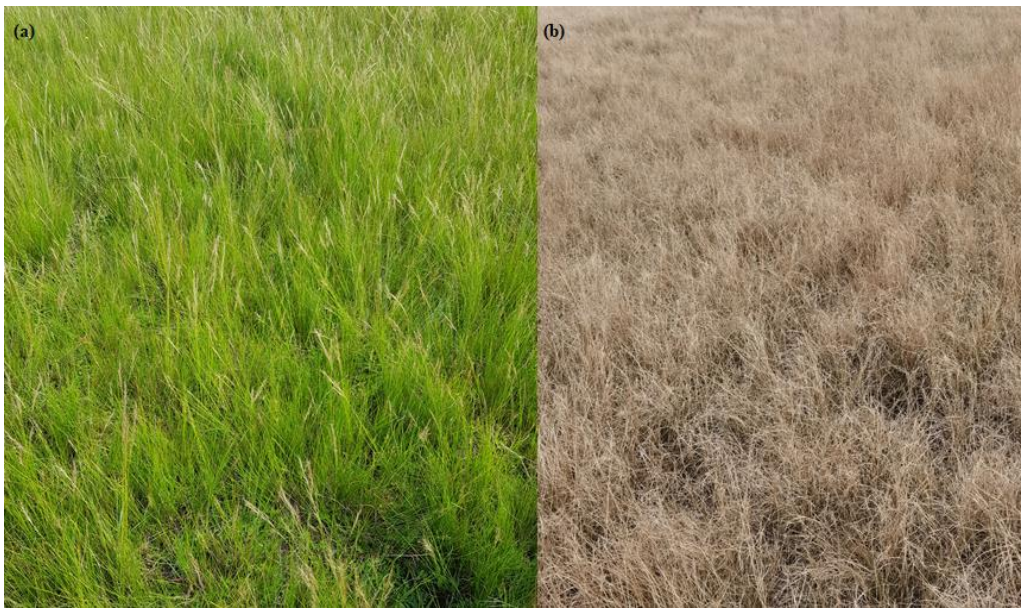

Figure 3.1 Photos of the nGongoni grass taken on the 22nd of March and 3rd of September 2020 in the study site to illustrate the conditions of the pre-senescent (a) and senescent (b) grasses, respectively.

3.2.2 Image acquisition

Two pre-processed Sentinel 2 images were downloaded from the Copernicus Open Access Hub using Quantum GIS (QGIS). The first image was acquired on the 20th March 2020 and represented the pre-senescence period while the second one on the 3rd September 2020 to represent the senescence phase. The choice of using Sentinel 2 data was determined by several factors, which include the free availability, extensive extent, improved resolution, and the coverage of the Red-Edge Position, among others. Similarly, numerous studies (i.e., Sibanda

et al. 2015; Shoko and Mutanga 2017a; Frampton *et al.* 2013) have explained dynamics in the physiological and biochemical properties of the vegetation, including grasses, using the Sentinel 2 data with satisfactory accuracies. However, bands 1, 9, and 10 were excepted from this study due to their insignificant contributions to vegetation assessments and analysis (Shoko and Mutanga 2017a).

3.2.3 Vegetation indices

The optimal performance of vegetation indices in characterizing vegetation attributes using remotely sensed data has been widely demonstrated (Royimani *et al.* 2019b; Sibanda *et al.* 2015; Frampton *et al.* 2013). In addition to the popular NDVIs (i.e., the traditional NDVI and the NDI45), several other NDVIs were computed in this study using the combination of different wavebands located in the Red-Edge Position, with the red band centred in the Visible region (Table 3.1). In addition, the Pigment Specific Simple Ratio (PSSR), Terrestrial Chlorophyll Index (TCI), Inverted Red-Edge Chlorophyll Index (IRECI), Green Normalised Difference Vegetation Index (GNDVI), as well as the Normalized Difference Red Edge ($NDVI_{705}$) were generated and considered in this study based on their optimal performance when estimating plant chlorophyll and biomass (Frampton *et al.* 2013; Sibanda *et al.* 2015; Mutanga *et al.* 2012; Matongera *et al.* 2017).

3.2.4 Statistical analysis

Field-measured chlorophyll and live-standing above-ground biomass of the nGongoni grass were tested for normality using the Shapiro-Wilk test. The requirement was to understand the extent to which the data deviated from the normal distribution curve as described in Sibanda *et al.* (2017b). Also, correlation tests were conducted between field-measured variables (i.e., chlorophyll and biomass) and the raw Sentinel 2 bands as well as between field-measured data and the vegetation indices using the cor.test function in R. In preparation for the establishment of the Random Forest Regression models, the various datasets were randomly split into 70% and 30% for training and testing purposes, respectively. The performance of the Random Forest models was validated based on the Root Mean Square Error (RMSE) and coefficient of determination (R^2) with combined highest R^2 and lowest RMSE values showing best performance and vice versa.

Table 3.1 Vegetation indices that were calculated in the present study.

Vegetation index name	Abbreviation	Standard formula	Bands used
Normalized Difference Vegetation Index	NDVI	(NIR − Red)/(NIR + Red)	(Band 8 − Band 4)/(Band 8 + Band 4)
Normalized Difference Vegetation Index	NDI45	(RE − Red)/(RE + Red)	(Band 7 − Band 4)/(Band 7 + Band 4)
Normalized Difference Vegetation Index	NDVI B5	(RE − Red)/(RE + Red)	(Band 5 − Band 4)/(Band 5 + Band 4)
Normalized Difference Vegetation Index	NDVI B6	(RE − Red)/(RE + Red)	(Band 6 − Band 4)/(Band 6 + Band 4)
Normalized Difference Vegetation Index	NDVI B8a	(RE − Red)/(RE + Red)	(Band 8a − Band 4)/(Band 8a + Band 4)
Terrestrial Chlorophyll Index	TCI	(RE − RE)/(RE − Red)	(Band 6 − Band 5)/(Band 5 − Band 4)
Inverted Red-Edge Chlorophyll Index	IRECI	(NIR − Red)/(RE1/RE2)	(Band 8 − Band 4)/(Band 5/Band6)
Pigment Specific Simple Ratio	$PSSR_a$	(NIR/Red)	(Band 8/Band 4)
Green Normalised Difference Vegetation Index	GNDVI	(NIR − G)/(NIR + Green)	(Band 8 − Band 3)/(Band 8 + Band 3)
Normalized Difference Red Edge	$NDVI_{705}$	$(R_{750} - R_{705})/(R_{750} + R_{705})$	(Band 6 − Band 5)/(Band 6 +Band 5)

Footnotes: RE and Red are the spectral reflectance from the Red-Edge and the red band, respectively. NDVI B5, NDVI B6, and NDVI B8a represents the NDVIs calculated using band 5, 6 and 8a with the red band, respectively.

3.2.5 Random Forest model establishment and optimization

Four sets of the Random Forest Regression model were built on R version 4.0.5 to predict the quality and quantity of the nGongoni grass during pre-senescence and senescence phenological stages, respectively (Figure 3.2). The Random Forest is an ensemble machine learning algorithm that explains and predicts parameters using measured-field variables (Odebiri *et al.* 2020). In operation, it uses the bagging (bootstrap) approach to construct multiple decision trees from a given set of predictors (i.e., Sentinel 2 bands and vegetation indices in the present case) and averages the outcome (Mutanga *et al.* 2012). The bootstrap aggregation function helps in reducing the variance error emanating from the decision trees. A splitting point,

otherwise known as a node, is defined based on field-measured data (i.e., biomass and chlorophyll) and the associated thresholds that retain the most matching partitions. At each splitting point, predictor variables and their associated thresholds are tested for possible selection, and, hence, determination of the best split.

In the present study, the process of data analysis was divided into four stages (Figure 3.2):
In stages 1 and 2 (i.e., models one and two), we tested the potential of the Sentinel 2 data in explaining grass quality during pre-senescence and senescence based on the March and September field-measured nGongoni grass chlorophylls, respectively, as surrogates. Due to the closure of the laboratories as a results of the national shutdown associated with Covid19 in South Africa, experimental analysis of grass nutrients could not be conducted. Therefore, we adopted chlorophyll as an indirect measure of grass quality. Two Random Forest Regression models were built to evaluate the bands of the Sentinel 2 jointly with derived vegetation indices in separately explaining grass quality during these two periods. Likewise, in stages 3 and 4 (i.e., models three and four), we explored the capability of the Sentinel 2 data in predicting grass quantity during pre-senescence and senescence using the live-standing above-ground biomass of the nGongoni grass (Figure 3.2). Again, two Random Forest Regression models were established to individually assess the Sentinel 2 bands together with subsequent indices in describing grass quantity over the pre-senescence and senescence stages.

In the preliminary analysis stages, we fitted all the variables (i.e., Sentinel 2 bands and vegetation indices) in the respective models, and the variable importance ranking was done to establish the best performing variables for the final and optimal predictions of the grass quality and quantity. The variable importance ranking was done based on the out of bag (OOB) error rating and the outputs (Mean Decrease Accuracies) were expressed in percentage. To identify the best performing variables, the models were individually and repeatedly executed while altering their *ntree* and *mtry* values until the highest R^2 and the lowest RMSE values were obtained. Tested *mtry* values ranged from 2 to 16 while *ntree* were between 100 and 2000. On the other hand, the *nodesize* was set to 1 throughout the analysis. The *ntree* is the number of trees built based on the bootstraps of the explanatory variables with a default value of 500 (Odebiri et al. 2020), while the *mtry* is the number of predictors tried at each node and has a default value of 1/3 of all the variables used in case of regression (Mutanga *et al.* 2012). On the other hand, the *nodesize* is the lowest size of the terminal nodes of the trees in the regression and it has a default value of 1 (Mutanga *et al.* 2012). Using the predicted forage quality and

quantity values and the Inverse Difference Weighted interpolation technique in ArcGIS, we produced the predicted forage quality and quantity maps for the pre-senescence and senescence periods in the study site.

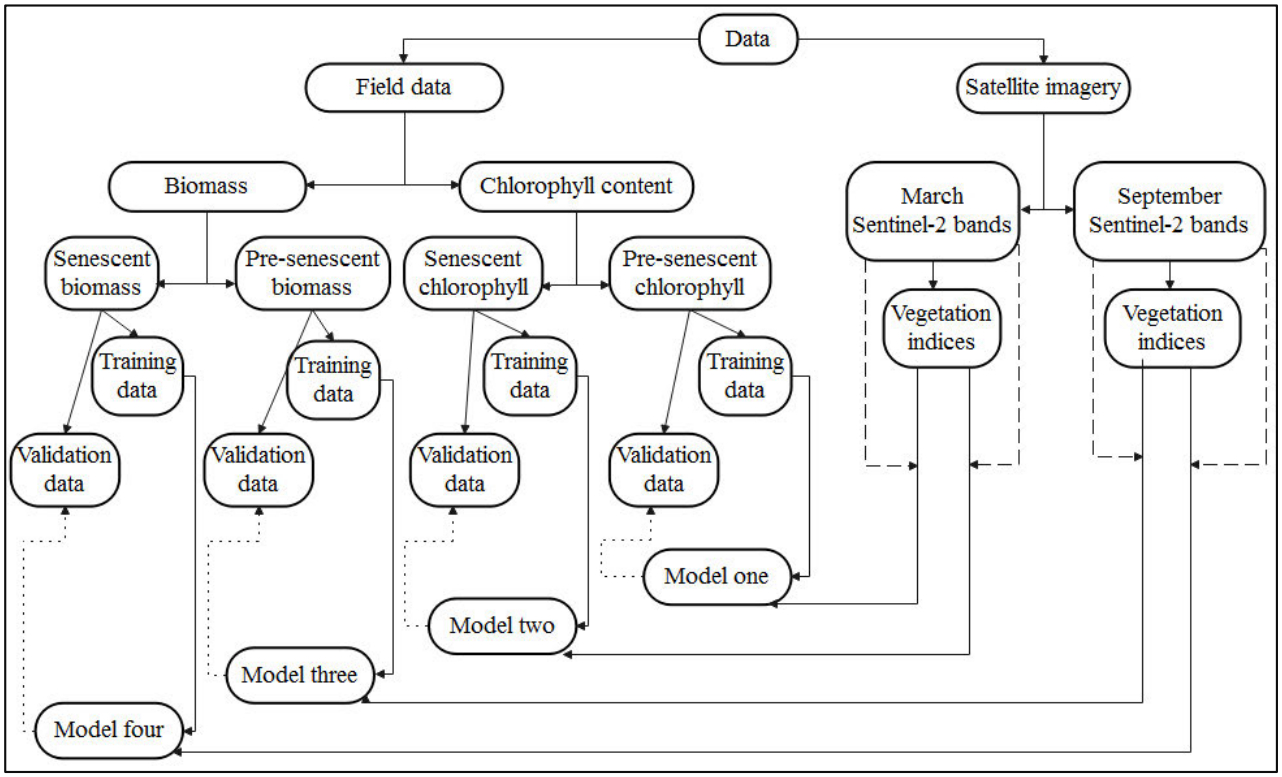

Figure 3.2 Data analysis framework adopted in estimating the quality and quantity of the nGongoni grass at pre-senescent and senescent stages.

3.2.6 Forage availability status from the pre-senescent and senescent nGongoni grasses

Currently, there are no established Thresholds of Potential Concern (TPC) to understand the status of availability in forage from a chlorophyll and biomass perspective. Therefore, to determine the amount of available forage from the nGongoni grass during the pre-senescent and senescent stages, we adopted the quantification of the DM content for these two periods. The formula for computing DM content is given in equation (3.1):

$$\text{DM}\ (\%/\text{m}^2) = \frac{\text{Dry Weight}}{\text{Wet Weight}} * 100 \quad \text{.....(3.1)}$$

where Dry Weight is the averaged weight of the grass biomass after oven drying while Wet Weight is the averaged weight of the fresh field-harvested biomass before oven drying. This approach (Equation 3.1) divides the mean weight of the sample after oven drying by the mean

weight of the sample before oven drying and multiplies the output by one hundred to get the DM content in percentage (Shipley and Vu 2002; De Waal 1990).

3.3 Results

3.3.1 Descriptive statistics

Descriptive statistics of the pre-senescent and senescent nGongoni grass quality and quantity as well as for the combined datasets (i.e., n = 160) are shown in Table 3.2. The quality varied between 2.50 and 33.50 and between 1.70 and 14.30 µg Chl/cm^2, for the pre-senescent and senescent grasses, respectively. The pre-senescent and senescent nGongoni grass quantity, on the other hand, varied between 0.98 and 3.40 and between 0.64 and 1.41 kg/m^2, respectively. The averaged grass quality during pre-senescence was 24.52 µg Chl/cm^2 while 7.34 µg Chl/cm^2 at senescent stage. Also, the averaged quantity varied between 2.11 and 1.22 kg/m^2 for the pre-senescent and senescent grass, respectively. Both, the pre-senescent and senescent quality content readings were higher than the quantity observations, with higher Standard Deviations (StDev) (Table 3.2).

Table 2.2 Pre-senescent and senescent chlorophyll content and biomass of the nGongoni grass.

Variables	No. of samples	Minimum	Maximum	Mean	StDev
Quality					
Pre-senescent Chl (µg Chl/cm^2)	80	2.50	33.50	24.52	8.48
Senescent Chl (µg Chl/cm^2)		1.70	14.30	7.34	3.13
Quantity					
Pre-senescent biomass (kg/m^2)	80	0.98	3.40	2.11	0.65
Senescent biomass (kg/m^2)		0.64	1.41	1.22	0.10
Combined variables					
Chl (µg Chl/cm^2)	160	1.70	33.50	15.93	10.71
Biomass (kg/m^2)		0.64	3.40	1.67	0.64

Footnotes: Chl = chlorophyll, StDev = Standard Deviation.

3.3.2 Correlation between field-measured and spectral variables

Table 3.3 illustrates the magnitude of agreement between field-measured (i.e., chlorophyll and biomass) and Sentinel 2 (i.e., spectral bands and vegetation indices) variables for the pre-senescent and senescent grasses. Generally, the study displayed a good positive relationship between the tested variables, both, at pre-senescent and senescent phenological stages. For instance, all the Sentinel 2 bands showed a good correlation with the quality and quantity of

the grass during pre-senescence. In addition, forage quality and quantity showed a good relationship, both, at pre-senescence (0.79) and senescence (0.77) stages.

Table 3.3 Correlation between Sentinel 2 variables and biomass as well as chlorophyll content of the nGongoni grass.

Variables	Pre-senescent Chl	Senescent Chl	Pre-senescent Biomass	Senescent Biomass
Raw bands				
Band 2	0.66	0.68	0.66	0.75
Band 3	0.72	0.76	0.73	0.82
Band 4	0.56	0.75	0.57	0.82
Band 5	0.72	0.84	0.75	0.91
Band 6	0.85	0.88	0.83	0.93
Band 7	0.86	0.89	0.83	0.93
Band 8	0.81	0.86	0.81	0.91
Band 8a	0.86	0.89	0.84	0.94
Band 11	0.65	0.73	0.66	0.78
Band 12	0.53	0.50	0.56	0.52
Vegetation indices				
$PSSR_a$	0.89	0.65	0.85	0.67
IRECI	0.70	0.37	0.63	0.37
MTCI	0.64	-0.08	0.63	-0.06
NDVI	0.83	0.72	0.74	0.78
NDVI B5	0.74	0.43	0.76	0.68
NDVI B6	0.93	0.62	0.84	0.66
NDI45	0.92	0.63	0.81	0.66
NDVI B8a	0.91	0.64	0.83	0.68
GNDVI	0.75	0.69	0.74	0.76
$NDVI_{705}$	0.74	0.73	0.73	0.77

In addition, at senescent stage, all the Sentinel 2 bands displayed reasonable correlations with either the quality or the quantity of the grass. Furthermore, the relationship between the calculated vegetation indices and the quality and quantity of the nGongoni grass at pre-senescence was significant. However, during senescence, the IRECI demonstrated poor correlations with either the quality or the quantity of the grass under investigation in the present study. Also, the MTCI showed a negative correlation with the quality and quantity of the nGongoni grass during pre-senescent and senescent stages.

3.3.3 Pre-senescent and senescent grass quality and quantity estimation using Sentinel 2 data

The Random Forest Regression models used in predicting the quality and quantity of the nGongoni grass in the present study yielded satisfactory results (Table 3.4). In stage one, which was the prediction of grass quality at the pre-senescent stage, the model obtained an RMSE of 2.12 µg Chl/cm^2 and an R^2 of 91.3%, while in stage two, which was the assessment of senescent grass quality, an RMSE and R^2 of 0.55 µg Chl/cm^2 and 96.6% were acquired, respectively. When explaining the quantity of the grass at pre-senescent stage, in stage three, the model reported an RMSE of 0.34 kg/m^2 and an R^2 of 70.9%. The fourth model, which evaluated grass quantity at senescent stage, recorded an RMSE and an R^2 of 0.02 kg/m^2 and 94.2%, respectively.

Table 3.4 Estimation accuracies of the nGongoni grass quality and quantity and the associated *ntree* and *mtry* values.

Stage of analysis	Model name	Model description	*ntree*	*mtry*	RMSE	R^2 (%)
1	Model one	Pre-senescent quality	100	6	2.12 (µg Chl/cm^2)	91.3
2	Model two	Senescent quality	300	8	0.55 (µg Chl/cm^2)	96.6
3	Model three	Pre-senescent quantity	200	8	0.34 (kg/m^2)	70.9
4	Model four	Senescent quantity	500	6	0.02 (kg/m^2)	94.2

After model optimization, prediction accuracies for the quality and quantity of the nGongoni grass at pre-senescent and senescent stages improved slightly (Figure 3.3). For instance, the optimal model for predicting grass quality during the pre-senescent phase yielded an R^2 of 92.9% and an RMSE of 1.91 µg Chl/cm^2 (Figure 3.3(a)). The predictive power of the model was boosted by the use of $PSSR_a$, Band 6, NDVI B6, Band 7, as the most important variables (Figure 3.4(a)). Equally, the optimal model that estimated grass quality during senescence exhibited an RMSE of 0.48 µg Chl/cm^2 and an R^2 of 97.4% (Figure 3.3(b)), with the Red-Edge Position (i.e., Band 7, 8a, 6, and 5), jointly with the Visible red band and the NIR, emerging as the most important regions (Figure 3.4(b)). Furthermore, optimum prediction of the nGongoni grass quantity during pre-senescence was explained by the $PSSR_a$, Band 8a, Band 6, NDVI B8a, (Figure 3.4(c)) as the most important variables. Again, an RMSE and an R^2 of 0.34 kg/m^2 and 71.1% were obtained, respectively (Figure 3.3(c)). Also, the optimal model that estimated

grass quantity during senescence produced an RMSE of 0.02 kg/m^2 and an R^2 of 96.1%. It can be observed that the NDVI B5, Band 6, Band 5, Band 7, NDVI B6, $PSSR_a$, and the Visible red band, in order of importance, were the most important variables when explaining the quantity of senescent grass (Figure 3.4(d)).

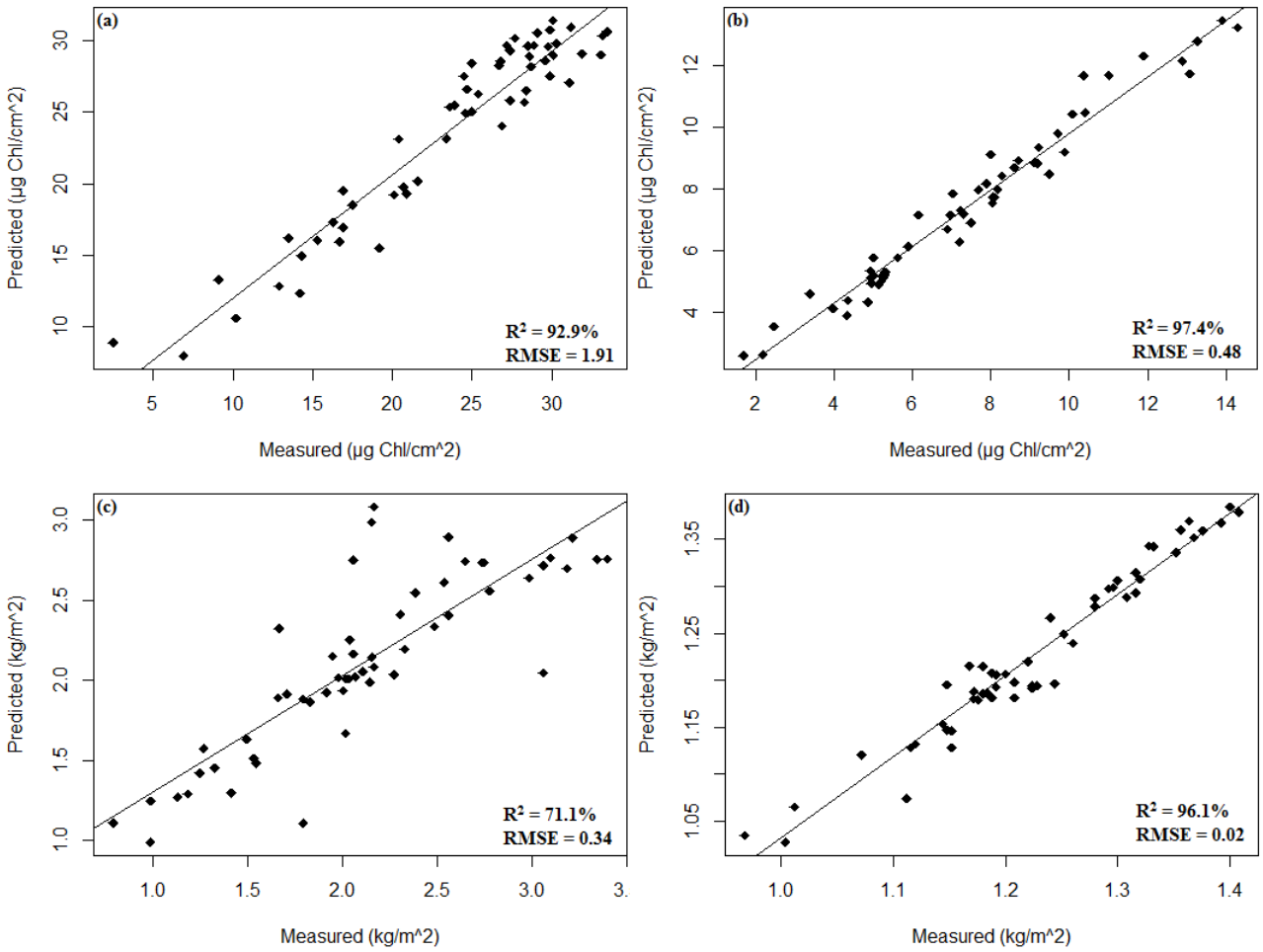

Figure 3.3 Relationship between measured and predicted nGongoni grass quality during the (a) pre-senescent and (b) senescent stages as well as quantity over the (c) pre-senescent and (d) senescent periods.

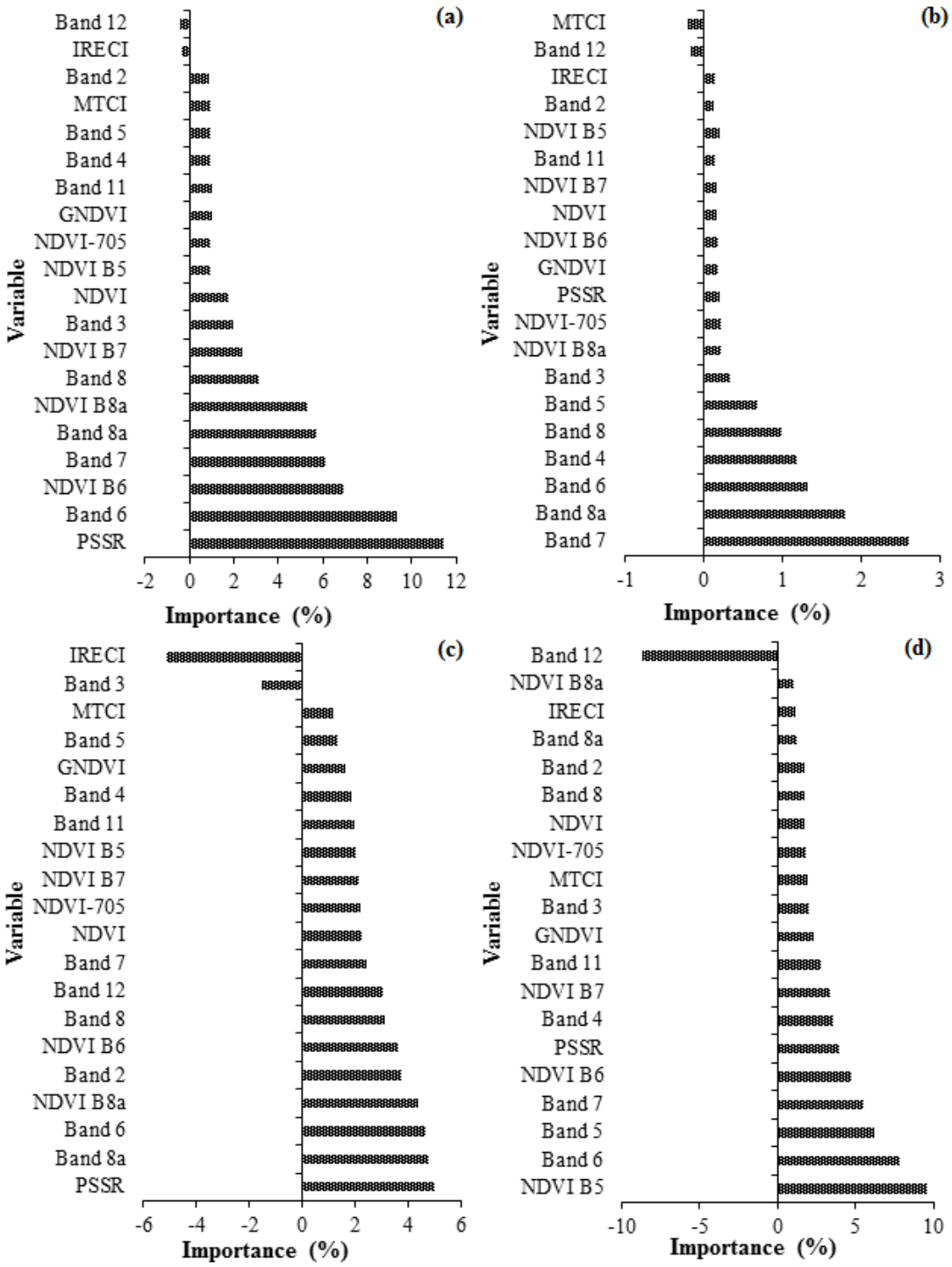

Figure 3.4 Variable importance ranking for the estimation of the nGongoni grass quality during the (a) pre-senescent and (b) senescent stages and quantity during the (c) pre-senescent and (d) senescent periods.

3.3.4 Decline in grass quality and quantity due to senescence and forage availability status

Figure 3.5 illustrates the averaged quality and quantity of the nGongoni grass measured on the field during the pre-senescent and senescent periods. Based on the figure (Figure 3.5), the maximum quality and quantity of the nGongoni grass at pre-senescence were 24.52 µg Chl/cm^2 and 2.11 kg/m^2, respectively. As a result of senescence, the quality and quantity of the nGongoni grass dropped substantially (i.e., 17.18 µg Chl/cm^2 and 0.89 kg/m^2) to 7.34 µg Chl/cm^2 and 1.22 kg/m^2. Besides, figure 3.5(a) and (b) shows that there was a greater reduction in quality than there was in quantity of the nGongoni grass because of senescence. With regards to the percentage DM and moisture contents of the nGongoni grass, a total of 68.5 and 78.2 %/m^2 DM as well as 31.5 and 21.8 %/m^2 moisture contents were, respectively, recorded for the pre-senescent and senescent grasses.

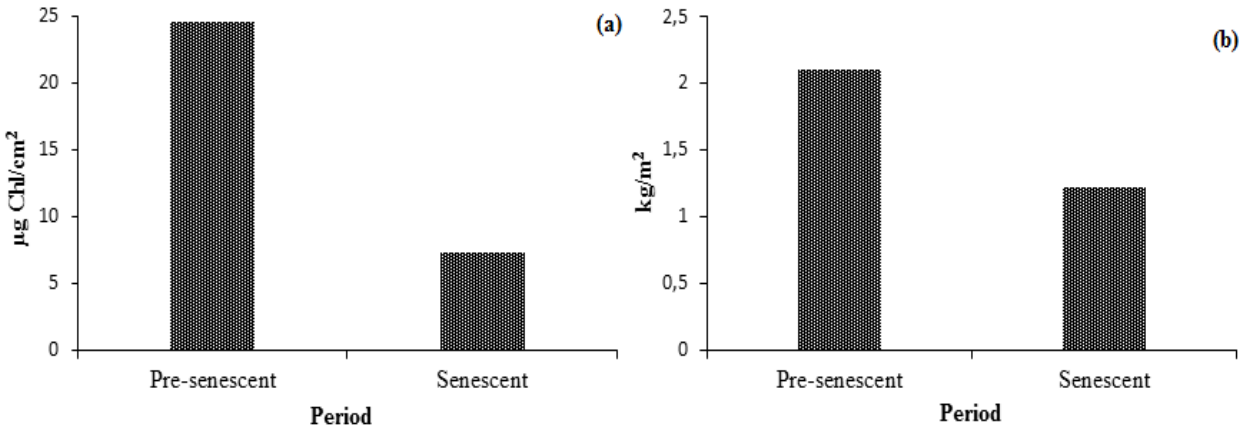

Figure 3.5 Decline in mean (a) chlorophyll content and (b) mean biomass of the nGongoni grass following senescence.

Moreover, figure 3.6 shows the spatial distribution of the predicted pre-senescent and senescent nGongoni grass quality and quantity in the study area. Specifically, figure 3.6(a) indicates that during the pre-senescent stage, high-quality grass tends to spread towards the south-eastern side of the study site, whereas the better quality senescent grass appears to be concentrated in specific areas (Figure 3.6(b)). Figure 3.6(c), also reveals that high biomass of pre-senescent nGongoni grass generally dominated the southern parts of the study area with patches in the north-western parts. It can be noted that the nGongoni grass quantity during senescence also tends to be confined in specific zones within the study site, although such a dynamic pattern was not apparent (Figure 3.6(d). However, the western, central, and north-eastern parts of the study area were generally characterized by low volumes of quality forage, both, during pre-senescent and senescent periods.

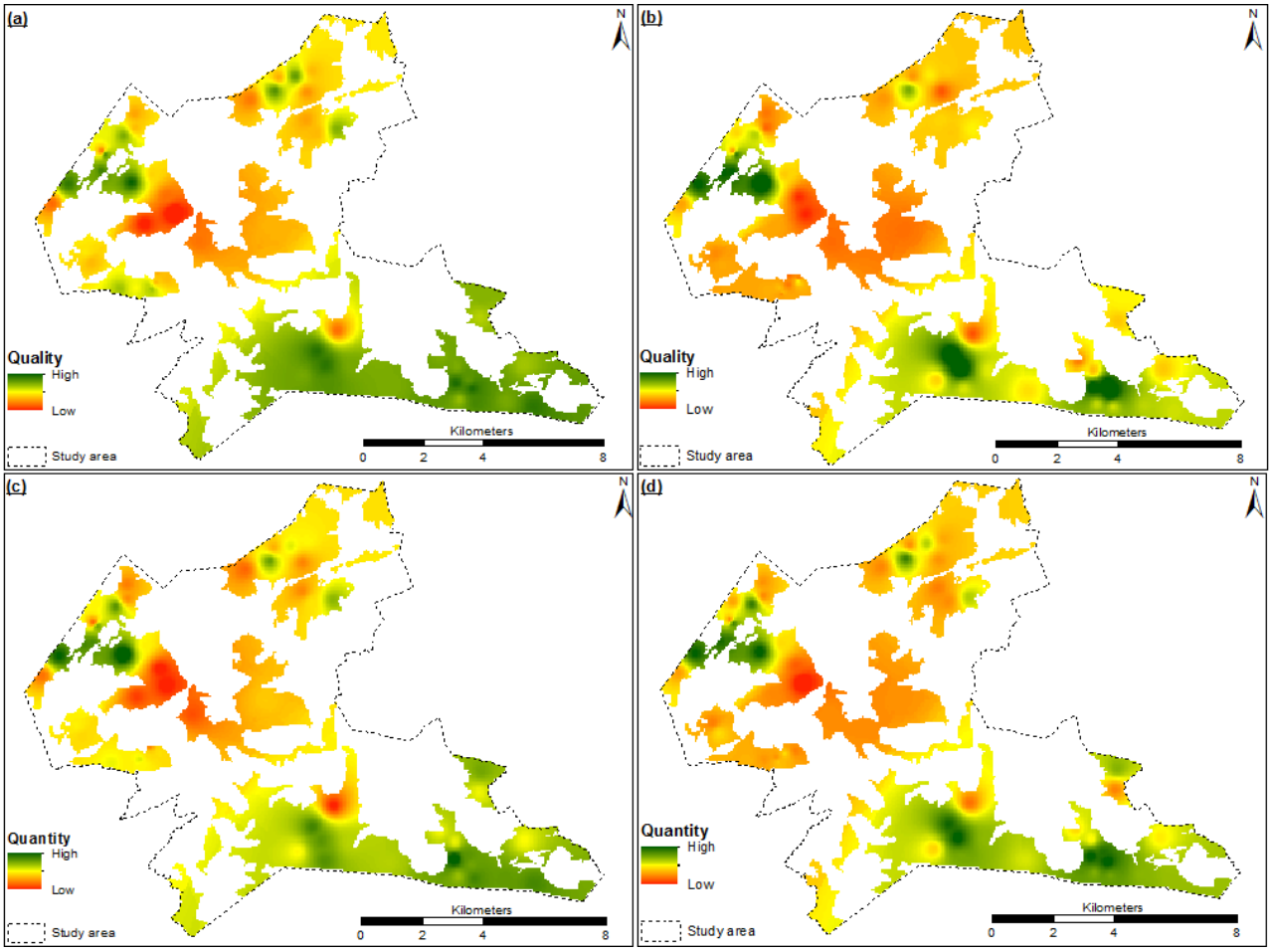

Figure 3.6 Spatial distribution of predicted grass quality at (a) pre-senescent and (b) senescent stages as well as the quantity during the (c) pre-senescent and (d) senescent periods. The empty or white spaces represent the other land use/land cover types which were masked in this study.

3.4 Discussion

3.4.1 Estimation of grass quality and quantity decline through senescence using Sentinel 2 data

The findings of this study showed that the quality and quantity of the nGongoni grass during pre-senescent and senescent phenological stages can be assessed successfully using the Sentinel 2 data, with a high degree of accuracy. Specifically, the Red-Edge Bands 6, 7, and 8a, jointly with their associated vegetation indices (i.e., NDVI B6, NDVI B7 and NDVI B8a) appeared to be the most important variables when estimating grass quality at pre-senescent stage. This could be attributed to the sensitivity of the Red-Edge Position of the spectrum to green features of the vegetation (Sibanda *et al.* 2021; Frampton *et al.* 2013), and the increased foliar chlorophyll of the nGongoni grass during pre-senescence. Sibanda *et al.* (2017b), highlighted the sensitivity of Sentinel 2's Red-Edge Position to foliar chlorophyll which is

dominant in green and healthy leaves of pre-senescent nGongoni grass. Again, the $PSSR_a$, which uses the information from the Near Infrared (NIR) and red bands, was very influential in characterizing grass quality at pre-senescence. Although the raw Sentinel 2 bands that are located in the Visible and NIR regions did not perform well in explaining grass quality at pre-senescence, the increased explanatory power of their subsequent indices ($PSSR_a$), on the other hand, could be justified by the fact that vegetation indices rely on the information from more than two wavebands (Sibanda *et al.* 2021). These results strengthen the findings from previous studies that have tested the robustness of vegetation indices derived from the Red-Edge in explaining green properties of the floral species (Sharma *et al.* 2015; Frampton *et al.* 2013; Mutanga *et al.* 2012).

More so, the poor performance of the Shortwave Infrared (SWIR) region observed when predicting foliar chlorophyll is not uncommon in remote sensing studies of plant pigment estimation (Sibanda *et al.* 2021). This is because the SWIR is sensitive to structural components and water content of the plants (Hunt Jr *et al.* 2016). Meanwhile, the relatively low predictive power of the Visible region compared to the Red-Edge in explaining grass quality at pre-senescence could be attributed to the low reflectance from the green leaves of the nGongoni grass during this period (Sims and Gamon 2002). Contrastingly, when chlorophyll content was reduced in the grass leaves because of senescence, the Visible red (Band 4) and the NIR regions along with the Red-Edge, emerged as the most important variables in explaining grass quality. The improved role of the Visible red in estimating grass quality during senescence is a consequence of the decrease in its chlorophyll, which promoted increased reflectance in this region. The spectral reflectance in the Visible red (Band 4) of the electromagnetic spectrum is known to be sensitive in dry structural features of the vegetation (Dube *et al.* 2021; Bremer *et al.* 2011) which are dominant in senescent nGongoni grass leaves (Cole *et al.* 2014).

This study further showed that the optimal estimation of grass quantity at pre-senescence was achieved using the $PSSR_a$, Band 8a, Band 6, and NDVI B8a, as the most important variables. Again, the majority of the influential variables when predicting grass quantity during pre-senescence were located in the Red-Edge and the NIR regions. During pre-senescence, the canopy of the nGongoni grass, like any other vegetation, is generally green and dominant, and that may have increased the spectral reflectance in the NIR section. Many studies have noted the sensitivity of the NIR and the Red-Edge Position jointly with subsequent indices in estimating the above-ground biomass (Shoko and Mutanga 2017a; Sibanda *et al.* 2015; Sharma

et al. 2015 Ramoelo and Cho 2014). Shoko and Mutanga (2017b), also highlighted the importance of the Red-Edge and the NIR regions of Sentinel 2 in discriminating between the C_3 and the C_4 grass species. Equally, the best prediction of the nGongoni grass quantity during senescence was achieved based on the NDVI B5, Band 6, 5, 7, NDVI B6, Visible red band, and the $PSSR_{a,}$ as the most important variables. These results highlighted the importance of the Visible red, NIR, and the Red-Edge Position of Sentinel 2 multispectral sensor in explaining the live-standing above-ground nGongoni grass quantity during senescence. This may be attributed to the widespread distribution of the hardy tufted nGongoni grasses during senescence (Wiseman *et al.* 2002), which minimizes the exposure of the soil background to the emitted radiation and subsequently the measured reflectance. Dube *et al.* (2021), also revealed a similar trend of importance of the Visible red and NIR regions of the electromagnetic spectrum when explaining above-ground grass biomass during dry seasons using the Landsat 8 multispectral instrument.

With regards to the distribution of quality in the nGongoni grass during the two senescent phenological periods under investigation in this study, our findings indicated that high-quality grasses were spread towards the southern and patchy in the north-western part of the study site during pre-senescence, while centred in specific zones during senescence. Although not dominant, a similar trend was observed with regards to the distribution of quantity of the nGongoni grass during pre-senescence and senescent periods. This implies that the southern side of the study area is generally characterized by high concentrations of quality nGongoni grasses, hence, livestock forage. Contrary, the western, central, and north-eastern sides appeared to be signified by low volumes of both quality and quantity nGongoni grasses, hence, low livestock feed. These findings also highlight an element of potential overuse of foraging resources, or rather grazing resources in bad condition, particularly in the western, central, and north-eastern parts of the study area, which were noted as closer to community residential areas. Egeru *et al.* (2019), and Oba (2012) reported that the condition of grazing fields that are close to the settlements is often poor. Again, Sun *et al.* (2011) noted that heavily grazed areas are often characterized by low grass biomass, and the proximity of the western, central, and north-eastern areas of the study site to the residential areas may have promoted increased livestock grazing there. Over and above, the strong relationship displayed between foraging resource quality and quantity suggest that, grass biomass decreases with decline in its quality.

3.4.2 Implications of the observed findings on rangeland's resource management

This study has demonstrated the magnitude of decrease in the quality and quantity of the nGongoni grass because of senescence, with a clear indication of the available forage DM content during pre-senescence and senescent stages. It is worth noting that the quality of the nGongoni grass drops substantially (17.18 µg Chl/cm^2) compared to its quantity (0.89 kg/m^2) during senescence and this may have negative implications to the availability status and conditions of the subsequent forage in the rangelands. For instance, the low-quality feed from the dry nGongoni grass during senescence may not adequately meet the dietary requirements of the grazing livestock. Generally, these results are consistent with previous studies that have confirmed plant nutrient decline following senescence (Gao and Li 2015; Guo and Gan 2014; Sarath *et al.* 2014). Over and above quantifying the magnitude of decrease in the quality of forage resources due to senescence, the study also estimated the decrease in quantity of the foraging resources. Although the DM content results give an impression that adequate forage may be available during senescence, as opposed to pre-senescent period, the is a challenge of forage quality. The hardy dry leaves of senescent nGongoni grass may not meet the grazing requirements of the livestock, unlike the green grass leaves which are known to be low in fibre and high in digestible nutrients and soluble proteins (Mutanga *et al.* 2003; Stichler 2002). Besides the quality aspect, it is also worth noting that the 78.2 %/m^2 DM content of the nGongoni grass during the senescent stage is not reflective of an increment from the pre-senescent 68.5 %/m^2 DM, but rather an indication of the lack of moisture content in senescent grass leaves. This is more challenges for rural livestock farmers who can barely afford the high cost of supplementary forage. With this knowledge, there is a need for adoption of robust models derived from Sentinel 2 data to monitor foraging resources for improved decision-making on effective stock densities and grazing approaches. This is a critical step towards understanding poverty alleviation and food security efforts, particularly in developing countries whose economies are largely dependent on the livestock farming, both, on commercial and subsistence scales (Ramoelo and Cho 2014).

3.5 Conclusion

The objective of the present study was to quantify the amount of decline in nGongoni grass quality and quantity because of senescence using *in-situ* and Sentinel 2 data. Based on the findings, it can be concluded that the Sentinel 2 data, when used in concert with the Random Forest Regression model presents not only a novel but rather a robust and effective method

towards prediction of grass quality and quantity at various stages of senescence. Despite the common notable decrease in the live-standing above-ground biomass of the vegetation with decline in quality during senescence, this study further revealed that the degree to which the quality drops is remarkable. This poses serious problems of potential insufficient forage for the livestock grazing, and, hence, requires effective management interventions to either regulate the stock densities or grazing patterns. The subsequent impact is expected to be more on rural livestock farmers who are often characterized by resource constraints in order to obtain supplementary forage. The importance of this study is not only limited to academia, but rather to the livestock farmers in general and to the communal livestock farmers in particular, especially in developing regions such as southern Africa, which are faced with resource constraints. Also, it is recommended that future studies must test the effectiveness of the adopted model on different grass species, or different regions, to verify the generalisation of the findings. Confirmation results from such studies will help in providing insightful information not only on the impact of senescence on foraging resource productivity, but rather to improve policy and decision-making on forage availability and livestock management. This is important because livestock farming forms a key livelihood option, especially in developing countries.

Chapter Four

4 Determining the onset of autumn grass senescence in subtropical sourveld grasslands using remote sensing proxies and the breakpoint approach

This chapter is based on:

Royimani, L., Mutanga, O., Odindi, J., Sibanda, M. & Chamane, S. 2022. Determining the onset of autumn grass senescence in subtropical sour-veld grasslands using remote sensing proxies and the breakpoint approach. *Ecological Informatics*, 69, 101651.

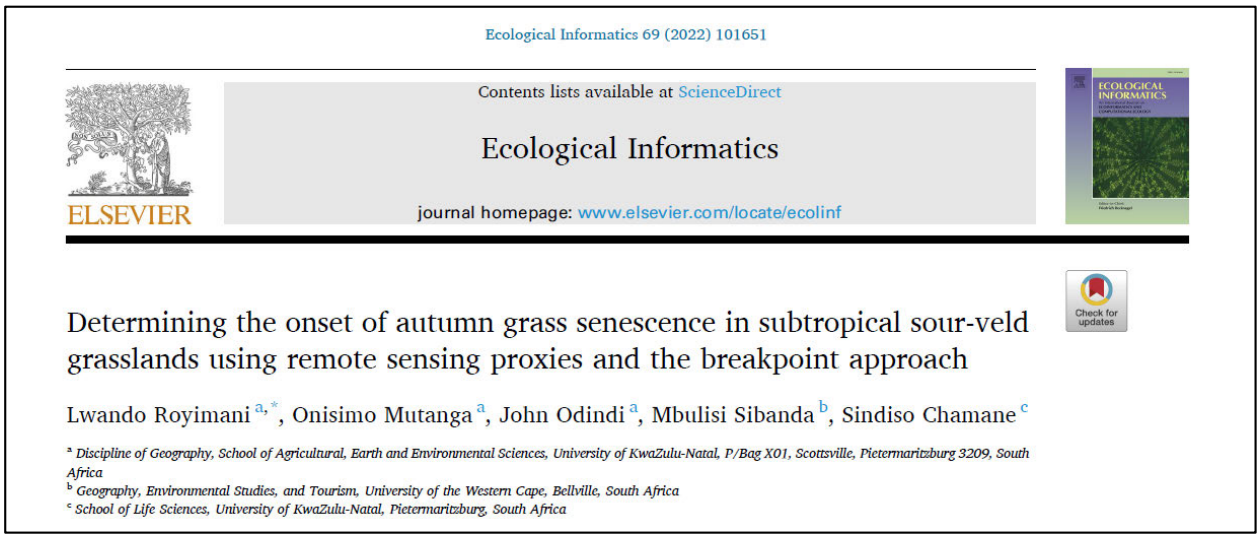

Ecological Informatics 69 (2022) 101651

Contents lists available at ScienceDirect

Ecological Informatics

journal homepage: www.elsevier.com/locate/ecolinf

Determining the onset of autumn grass senescence in subtropical sour-veld grasslands using remote sensing proxies and the breakpoint approach

Lwando Royimani [a,*], Onisimo Mutanga [a], John Odindi [a], Mbulisi Sibanda [b], Sindiso Chamane [c]

[a] Discipline of Geography, School of Agricultural, Earth and Environmental Sciences, University of KwaZulu-Natal, P/Bag X01, Scottsville, Pietermaritzburg 3209, South Africa
[b] Geography, Environmental Studies, and Tourism, University of the Western Cape, Bellville, South Africa
[c] School of Life Sciences, University of KwaZulu-Natal, Pietermaritzburg, South Africa

Abstract

Information on the onset of autumn grass senescence in subtropical grasslands is essential for ascertaining the duration of poor forage quality. It is well-established that during senescence, grass leaves lose their nutrients to the rooting systems; which affects the quality and quantity of forage resources. The timing of the onset of autumn grass senescence is critical in determining the potential lifespan through which the provision of quality forage can be sustained in grazing lands. However, objective and robust methods for estimating the onset of autumn grass senescence at a rangeland scale are limited. Hence, this study sought to characterize the onset of autumn senescence in mesic subtropical sourveld grasslands using remotely sensed data. Ten monthly vegetation indices were generated from the Sentinel 2 data and used as proxies to explain the onset of autumn grass senescence. The performance of the proxies was validated using the corresponding field-measured monthly grass chlorophylls. Results showed that the Chlorophyll Red-Edge (CHL-RED-EDGE) and the Normalized Difference Red Edge Index ($NDVI_{705}$) were the most important proxies for characterizing the autumn grassland senescence. In addition, monthly (i.e., January to June) mean values of the two best proxies were fitted in a piecewise linear regression model with a breakpoint approach to determine the start of autumn grass senescence. The first proxy (i.e., $NDVI_{705}$) predicted that the grass in the study area starts senescing on day number ± 98 of the year (R^2 = 0.97, RMSE = 0.024), while the second (i.e., CHL-RED-EDGE) suggested day number ± 106 of the year (R^2 = 0.96, RMSE = 0.052). Overall, this study demonstrated the value of remote sensing proxies in estimating the autumn grass senescence and in determining its onset. These results provide a basis for understanding the impact of autumn senescence on foraging resource provision in rangeland ecosystems.

Keywords: Grass senescence, forage, autumn onset, Sentinel 2, remote sensing proxy, breakpoint analysis.

4.1 Introduction

Quantifying the onset of autumn grass senescence is a critical step towards understanding its ecological implications as well as the dynamics in the provision and supply of quality forage in rangeland environments (Yang and Udvardi 2018; Ren *et al.* 2017). This is primarily important for two major reasons; firstly, grasses constitute the greatest portion of the natural pastures and secondly, they degrade during senescence; hence, losing their grazing value (Royimani *et al.* 2021). Even though it is noted that grasses may senesce individually because of, among others, physical damages and genetically related conditions (Royimani *et al.* 2021),

the impact of such senescence is not significant to forage productivity due to the disjointed nature of its occurrence. Instead, the autumn senescence, which is described as the seasonal plant wilting due to old age and the climatic conditions associated with autumn (Mariën *et al.* 2019) has generated interest due to its relative uniformity across the landscape. Besides, the onset of autumn grass senescence can be accelerated or delayed due to changes in seasonal and climatic conditions; in turn, reducing or extending forage quality and quantity (Royimani *et al.* 2021). For instance, studies indicate that the early onset of senescence reduces the growing period of the flora and the subsequent productivity, while delayed onset allows for maximum growth and maturity that increases forage quality (Gehrmann *et al*. 2021; Mariën *et al*. 2021; Anderegg *et al.* 2020; Guo and Gan 2014). Therefore, an accurate and timely assessment of the onset of autumn grass senescence is required to forecast the period through which quality forage provision can be ascertained in grazing lands.

Current methods for assessing the start of autumn plant senescence have largely been based on field observations of changes in chlorophyll and nitrogen pigments as well as visual scoring of leaf coloration and fall (Anderegg *et al.* 2020; Mariën *et al.* 2019; Michelson *et al*. 2018). However, the drawbacks of such methods include the high cost of labour, time, and money and are limited to plot and field-scale applications (Mariën *et al.* 2019; Royimani *et al.* 2019a). Besides, leaf coloration and fall approaches are impeded by their subjectivity and the effect of time lag (i.e., they can only occur beyond a given decline in chlorophyll threshold) (Mariën *et al.* 2019). Hence, these approaches are inadequate in monitoring rangeland's phenology at reasonable spatial extents (Makanza *et al*. 2018). On the other hand, remote sensing has been instrumental in providing near real-time high-quality data useful in explaining changes in plant pigments like chlorophyll over large spatial extents (Morley *et al.* 2020; Frampton *et al.* 2013; Di Bella *et al.* 2004). As a result, many remote sensing proxies that are sensitive to changes in chlorophyll e.g., the Normalized Difference Vegetation Index (NDVI), Plant Senescence Reflectance Index (PSRI), MERIS Terrestrial Chlorophyll Index (MTCI), Enhanced Vegetation Index (EVI), Chlorophyll Red Edge Index (CHL-RED-EDGE), and the Green-Red Ratio Index (GRVI) have been developed and used to optimize the quantification of plant senescence (Lang *et al.* 2019; Yu *et al.* 2019; Dash *et al.* 2010). For instance, Mariën *et al.* (2019) estimated the onset of autumn senescence in European beech (*Fagus sylvatica* L.) trees in Antwerp, Belgium, using a combination of field-based (i.e., chlorophyll content, nitrogen concentration, leaf coloration, and fall) and remote sensing (i.e., NDVI, EVI, CHL-RED-EDGE, PSRI, and the MTCI) proxies with the breakpoint analysis. Based on their findings, the

start of autumn senescence in the vegetation was best explained by the CHL-RED-EDGE and the NDVI, with an inflection point on day number ± 248 of the year. Makanza *et al.* (2018), also investigated the utility of the Unmanned Aerial Vehicle (UAV) technology in assessing canopy senescence in crop plantations, in Harare, Zimbabwe, while Renier *et al.* (2015a), detected the onset of vegetation senescence in Mauritania using a time series analysis of the NDVI and the Normalized Difference Tillage Index (NDTI) generated from MODIS with three different classification techniques. Using the decision tree, the maximum likelihood, and the support vector machine classification techniques, they achieved 71.5%, 61.4%, and 72.3% classification accuracies, respectively. Generally, the estimation of the onset of plant senescence relies on the ongoing monitoring of dynamics in the trajectory of the chlorophyll through time.

However, to the best of our knowledge, no study has estimated the onset of autumn senescence in subtropical grasslands using remote sensing techniques. Therefore, this study is the first attempt in testing the potential of vegetation metrics derived from the remotely sensed Sentinel 2 dataset to explain the onset of autumn senescence in mesic subtropical sourveld grasslands. To achieve this objective, ten monthly vegetation indices were retrieved as proxies for the assessment of grass senescence for the period between March and June 2021. The performance of the vegetation indices was evaluated using corresponding monthly grass chlorophyll contents collected on the field and the best proxies were established. Mean monthly values of the best proxies were calculated for the detection of the onset of autumn grass senescence using the piecewise linear regression model and the breakpoint analysis (Mariën *et al.* 2019; Odindi and Kakembo 2011). The approach captures the inflection point, where the change in the slopes of the two or more datasets (i.e., from negative to positive or vice versa) occurs (Tomé and Miranda 2004). Our study hypothesized that the start of autumn senescence in the grass can be determined by explaining the inflection point in its monthly chlorophyll.

4.2 Methods and materials

4.2.1 Sampling strategy

Monthly grass chlorophyll content values for this study were collected using a SPAD-502 meter between March and June 2021 (Table 4.1). The assumption was that during March, the chlorophyll content in the grass leaves is at the peak due to maturity while at the lowest in June because of senescence (Table 4.2). A total of 110, 10 m-by-10 m plots were established at 150 m distance apart using a purposive sampling approach (Royimani *et al.* 2019b). The 10 m-by-10 m plots were located within bigger homogeneous plots of approximately 15 m-by-15 m to

minimize the potential errors arising from geolocation mismatch with the satellite imagery. Centre coordinates of the plots were taken using a Trimble GPS receiver with a sub-meter accuracy to facilitate tracing and identification during subsequent site visits. Although the measurements of plant chlorophyll when using the SPAD-502 meter are often taken at the leaf level, the narrow leaf surface area of the sampled grass leaves was inappropriate for this approach. Therefore, chlorophyll measurements were taken at the plant level, in the region between culm and inflorescence, and the SPAD-502 sensor was fully covered by the grass leaves. A calibration set of five simultaneous SPAD-502 readings were taken and averaged to determine a measurement. This exercise was reiterated three times in each plot and the outcomes were averaged to get one value for the plot. Also, mean values of the monthly grass chlorophylls were generated and plotted to understand the pattern in the temporal behavior of the chlorophyll for the duration of the study (Figure 4.1). However, using the March to June mean monthly chlorophylls, the trajectory of the grass chlorophyll was shown to be already on a down falling slope. To determine the behavior of the grass chlorophyll before senescence was visible, we extrapolated the mean values of the grass chlorophyll for January and February using a linear regression model in R. The extrapolated January and February mean chlorophylls corresponded to the ± 27^{th} and 55^{th} days of the year, respectively (Table 4.1).

Table 4.1 Field data collection dates and the variables collected, frequency, and sampling scale.

Date	**Corresponding DOY**	**Variables collected**	**Frequency**	**Sampling scale**
-	27	-	-	-
-	55	-	-	-
23 – 29 March 2021	85	Chlorophyll content	Monthly	Plant
26 – 30 April 2021	118			
24 – 28 May 2021	146			
21 – 25 June 2021	174			

Footnote: DOY = Day of the year.

Table 4.2 Field captured visuals of the grass between March and June 2021 to illustrate the condition of the grass from the pre-senescent through to senescent phase.

Month	**DOY**	**Coloration stage**	**Photo**
March	85	Deep green	
April	118	Pale green	
May	146	Yellow	
June	174	Brown	

4.2.2 Remote sensing proxies

4.2.2.1 Sentinel 2 multispectral image acquisition

Six pre-processed (i.e., L2A processing level) monthly scenes of the Sentinel 2 Multi-Spectral Instrument (MSI) were freely downloaded from the Copernicus Open Access Hub data repository (https://scihub.copernicus.eu/dhus/#/home). The acquisition dates of these Sentinel 2 images are presented in table 4.3. These image dates were chosen because they overlapped with field data collection dates in this study (Table 4.1). All the Sentinel 2 images were georeferenced using the first-order polynomial transformation available in ArcGIS version 10.6. The standard errors obtained are reported in table 4.3. In the process, the ArcMap's base-map imagery was used as a benchmark and recognizable features like crossroads and water bodies were identified as Ground Control Points (GCPs) to geometrically rectify the Sentinel 2 images. This was necessary to avoid possible spatial or geometric inconsistencies in pixel locations across the multiple images.

Table 4.3 Sentinel 2 image acquisition dates and the cloud cover proportions.

Sensor	Acquisition date	Corresponding DOY	Cloud cover (%)	Standard error (RMSE) (m)
Sentinel 2	22-Jan-21	27	0.063	1.879
	24-Feb-21	55	0.571	2.271
	29-Mar-21	85	0.167	1.911
	21-Apr-21	118	0.029	2.089
	23-May-21	146	0.126	1.893
	25-Jun-21	174	2.950	1.287

Footnote: DOY = Day of the year, Standard error = georectification error.

The broadband multispectral remote sensing sensors like Sentinel 2 have been commended for rangeland monitoring and management due to their extensive coverage and free availability (Shoko *et al.* 2020). The high (i.e., 5-day) temporal resolution of the Sentinel 2 imagery

satisfies the requirements for the ongoing earth observation required for the detection of the onset of plant senescence. Also, the Sentinel 2 provides the coverage of the Red Edge Position (REP) (Frampton *et al.* 2013), which is required to explain subtle changes in plant pigments like chlorophyll through senescence.

4.2.2.2 Vegetation index extraction

Ten monthly vegetation indices were calculated and used as proxies for the period of the field data collection to estimate autumn grass senescence. The chosen indices included the CHL-RED-EDGE, PSRI, MTCI, GRVI, Normalized Difference Senescent Vegetation Index (NDSVI), NDTI, and the four NDVIs. In addition to the traditional NDVI and the Normalized Difference Red Edge Index ($NDVI_{705}$), two other NDVIs (i.e., NDVI-B8A and NDVI-B7) were explored using a combination of bands in the Near Infrared and the Red-Edge Band 8A and Band 7, respectively. The choice of the indices was motivated by their success in previous applications of plant senescence estimation (Mariën *et al.* 2019; Lang *et al.* 2019; Yu *et al.* 2019) or due to the sensitivity of the region that contains the associated bands in detecting plant chlorophyll. Additional indices were generated using the best performing proxies for January and February 2021. Detailed descriptions of the indices used in this study together with their formulae are given in table 4.4.

4.2.3 Statistical analysis

All statistical analysis in the study were performed using R version 4.0.5 (R Core Team, 2021). Also, figures were coded in R using embedded packages like the plot and the segmented function. The monthly grass chlorophylls, as response variables, as well as the remotely sensed data, as predictors, were tested for normality using the Shapiro-Wilk test based on the p-value. The accuracies of the models and approaches employed were individually or collectively evaluated using the coefficient of determination (R^2), Root Mean Square Error (RMSE), the Mean Square Error (MSE), and the level of significance (*p*-value).

Table 4.4 Chosen vegetation indices in the present study.

Index name	Abbreviation	Formula	Reference
Green Red Ratio Index	GRVI	B03 - B04 / B03 + B04	Lang *et al.* (2019)
Normalized Difference Senescent Vegetation Index	NDSVI	B11 - B04 / B11 + B04	Yu *et al.* (2019)
Normalized Difference Tillage Index	NDTI	B11 - B12 / B11 + B12	Mariën *et al.* (2019)
Normalized Difference Vegetation Index	NDVI	B08 - B04 / B08 + B04	Anderegg *et al.* (2020)
Normalized Difference Vegetation Index	NDVI-B7	B07 - B04 / B07 + B07	-
Normalized Difference Vegetation Index	NDVI-B8A	B08A - B04 / B08A + B04	-
Plant Senescence Reflectance Index	PSRI	B04 - B02 / B06	Anderegg *et al.* (2020)
Chlorophyll Red Edge	CHL-RED-EDGE	B05 / B08	Mariën *et al.* (2019)
Normalized Difference Red Edge	$NDVI_{705}$	B06 - B05 / B06 + B05	Dong *et al.* (2015)
MERIS terrestrial Chlorophyll index	MTCI	B06 - B05 / B05 - B04	Mariën *et al.* (2019)

4.2.4 Optimal remote sensing proxies for estimating autumn grass senescence

In identifying remote sensing proxies (i.e., predictors) that can explain autumn grass senescence with superior accuracies, the capabilities of the retrieved vegetation indices were tested based on the field-measured monthly grass chlorophylls (i.e., responses) using the Pearson's Product correlation test. The importance of the proxy or predictor variable in detecting autumn grass senescence was determined based on the R^2, RMSE and *p*-value obtained. The requirement for the best proxy was that it must be consistently significant ($p < 0.001$) with a consistently high R^2 and low RMSE values across all the four months considered for the analysis. Ultimately, proxies that satisfied all these requirements were chosen and used to estimate the timing of the start of autumn grass senescence in the study area.

4.2.5 Detecting the inflection point in grass chlorophyll during autumn senescence

To explain the inflection point in the onset of autumn grass senescence, we separately averaged all the monthly 110 points and we ended up with monthly mean values. Next, the monthly means of grass chlorophyll, as expressed by the best proxy, were used starting from January to June 2021. Subsequently, the study employed a piecewise linear regression model with a breakpoint (Mariën *et al.* 2019; Odindi and Kakembo 2011), using the monthly means of the best proxies. The formula for the piecewise linear regression with a breakpoint is given in equation 4.1.

$$Y = b_0 + b_1 * X + b_2 * (X - \text{breakpoint}) * (X > \text{breakpoint}) \quad \text{(4.1)}$$

where; X is the time (in days), Y is the remote sensing based chlorophyll content (in µg Chl/cm^2), b_0 is the intercept, b_1 and b_2 are the slopes of chlorophyll before and after the breakpoint. This function (equation 4.1) is composed of two expressions (equation 4.2 and 4.3) with formulae:

$$Y = b_0 + b_1 * X \quad \text{(4.2)}$$

and

$$Y = b_0 + b_1 * X + b_2 * (X - \text{breakpoint}) \quad \text{(4.3)}$$

Equation 4.2 deals with chlorophyll values of the grass before the breakpoint while equation 4.3 takes care of grass chlorophyll after the breakpoint.

In addition, effective detection of the inflection point using the regression with a breakpoint approach requires the definition of the actual breakpoint (Odindi and Kakembo 2011). To define the best breakpoint, a wider range of breakpoints was created using the four dates that fall in the middle of all the dates considered in this analysis. Specifically, these dates were day numbers ± 55, 85, 118, and 146 corresponding to February, March, April, and May, respectively (Table 4.1 and Figure 4.1). The optimal breakpoint was established through an iterative search between these four dates and was identified based on the lowest residual or Mean Square Error (MSE). The inflection point was defined as the point where the two slopes (i.e., before and after the onset of autumn grass senescence) meet. Using the means of the two predicted dates of the start of autumn grass senescence, we established the actual onset of autumn grass senescence in the study area (equation 4.4).

$$\text{Actual Onset of Autumn Grass Senescence (AOAGS)} = M_1 + M_2 / \text{n} \quad \text{(4.4)}$$

where M_1 and M_2 are predicted dates for models one and two, respectively, while n is the number of models considered.

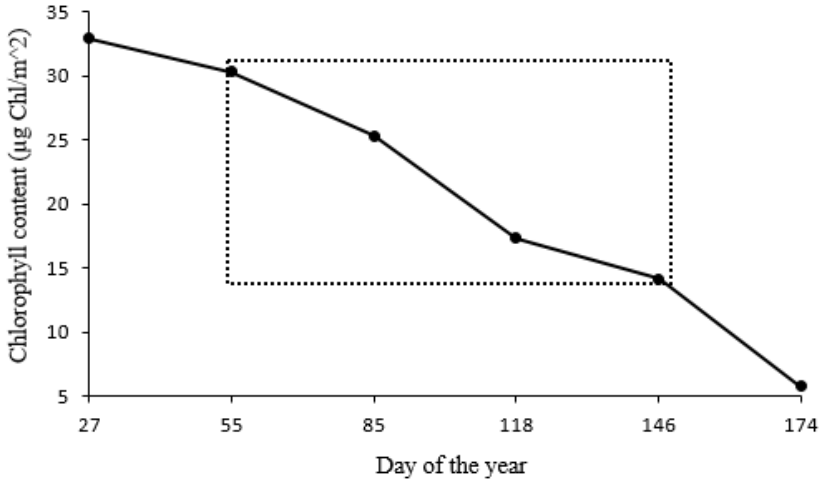

Figure 4.1 Schematic representation of the mean monthly grass chlorophylls with extrapolated values for day number ± 27 and 55 to represent the January and February months, respectively. The black dotted rectangle at the centre of the figure illustrates the four dates used to determine the best breakpoint.

4.3 Results

4.3.1 Descriptive statistics

Table 4.5 shows the descriptive statistics of the field-measured monthly grass chlorophyll for the study period. Overall, the grass chlorophyll varied widely with a maximum and minimum of 29.4 µg Chl/cm^2 and 2.2 µg Chl/cm^2 in March and June, respectively. High grass chlorophyll contents (mean, maximum, and minimum) were recorded in March while low values were obtained in June. In addition, a gradual decrease in monthly grass chlorophyll was observed from March to June (Table 4.5 and Figure 4.2). Normality tests indicated that, field-collected monthly grass chlorophyll did not deviate from the normal distribution ($p > 0.05$) with most of the data centred around the mean for all the months considered (Figure 4.2).

Table 4.5 Descriptive statistics of the field-measured grass chlorophyll content.

Variable	No. of samples	Month	Minimum	Maximum	Mean	Standard deviation
Chlorophyll content (µg Chl/cm^2)	110	March	20.1	29.4	25.3	2.4
		April	10.3	25.9	17.3	3.4
		May	4.4	21.7	14.2	3.8
		June	2.2	11.6	5.8	2.0

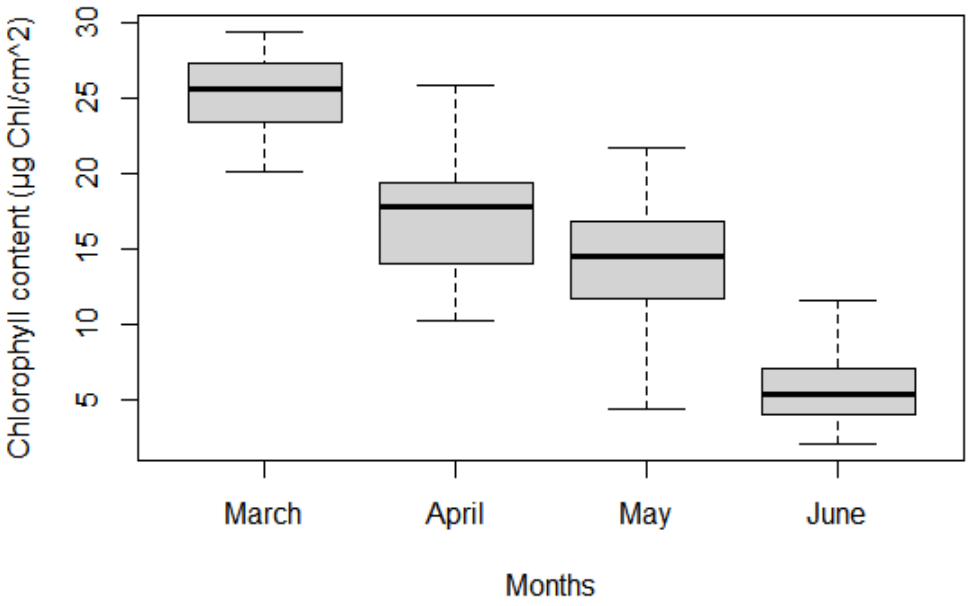

Figure 4.2 Distribution of field-collected chlorophyll content of the grass.

4.3.2 Optimal remote sensing proxy for detection of autumn grass senescence

Based on the Pearson's Product correlation test result in table 4.6, all the remote sensing proxies calculated in this study, except the NDSVI, showed a good relationship ($p < 0.001$) with grass chlorophyll for most of the months considered. Again, the performance of the GRVI decreased substantially in May and June (Table 4.6). The MTCI was only insignificant ($p > 0.001$) in June. The PSRI and the CHL-RED-EDGE, on the other hand, demonstrated a negative correlation with the response variable (i.e., grass chlorophyll) for all the months considered in this investigation. Although all remote sensing proxies were generally significant in estimating the autumn grass senescence, their inconsistency throughout the study disqualified them in the selection of the best proxy. Contrary, the $NDVI_{705,}$ and CHL-RED-EDGE emerged as the most

important and consistent proxies in explaining autumn grass senescence in all the months, with high R^2 and low RMSE values (Figure 4.3 and Table 4.6).

Table 4.6 Correlation coefficients between the chlorophyll content of the grass and remote sensing proxies. Values in bold are insignificant at p > 0.001.

Variables	March		April		May		June	
	R^2	RMSE (µg Chl/cm^2)	R^2	RMSE (µg Chl/cm^2)	R^2	RMSE (µg Chl/cm^2)	R^2	RMSE (µg Chl/cm^2)
GRVI	0.70***	0.08	0.69***	0.08	0.49***	0.09	**0.20****	0.15
NDSVI	**0.32****	0.05	**0.18***	0.06	**0.07***	0.13	**-0.24****	0.07
NDTI	0.50***	0.03	0.59***	0.05	0.61***	0.09	0.61***	0.13
NDVI	0.83***	0.08	0.81***	0.11	0.76***	0.08	0.68***	0.13
NDVI-B7	0.83***	0.09	0.82***	0.12	0.76***	0.08	0.67***	0.14
NDVI-B8A	0.83***	0.09	0.83***	0,11	0.75***	0.08	0.64***	0.14
PSRI	-0.77***	0.04	-0.74***	0.06	-0.71***	0.05	-0.51***	0.10
$NDVI_{705}$	0.87***	0.07	0.84***	0.06	0.83***	0.05	0.80***	0.07
CHL-RED-EDGE	-0.88***	0.06	-0.89***	0.06	-0.87***	0.04	-0.81***	0.05
MTCI	0.79***	0.06	0.70***	0.05	0.60***	0.03	**0.15***	0.20

Footnote: * $p < 0.05$, ** $p < 0.01$ and *** $p < 0.001$.

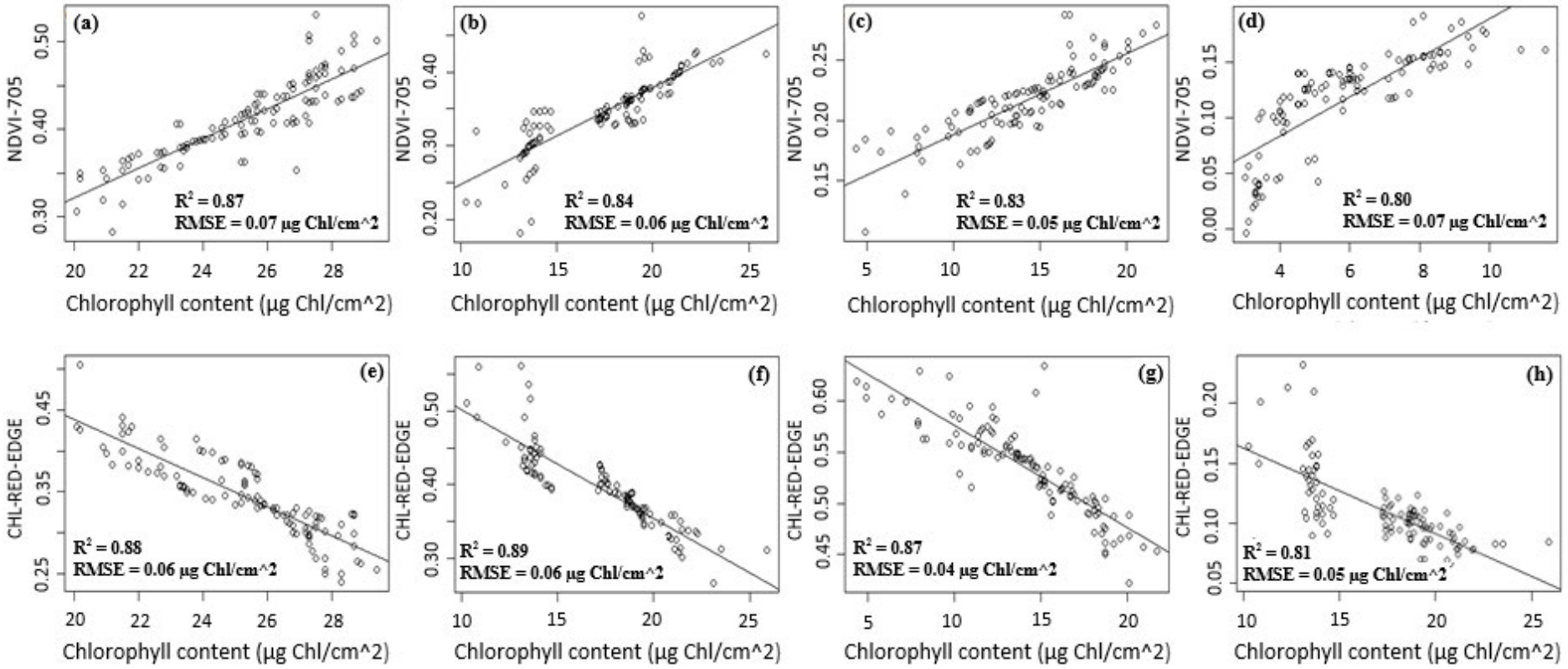

Figure 4.3 Relationship between field-measured (SPAD-502 values) and predicted grass chlorophyll based on optimal remote sensing proxies for all the months of data collection. The top row illustrates the correlation between grass chlorophyll and the $NDVI_{705}$ for (a) March, (b) April, (c) May, and (d) June, while the bottom row shows the grass chlorophyll against the CHL-RED-EDGE for (e) March, (f) April, (g) May and (h) June.

4.3.3 Onset of autumn grass senescence

The wider range of breakpoints set to determine the optimal breakpoint identified day number ± 118 of the year, which is breakpoint number 3.0 in figure 4.4, as the most suitable date for explaining the inflection point in grass chlorophyll. This day (i.e., number ± 118) complemented the April field data collection date, thereby, indicating that the breaking point in the temporal trajectory of grass chlorophyll in this area is in April. According to figure 4.5(a), which shows the estimated date of the inflection point in grass chlorophyll based on the $NDVI_{705}$, the onset of autumn grass senescence in the study area occurs on day number ± 98 of the year (R^2 = 0.97, RMSE = 0.024). On the other hand, figure 4.5(b), which illustrates the inflection point in grass chlorophyll using the CHL-RED-EDGE, predicted day number ± 106 of the year (R^2 = 0.96, RMSE = 0.052) as the day in which autumn grass senescence begins. Averaging these two predicted dates, a mean day in which the onset of autumn grass senescence occurs was established to be day number ± 102. The inflection point is shown by the red vertical lines in both figures (Figures 4.5(a) and (b)). Also, it can be noted that the slope of the grass chlorophyll based on the $NDVI_{705}$ changed from positive, before the onset of senescence, to negative, after senescence onset, while the reverse was observed for the CHL-RED-EDGE (Table 4.7).

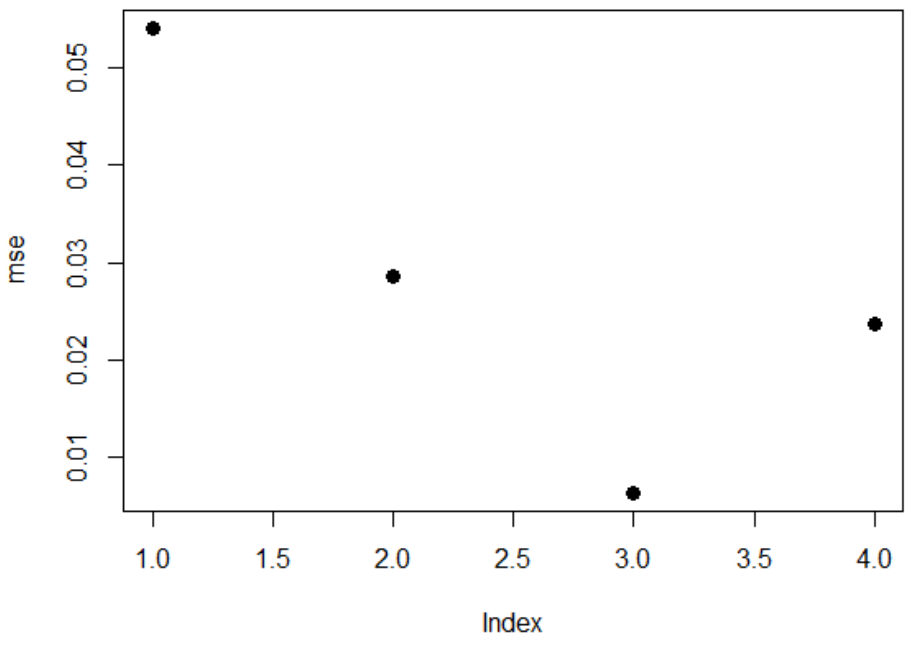

Figure 4.4 Four chosen breakpoints to estimate the onset of autumn grass senescence and their prediction accuracy in terms of the Mean Square Error (MSE).

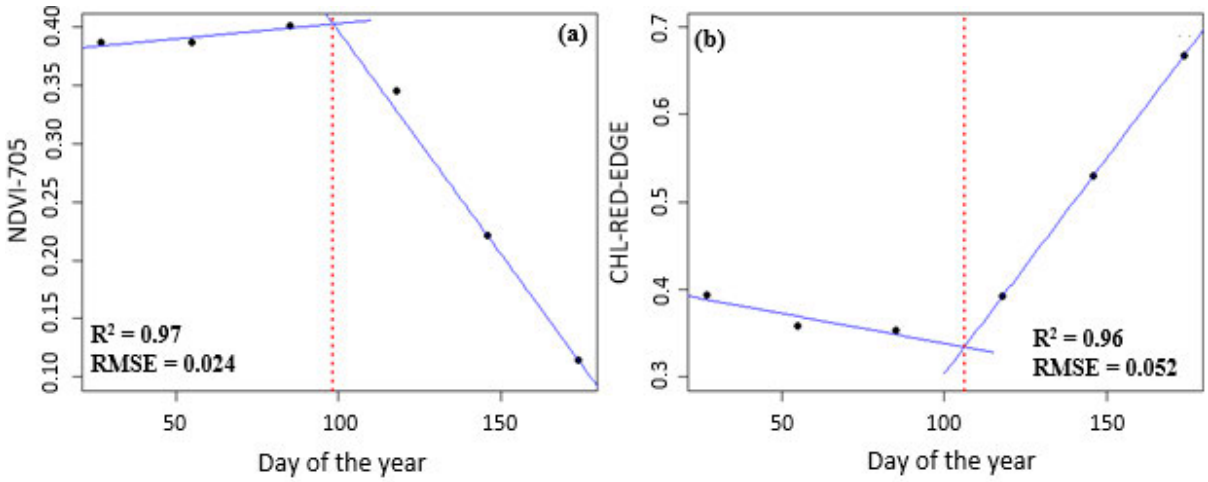

Figure 4.5 Estimated onset of autumn grass senescence based on the (a) $NDVI_{705}$ and the (b) CHL-RED-EDGE remote sensing proxies.

Table 4.7 Chlorophyll content slopes and intercepts before and after the breakpoint.

Proxy	Slope before breakpoint	y-intercept	Slope after breakpoint	y-intercept
$NDVI_{705}$	0,000264	0,376845	-0,00382	0,778807
CHL-RED-EDGE	-0,00068	0,406782	0,004924	-0,18897

4.4 Discussion

This study has demonstrated the potential of remote sensing proxies derived from the Sentinel 2 multispectral data in explaining the onset of autumn senescence in mesic subtropical sourveld grasslands of the KwaZulu-Natal midlands region, South Africa. Specifically, these results highlighted that the CHL-RED-EDGE and the $NDVI_{705}$ were the most sensitive proxies for detecting the autumn grassland senescence. One explanation for that is the sensitivity of the region of the electromagnetic spectrum that contains the bands that are used to generate these proxies. Both the CHL-RED-EDGE and the $NDVI_{705}$ are retrieved using the strategically positioned bands located in the REP of the electromagnetic spectrum. The strength of the REP in explaining dynamics in plant pigments such as chlorophyll is well documented in the literature (Shoko and Mutanga 2017a; Sibanda *et al.* 2017a; Shoko and Mutanga 2017b; Frampton *et al.* 2013). Moreover, the positive relationship observed between field-measured monthly grass chlorophylls and the $NDVI_{705}$ suggests that this proxy explains grass senescence

based on the chronological changes in its chlorophyll. Considering the "blue shift of the red edge" phenomenon in the shorter wavelengths of the REP due to senescence (Clark *et al.* 1995a), it is befitting to have the $NDVI_{705}$ ranked among the most important proxies for characterizing the autumn grass senescence. This also justifies the failure of the other indices (i.e., GRVI, NDVI, NDVI-B7, NDVI-B8A) to meet the set criteria for selection of the best proxy, despite their known sensitivity in plant pigments like chlorophyll (Lang *et al.* 2019; Ren *et al.* 2017; Di Bella *et al.* 2004). The NDVSI and NDTI, on the other hand, are mainly generated using bands that are located in the Shortwave Infrared region of the electromagnetic spectrum, which is less sensitive to plant chlorophyll but rather to water content and other biochemical constituents such as cellulose and lignin (Sibanda *et al.* 2021; Ceccato *et al.* 2001; Ben-Dor *et al.* 1997).

Our findings contrast Mariën *et al.* (2019), who noted that detecting plant senescence onset based on changes in carotenoid derivatives (e.g., leaf coloration and fall) are often inaccurate. In our study, the CHL-RED-EDGE, which is sensitive to changes in plant carotenoid content, emerged as one of the best proxies for explaining the autumn grass senescence. This could be attributed to the strong relationship that exists between plant carotenoid and chlorophyll (Niroula *et al.* 2019). Other studies have further emphasized this inverse relationship between plant chlorophyll and carotenoid, noting the consistent increase in carotenoid with decrease in chlorophyll (Royimani *et al.* 2021; Merzlyak *et al.* 1999; Peñuelas and Filella 1998). Additionally, this discussion suggests that the known time lag problem common between plant chlorophyll decline and carotenoid ascendancy when assessed through field observations and visual scorings (Mariën *et al.* 2019), can be overcome by the use of remote sensing proxies. The sensitivity of regions such as the REP can detect small changes in plant pigments, unlike the use of subjective field observations and visual scorings which introduces the issue of time lag (Mariën *et al.* 2019; Makanza *et al.* 2018). Furthermore, the explanatory power of the CHL-RED-EDGE in optimally detecting autumn grass senescence in the present study is assumed to have been boosted by the sensitivity of the subsequent bands to carotenoid, which is strongly and inversely related to chlorophyll.

With regards to the timing of the onset of autumn grass senescence, the two linear regression models established, based on the $NDVI_{705}$ and the CHL-RED-EDGE, were successful in defining the days of the year in which the start of grass senescence can be expected in the area during autumn. The first model (i.e., $NDVI_{705}$) indicated that the onset of autumn grass senescence is on day number ± 98 of the year (R^2 = 0.97, RMSE = 0.024) while the second

model (i.e., CHL-RED-EDGE) suggested day number ± 106 of the year (R^2 = 0.96, RMSE = 0.052). Based on averaging these two predicted dates, the actual start of autumn grass senescence in the area was estimated to be on day number ± 102 of the year, which is in April. This attests to the observational evidence gathered in the area during field data collection. Again, this complements the evidence presented in table 4.2, using the monthly visuals of the conditions of the grass acquired in the study area. For instance, the clear change in grass colour from deep green in March (i.e., day number ± 85) to pale green in April (i.e., day number ± 118) confirms this predicted date of the start of autumn grass senescence in this area.

The findings of this study are crucial to rangeland users and managers as they provide a basis for knowledge on the potential duration of forage quality and quantity in the rangelands. The delayed onset of autumn senescence in grasslands postpones the time in which the nutrients could be relocated from the leaves to the roots, thereby extending the duration of their accessibility to the grazing livestock (Anderegg *et al.* 2020). Therefore, this information on the actual start of autumn grass senescence will inform local livestock farmers and range managers on the potential deficit of forage production in their grazing area, hence, the adoption of appropriate measures to minimize the possible impact on the livestock productivity. For instance, in the case of early onset of autumn grass senescence, these livestock managers can be empowered to make informed decisions regarding selling some of their livestock while still healthy, as opposed to waiting for later stages of senescence when the economic value of the animals has declined. This is particularly important in communal rangelands of developing regions where forage enhancement measures like fertilizer applications and supplements are limited due to resource constraints (Rabumbulu and Badenhorst 2017). Empirical evidence also highlights the ecological importance of understanding the start of autumn plant senescence. For instance, Royimani *et al.* (2021) noted that during senescence, the surface area and the stomatal pores of the grass leaves are significantly reduced, thereby, decreasing the amount of sequestrated carbon, while Anderegg *et al.* (2020), reported the value of increased stay-green or delayed onset of senescence in vegetation for carbon assimilation. These findings further stress the importance of understanding the timing of the start of autumn grass senescence for its implications on climate regulatory initiatives.

4.5 Conclusion

This study has established remote sensing-based proxies for estimating the onset of autumn senescence in grassland ecosystems. The identified best proxies were the $NDVI_{705}$ and the CHL-RED-EDGE and they, respectively, explained the onset of autumn grass senescence based on changes in chlorophyll and carotenoid content of the grass. The explanatory power of the best proxies is believed to have been boosted by the utility of the bands in the REP of the electromagnetic spectrum. Based on the $NDVI_{705}$, the estimated start of autumn grass senescence was on day number ± 98, while on day number ± 106 for the CHL-RED-EDGE. The mean day, which represents the actual start of grass senescence during the autumn season in the study area, was predicted to be day number ± 102 of the year. All the predicted dates of the start of autumn grass senescence in this study fall within the month of April which attests to the observational evidence. This reinforces the evidence presented in table 4.2 using field acquired photographs. This research provides baseline knowledge on the potential duration of forage provision and supply in rangeland ecosystems. Whereas our study provides a novel approach for determining the onset of autumn grass senescence, it is based on a single-season analysis, which may vary from year to year as per changing climatic conditions. Future studies should, therefore, consider long-term multi-temporal chlorophyll changes to determine a universal period of grass senescence onset in this area.

Chapter Five

5 Multi-temporal assessments of remotely sensed autumn grass senescence across climatic and topographic gradients

The chapter is based on:

Royimani, L., Mutanga, O., Odindi, J. & Slotow, R. Multi-temporal assessment of remotely sensed autumn grass senescence across climatic and topographic gradients. *Land*, 14, 183.

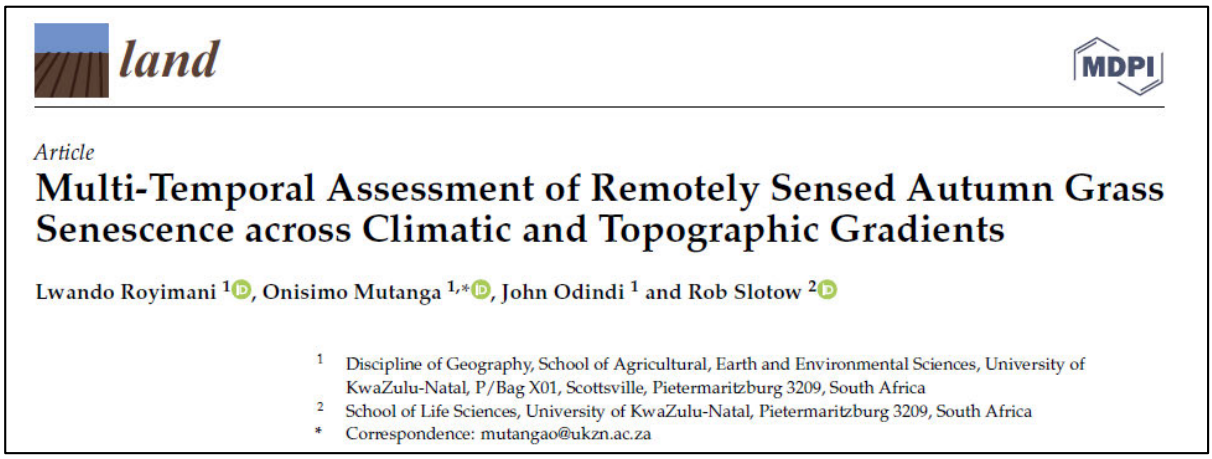

land

MDPI

Article

Multi-Temporal Assessment of Remotely Sensed Autumn Grass Senescence across Climatic and Topographic Gradients

Lwando Royimani [1], Onisimo Mutanga [1,*], John Odindi [1] and Rob Slotow [2]

[1] Discipline of Geography, School of Agricultural, Earth and Environmental Sciences, University of KwaZulu-Natal, P/Bag X01, Scottsville, Pietermaritzburg 3209, South Africa
[2] School of Life Sciences, University of KwaZulu-Natal, Pietermaritzburg 3209, South Africa
* Correspondence: mutangao@ukzn.ac.za

Abstract

Climate and topography are influential variables in the autumn senescence of grassland ecosystems. For instance, extreme weather can lead to earlier or later senescence than normal, while higher altitudes often favour early grass senescence. However, to date, there is no comprehensive understanding of key remote sensing-derived environmental variables to determine the occurrence of autumn grass senescence, particularly in tropical and subtropical regions. Meanwhile, knowledge of the relationship between autumn grass senescence and environmental variables is required to aid the formulation of optimal rangeland management practices. Therefore, this study aimed to examine the spatial autocorrelations between remotely sensed autumn grass senescence *vis-a-vis* the climatic and topographic variables in the subtropical grasslands. Sentinel 2's Normalized Difference Red Edge Index ($NDVI_{705}$) and the Chlorophyll Red-Edge (CHL-RED-EDGE) indices were used as proxies to explain the occurrence of autumn grass senescence, while monthly (i.e., March to June) values of the remotely sensed autumn grass senescence were examined against their corresponding climatic and topographic factors using the Partial Least Square Regression (PLSR), the Multiple Linear Regression (MLR), the Classification and Regression Trees (CART) and the Random Forest Regression (RFR) models. The RFR model displayed a superior performance on both proxies. Next, the mean monthly values of the remotely sensed autumn grass senescence were separately tested for significance against the average monthly climatic (i.e., minimum (T_{min}) and maximum (T_{max}) air temperatures, rainfall, soil moisture, and solar radiation) and topographic (i.e., slope, aspect, and elevation) factors to determine the environmental drivers of autumn grass senescence. Overall, the results indicated that T_{max}, (p = 0.000 and 0.005 for the $NDVI_{705}$ and the CHL-RED-EDGE, respectively), T_{min} (p = 0.021 and 0.041 for the $NDVI_{705}$ and the CHL-RED-EDGE, correspondingly) and the soil moisture (p = 0.031 and 0.040 for the $NDVI_{705}$ and the CHL-RED-EDGE, respectively) were the most influential autumn grass senescence drivers. Overall, these results have shown the role of remote sensing techniques in assessing the autumn grassland senescence along climatic and topographic gradients as well as in determining key environmental drivers of this senescence in the study area.

Keywords: Autumn senescence, grass, climate, remotely sensed, topographic factors.

5.1 Introduction

Climate and topography are key drivers of plant phenology in terrestrial environments (Tao *et al.* 2021; Shoko *et al.* 2019; Wu *et al.* 2018; Liu *et al.* 2018; Tao *et al.* 2018; Liu *et al.* 2016;

McKean *et al.* 1991). Their variability often influences the occurrence, rate, and duration of key phenological stages such as the autumn grassland ecosystem senescence. For instance, Liu *et al.* (2016) noted a variation in the start of grass senescence in the low-lying Inner Mongolian grasslands than the higher Qinghai-Tibetian Plateau. However, the extent and significance of the overlaps between autumn grass senescence and environmental factors such as climate and topography have not been established, especially from a remote sensing point of view. Meanwhile, understanding the relationship between autumn grass senescence and environmental variables is vital, given that senescence markedly decreases photosynthetic activities and plant productivity (Gepstein *et al.* 2003), which in turn affects forage quality, production and availability. Royimani *et al.* (2021), also noted that senescence can either extend or reduce floral species growing season, with serious implications on forage productivity. In addition, studies (e.g., Royimani *et al.* 2022; Royimani *et al.* 2021; Anderegg *et al.* 2020) have noted the socioeconomic and ecological impact of grassland senescence including their regulatory role in the climate-biosphere interactions and potential contribution to land degradation (Liu *et al.* 2016). Given the importance of rangelands and the livestock farming for subsistence and commercial purposes, particularly in the developing world (Shoko *et al.* 2019), understanding the impact of senescence on foraging resource productivity in response to climatic and topographic gradients is increasingly becoming an area of research interest. This information is required to monitor the impact of autumn senescence on foraging resource productivity (Munné-Bosch and Alegre 2004), hence, guiding planning and decision-making on, among others, grazing patterns and stock densities.

Useful assessment of the links between the occurrence of autumn grass senescence and environmental variables at a rangeland scale requires repeated observations acquired at extensive spatial extents. However, the commonly used methods for assessing plant senescence, such as visual scoring of leaf coloration and fall (Anderegg *et al.* 2020), do not effectively satisfy these requirements. Furthermore, these methods are generally not objective and they suffer from the time lag effect (Mariën *et al.* 2021). Contrary, remote sensing techniques offer repeated synoptic viewing of the earth surface (Royimani *et al.* 2019a; Royimani *et al.* 2019b; Sibanda *et al.* 2016), which may benefit the assessment of the spatial autocorrelations between grass senescence and environmental factors during the autumn season. Although many studies have examined plant senescence dynamics based on remote sensing techniques (Mariën *et al.* 2021; Makanza *et al.* 2018; Renier *et al.* 2015b), few have focused on the interactions between autumn senescence and environmental parameters. For

instance, Liu *et al.* (2016) assessed the effect of temperature, insolation and precipitation in temperate regions of China during the maturity stage using a 30-year (1981 - 2011) Normalized Difference Vegetation Index (NDVI) derived from the Global Inventory Modelling and Mapping Studies (GIMMS). Their findings showed that temperature was a decisive factor to the end of the growing season. However, the study was generalized across biomes, hence, did not offer an opportunity for a greater understanding of the autumn-senescence-environmental factors relationship in grassland environments, particularly in the subtropical regions.

In addressing this knowledge gap, the current study examined the spatial autocorrelations between remote sensing derived autumn grass senescence and environmental parameters (i.e., climatic factors and topography) in the subtropical sourveld grasslands of the Midlands region, KwaZulu-Natal, South Africa, where autumn senescence is a key factor on forage quality and quantity (Royimani *et al.* 2021). Such information is critical to ascertain the understanding of the dynamics around the occurrence of autumn grass senescence and to accurately determine grass wilting for improved planning and decision-making on grazing patterns and overall rangeland management. Specifically, a better understanding of the influence of environmental factors on autumn grass senescence will help improve the projection of the onset and duration of autumn grassland senescence, hence, reliably determining the period of low and poor forage quality for grazing, while minimizing the subsequent impact on the livestock and wildlife. To achieve this aim, this study adopted two Sentinel 2 derived vegetation indices (i.e., the $NDVI_{705}$ and the CHL-RED-EDGE) that have been identified as the most sensitive proxies for explaining the occurrence of autumn grass senescence within the study area (Royimani *et al.* 2022). Remotely sensed monthly (i.e., March to June) estimates of autumn grass senescence were assessed for sensitivity against their corresponding climatic (i.e., minimum (T_{min}) and maximum (T_{max}) air temperatures, soil moisture, solar radiation, and rainfall) and topographic (i.e., slope, aspect, and elevation) factors using the Partial Least Square Regression (PLSR), the Multiple Linear Regression (MLR), the Classification and Regression Trees (CART) and the Random Forest Regression (RFR) models. Next, monthly averages of the remotely sensed autumn grass senescence were tested against monthly mean values of the climatic and topographic variables using Pearson's product-moment correlation approach to understand possible environmental drivers of autumn grassland senescence. We hypothesized that the occurrence of autumn grass senescence in this area can be explained by the dynamics in the micro-climatic and topographic gradients.

5.2 Materials and Methods

5.2.1 Field data collection

A purposive sampling approach was used in the study area (Figure 1.1) to establish 110 plots measuring about 10m by 10m and their centre coordinates were recorded. The plots were designed to provide a representation of the topography of the study site, particularly with regards to the elevation, aspect and slope. For instance, some plots were created in low, middle and high altitudinal areas, while considering the effect of south, east, west and north facing slopes. Equally, we considered the effect of the slope gradient, whereby some plots were designed on steeper, while others on gentle slopes. Soil moisture content readings were collected monthly within the plots using the ML3 ThetaProbe Soil Moisture Sensor between the 20th of March and 30th of June 2021. The ML3 ThetaProbe Soil Moisture Sensor measures soil moisture from the earth surface to the depth of 7 cm and the measurements are often expressed in percentage per volumetric water content (%/VWC) (Goodchild *et al.* 2014). In this study five measurements were randomly taken within each plot and averaged to obtain a value for the plot. Subsequently, we created four monthly point maps of the soil moisture with the corresponding coordinate points for the months of March, April, May and June.

5.2.2 Remotely sensed autumn grass senescence

Two vegetation indices (i.e., the $NDVI_{705}$ and the CHL-RED-EDGE), identified as the best proxies in explaining the occurrence of autumn grass senescence within the study area were adopted (Royimani *et al.* 2022). These indices were derived from the Sentinel 2 data acquired between March and June 2021. For detailed explanation on the establishment and validation of the named indices, readers are directed to Royimani *et al.* (2022). The considered indices were derived on monthly basis representing March, April, May and June 2021. In total, eight vegetation index maps were generated, with four monthly indices generated using the $NDVI_{705}$ and the CHL-RED-EDGE.

5.2.3 Climatic and topographic variables

Daily rainfall and minimum (T_{min}) and maximum (T_{max}) air temperature data for the study area were sourced from the South African Weather Service (SAWS). The daily rainfall and temperature values were aggregated to obtain monthly records. However, this data was provided as point data for the city of Pietermaritzburg, hence, inadequate for analysis. Therefore, additional monthly T_{min} and T_{max} and rainfall data were downloaded from the

KwaZulu-Natal Sugarcane Research Institute (KZN-SRI) website. Whereas the KZN-SRI has many weather stations distributed throughout the province of KwaZulu-Natal, we only used data from stations surrounding the study site. Next, we interpolated the combined KZN-SRI and SAWS data using the Inverse Difference Weighted (IDW) technique in ArcGIS 10.7 to generate a comprehensive T_{min} and T_{max} as well as rainfall data for the study site. Detailed descriptions of the topographic and climatic factors considered in the current assessment are given in table 5.1.

Table 5.1 Topographic plus climatic variables used in this study.

Variable	Units of measurement	Source
Topographic factors		
Aspect	Degrees North (^oN)	ASTER DEM
Elevation	Meters (m)	ASTER DEM
Slope	Degrees (^{o})	ASTER DEM
Climatic factor		
T_{min}	Degrees Celsius (^oC)	SAWS, KZN-SRI
T_{max}	Degrees Celsius (^oC)	SAWS, KZN-SRI
Rainfall	Millimeters (mm)	SAWS, KZN-SRI
Radiation	Watts Hours per square meter (Wh/m^2)	ASTER DEM

Footnote: ASTER = Advanced Spaceborne Thermal Emission and Reflection Radiometer, DEM = Digital Elevation Model.

Aspect, slope, elevation and radiation were generated using the 30 m ASTER Digital Elevation Model (DEM) in ArcGIS. Specifically, aspect and slope were, respectively, calculated using the aspect and slope functions under the surface tools in Spatial Analysis Tools, ArcGIS 10.7. Similarly, radiation was derived using the Area Solar Radiation extension found under surface tools of the Spatial Analysis Tools, ArcGIS 10.7. Studies show that the application of modelled solar radiation from the DEM is a widely accepted practice in ecological remote sensing (Shoko *et al.* 2019; Dube and Mutanga 2016; Ruiz-Arias *et al.* 2009; Kumar *et al.* 1997).

5.2.4 Data processing and statistical analysis

To ensure compatibility and consistency, all the generated monthly maps (i.e., sections 5.2.2 and 5.2.3) were standardized to a common resolution based on the nearest neighbour resampling approach in ArcGIS 10.7. We then overlaid all the monthly vegetation indices plus

topographic and climatic maps with their respective monthly point maps to extract the corresponding monthly climatic, topographic and remotely sensed autumn grass senescence information. Ultimately, we generated four spreadsheets with the monthly climatic and topographic information jointly with corresponding monthly soil moisture content and remotely sensed derived autumn grass senescence values. The four monthly spreadsheets were further split into eight spreadsheets based on the vegetation index (i.e., the $NDVI_{705}$ or the CHL-RED-EDGE) as predictor variables. The data were separately imported into R version 4.1.3 (R Core Team) for further analysis. Again the data we split into 80% and 20% for training and testing, respectively. Four popular regression algorithms (i.e., the PLSR, MLR, RFR, and CART) were employed in each monthly $NDVI_{705}$ and CHL-RED-EDGE spreadsheet to test the association between the remotely sensed autumn grass senescence and the climatic factors and topography. A 10-fold-cross validation approach was used at each stage of analysis to evaluate the model performances based on the obtainable Root Mean Square Error (RMSE), the coefficient of determination (R^2) and the Mean Absolute Error (MAE).

5.2.5 Model optimization and identification of key environmental determinants of autumn grass senescence

Based on the performance of the four popular algorithms employed in section 5.2.4, one superior model was identified using the RMSE, R^2, and MAE. The model was identified by averaging all the RMSEs, MAEs and R^2s obtained throughout the four months of investigation. The model that yielded the lowest MAE and RMSE jointly with the highest R^2 was determined to be the best, hence, selected for the final prediction of remotely sensed autumn grass senescence with climatic factors and topography. As the superior algorithm, the RFR was adopted and eight final models were built to individually relate the monthly remotely sensed autumn grass senescence values (i.e., the $NDVI_{705}$ and the CHL-RED-EDGE) with their respective monthly climatic and topographic factors. These final models were optimized by tuning their *ntree*, *mtry* and *nodesize* values. The *ntrees*, ranged between 300 and 1200, *mtrys* were between 2 and 16, while the *nodesizes* were put to 1 throughout the analysis. The final prediction results were judged based on the RMSEs and their R^2s. Next, we averaged all the monthly predictor (i.e., the $NDVI_{705}$ and the CHL-RED-EDGE) and response (i.e., climatic and topographic) variables. The outcome was a set of two spreadsheets, first with the $NDVI_{705}$ and second with the CHL-RED-EDGE as predictors along with their monthly averages of topographic and climatic factors. Pearson's product-moment correlation tests were conducted in each set of the spreadsheet to determine the sensitivity of each climatic and topographic

factor to the remotely sensed autumn grass senescence. The significance of each topographic or climatic variable in influencing the occurrence of autumn grassland senescence was determined based on the p-value ($P \leq 0.05$).

5.3 Results

5.3.1 Descriptive statistics

Table 5.2 provides the descriptive statistics of the remotely sensed autumn grass senescence plus climatic and topographic variables used in this study. Overall, the estimates of autumn grass senescence based on the $NDVI_{705}$ increased with a decrease in the CHL-RED-EDGE across the four-month period. Besides, there were no significant variations between the $NDVI_{705}$ and the CHL-RED-EDGE values of autumn grass senescence from March to June. However, in March the values of the $NDVI_{705}$-based autumn grass senescence were higher than those of the CHL-RED-EDGE derived autumn grass senescence. In addition, the monthly means of all the climatic variables (i.e., T_{min} and T_{max}, soil moisture, rainfall and solar radiation) also showed notable variations. Specifically, the means of the solar radiation, T_{min} and T_{max} demonstrated consistent declines throughout the four months, whereas the observable decreases in rainfall and soil moisture from March to May were followed by an increase in June (Table 5.2).

5.3.2 Remotely sensed autumn grass senescence with climatic and topographic variables

Based on the results from the preliminary analysis (Table 5.3), the prediction outputs of the four popular regression models (i.e., the PLSR, MLR, CART and the RFR) adopted in the study were generally significant. Specifically, the RFR outperformed all the other algorithms when using both the $NDVI_{705}$ and the CHL-RED-EDGE as predictors throughout the four months considered in this investigation. This was demonstrated by the low RMSE and MAE with high R^2. These results (Table 5.3) further indicated that the CART was the second most important algorithm in the four months of analysis. On the other hand, the performance of the PSLR was generally inferior throughout the various stages of the analysis.

Table 5.2 Descriptive statistics of the data collected and extracted for analysis.

Month	Variable	Min	Max	Mean	Stdv
March	$NDVI_{705}$	0.248	0.532	0.396	0.057
	CHL-RED-EGDE	0.239	0.519	0.357	0.058
	Aspect	7.723	340.649	144.777	87.127
	Elevation	1273	1412	1340	30.359
	Slope	0.512	19.411	5.702	3.860
	T_{max}	25.5	25.85	25.65	0.131
	T_{min}	13.68	14.66	14.13	0.398
	Radiation	22878	232161	150843	65496.12
	Rainfall	69.44	87.65	79.39	7.095
	Soil moisture	12.5	34.9	22.43	3.764
April	$NDVI_{705}$	0.182	0.477	0.346	0.051
	CHL-RED-EGDE	0.266	0.562	0.390	0.056
	Aspect	7.723	350.73	146.931	90.342
	Elevation	1273	1410	1340	31.702
	Slope	0.512	19.411	6.11	3.922
	T_{max}	24.51	25.08	24.78	0.217
	T_{min}	11.25	12.21	11.71	0.387
	Radiation	20736	256029	138918	75657.96
	Rainfall	58.5	64.74	62.04	2.137
	Soil moisture	10.1	30.1	16.36	4.505
May	$NDVI_{705}$	0.108	0.291	0.223	0.034
	CHL-RED-EGDE	0.266	0.562	0.390	0.049
	Aspect	7.723	350.73	145.929	89.772
	Elevation	1273	1410	1340	31.298
	Slope	0.512	19.411	5.791	3.689
	T_{max}	22.2	22.85	22.51	0.262
	T_{min}	8.481	9.672	9.057	0.488
	Radiation	19653	304608	137763	87583.85
	Rainfall	13.86	15.25	14.64	0.401
	Soil moisture	0.685	21.030	11.269	4.289
June	$NDVI_{705}$	-0.004	0.203	0.113	0.050
	CHL-RED-EGDE	0.522	1.076	0.666	0.111
	Aspect	7.723	350.73	141.185	87.491
	Elevation	1273	1412	1340	31.881
	Slope	0.512	19.411	6.125	3.850
	T_{max}	20.43	21.14	20.77	0.283
	T_{min}	6.876	7.919	7.379	0.418
	Radiation	22430	303014	131301	89098.69
	Rainfall	30.46	37.7	34.34	2.862
	Soil moisture	10.8	26.7	18.97	3.898

Table 5.3 Performance of the adopted algorithms based on the R^2, MEA and the RMSE.

Month	Predictor variable	Algorithm	RMSE	R^2	MAE
March	$NDVI_{705}$	PLS	0.046	0.39	0.037
		CART	0.042	0.47	0.033
		MLR	0.041	0.46	0.032
		RFR	0.039	0.50	0.031
	CHL-RED-EGDE	PLS	0.053	0.38	0.042
		CART	0.045	0.45	0.037
		MLR	0.046	0.46	0.036
		RFR	0.044	0.50	0.035
April	$NDVI_{705}$	PLS	0.038	0.35	0.031
		CART	0.034	0.63	0.028
		MLR	0.038	0.50	0.030
		RFR	0.035	0.62	0.026
	CHL-RED-EGDE	PLS	0.042	0.34	0.034
		CART	0.041	0.42	0.031
		MLR	0.043	0.42	0.034
		RFR	0.041	0.55	0.032
May	$NDVI_{705}$	PLS	0.024	0.52	0.020
		CART	0.024	0.50	0.018
		MLR	0.026	0.49	0.021
		RFR	0.022	0.53	0.017
	CHL-RED-EGDE	PLS	0.043	0.30	0.033
		CART	0.036	0.46	0.029
		MLR	0.043	0.36	0.036
		RFR	0.036	0.56	0.028
June	$NDVI_{705}$	PLS	0.041	0.36	0.033
		CART	0.046	0.42	0.035
		MLR	0.041	0.47	0.034
		RFR	0.033	0.68	0.026
	CHL-RED-EGDE	PLS	0.091	0.35	0.077
		CART	0.082	0.53	0.060
		MLR	0.101	0.33	0.078
		RFR	0.081	0.60	0.058

Moreover, the averaged prediction outputs of the adopted algorithms across the four month-period of the investigation maintained the findings presented in Table 5.3 that the RFR was the most useful model in associating the remotely sensed autumn grass senescence with climatic and topographic factors (Figure 5.1). A closer look at Figure 5.1(a), (b) and (c) indicates that the RFR is the only algorithm that had a low RMSE and MAE with a high R^2 followed by CART. On the contrary, the PLSR displayed inferior performance based on two of the three model evaluation matrices (i.e., the R^2 and the MAE).

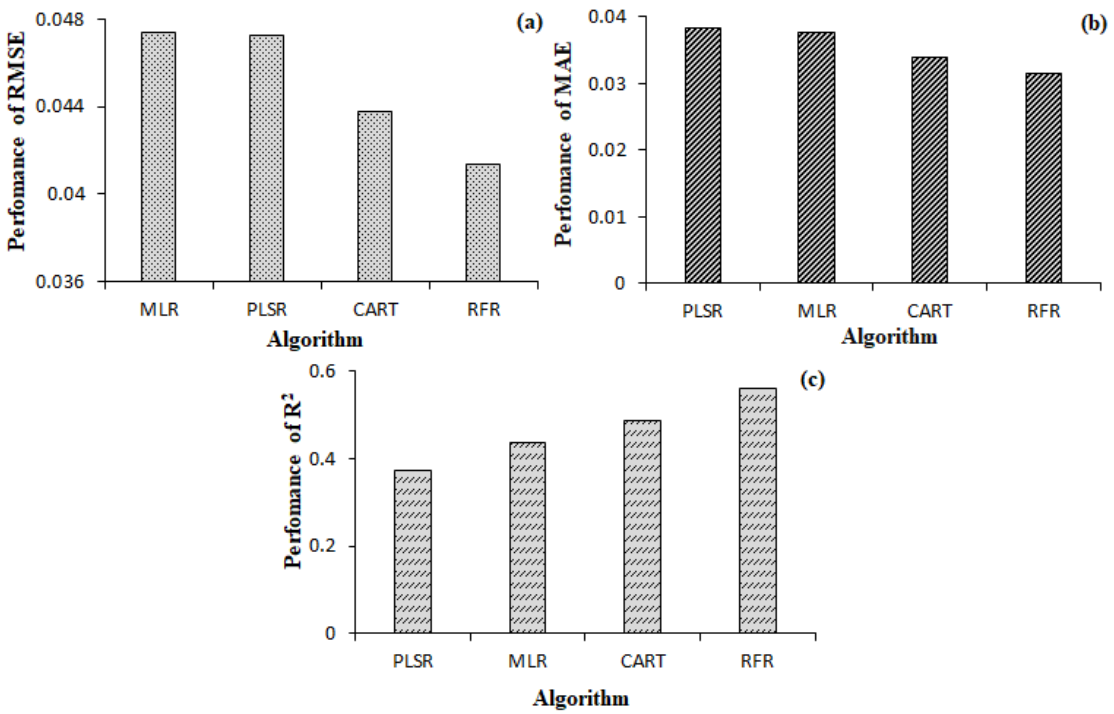

Figure 5.1 Algorithm's performances based on the (a) RMSE, (b) MAE and the (c) R^2.

The final RFR models showed an improved explanation of the association between the remotely sensed autumn grass senescence and the topographic and climatic factors when using both predictors across the four months considered (Table 5.4). For instance, when using the $NDVI_{705}$ and the climatic and topographic factors in March, the model yielded an RMSE of 0.017 and an R^2 of 0.69, while obtaining an RMSE and an R^2 of 0.023 and 0.59, respectively, when using the CHL-RED-EDGE. Likewise, the $NDVI_{705}$ recorded an RMSE of 0.012 and an R^2 of 0.71 in April, whereas the CHL-RED-EDGE produced an RMSE of 0.018 and R^2 of 0.60. Similarly, both the $NDVI_{705}$ and the CHL-RED-EDGE reported RMSEs and R^2s of 0.056 and

0.014 as well as 0.56 and 0.69 in May. Moreover, the $NDVI_{705}$ showed an RMSE and R^2 of 0.013 and 0.71, while the CHL-RED-EDGE obtained an RMSE of 0.056 and R^2 of 0.72 in June. Important variables for the final prediction models are presented in Figure 5.2. The predictive performance of each variable was assessed based on the obtainable Out of Bag Error Rate, which increases with significance.

Table 5.4 Optimal RFR results for the relationships between remotely sensed grass senescence and climatic factors and topography.

	$NDVI_{705}$		**CHL-RED-EDGE**	
Month	**RMSE**	**R^2**	**RMSE**	**R^2**
March	0.017	0.69	0.023	0.59
April	0.012	0.71	0.018	0.60
May	0.056	0.56	0.014	0.69
June	0.013	0.71	0.056	0.72

5.3.3 Climatic and topographic drivers of the autumn grassland senescence

Using the monthly averages of the predictors (i.e., the $NDVI_{705}$ and the CHL-RED-EDGE) against the response variables (i.e., topographic and climatic variables), we identified the key drivers that influence the occurrence of autumn grass senescence (Table 5.5). However, the majority of the CHL-RED-EDGE based R^2 values were negative, indicating the inverse relationship that exist between this index and the predictor variables. Overall, our findings showed that only the climatic factors were sensitive to the occurrence of autumn grassland senescence. Specifically, the T_{min} and T_{max}, jointly with soil moisture were identified as the most influential factors in the occurrence of autumn grass senescence as shown by their significance levels ($P \leq 0.05$). Obtainable R^2 values for the three climatic factors that significantly influence the occurrence of autumn grass senescence were; 1.00, 0.98, and 0.81 based on the $NDVI_{705}$ and -1.00, -0.96, and -0.78 when using the CHL-RED-EDGE. Conversely, even though they displayed good R^2 values (i.e., between 0.76, and 0.93), the insignificant *p*-values ($P \geq 0.05$) highlighted the poor contribution of these other climatic variables in explaining the occurrence of autumn grass senescence in the study area. With regards to the topographic factors, only the slope showed good R^2 values (i.e., -0.80 and 0.75 when using the $NDVI_{705}$ and the CHL-RED-EDGE, respectively), otherwise, they were all

insignificant when considering the *p*-value ($P \geq 0.05$). Table 5.5 shows the contribution of environmental factors on autumn grassland senescence, with significant variables in bold.

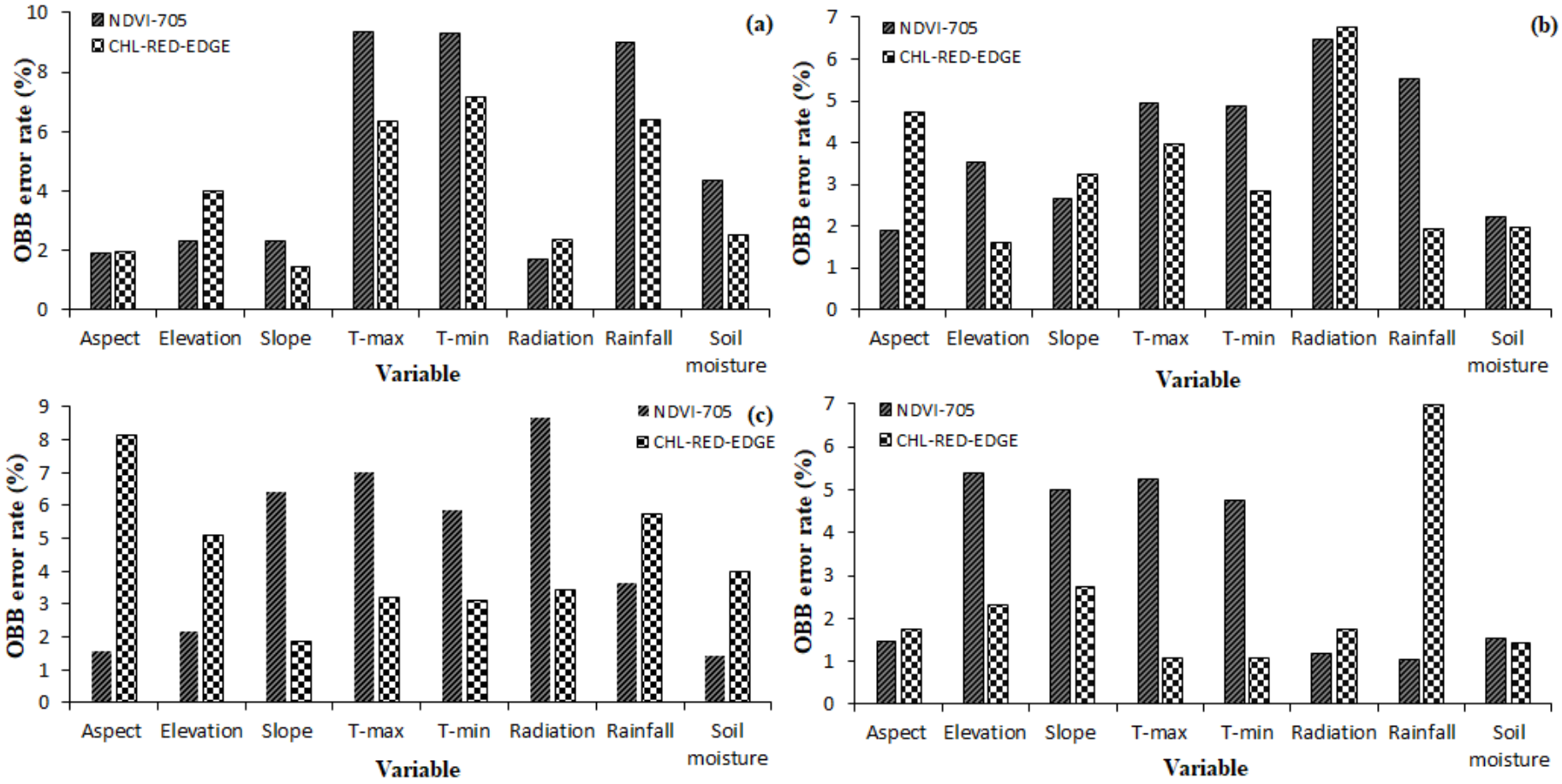

Figure 5.2 RFR model's variable importance for assessing the response of remotely sensed autumn grass senescence against the climatic and topographic factors in (a) March, (b) April, (c) May, and (d) June.

The sensitivity of the topographic and climatic factors in influencing the occurrence of autumn grass senescence in the study area was further emphasized by the value of the *t*-statistics, with higher values signifying the importance and vice versa.

Table 5.5 Correlations between remotely sensed grass senescence and climatic factors and topography. Influential variables are shown in bold.

	$NDVI_{705}$			**CHL-RED-EDGE**		
Variable	***t*-statistics**	***p*-value**	**R^2**	**t-statistics**	***p*-value**	**R^2**
Topographic factors						
Aspect	-0.597	0.611	-0.39	0.492	0.672	0.33
Elevation	0.163	0.886	0.11	-0.276	0.809	-0.19
Slope	-1.865	0.203	-0.80	1.588	0.253	0.75
Climatic factors						
T_{max}	55.095	**0.000**	1.00	-14.388	**0.005**	-1.00
T_{min}	6.832	**0.021**	0.98	-4.806	**0.041**	-0.96
Radiation	3.502	0.073	0.93	-2.852	0.104	-0.90
Rainfall	1.881	0.201	0.80	-1.661	0.239	-0.76
Soil moisture	6.579	**0.031**	0.81	-4.461	**0.040**	-0.78

Figure 5.3 shows the response of the remotely sensed autumn grass senescence (i.e., the $NDVI_{705}$ and the CHL-RED-EDGE) to the most influential variables (i.e., T_{min}, T_{max}, and the soil moisture). Figure 5.3 (a-c) illustrates the remotely sensed autumn grass senescence based on the $NDVI_{705}$, while Figure 5.3 (d-f) displays the remotely sensed autumn grass senescence based on CHL-RED-EDGE. Overall, the effect of time lag was evident between the occurrence of autumn grass senescence and the change in sensitive variables. The $NDVI_{705}$-based autumn grass senescence indicated a continuous decline with a decrease in both the T_{min} and T_{max} during the autumn season. On the other hand, a synonymous decline in the $NDVI_{705}$-based autumn grass senescence with soil moisture was followed by a sudden increase in soil moisture in June. Figure 5.3 (d-f) indicates an inverse relationship between the CHL-RED-EDGE-based autumn grass senescence and the influential variables. Generally, the consistent drop in T_{min}, T_{max}, and the soil moisture values was concurrent with the increasing CHL-RED-EDGE-based autumn grass senescence estimates.

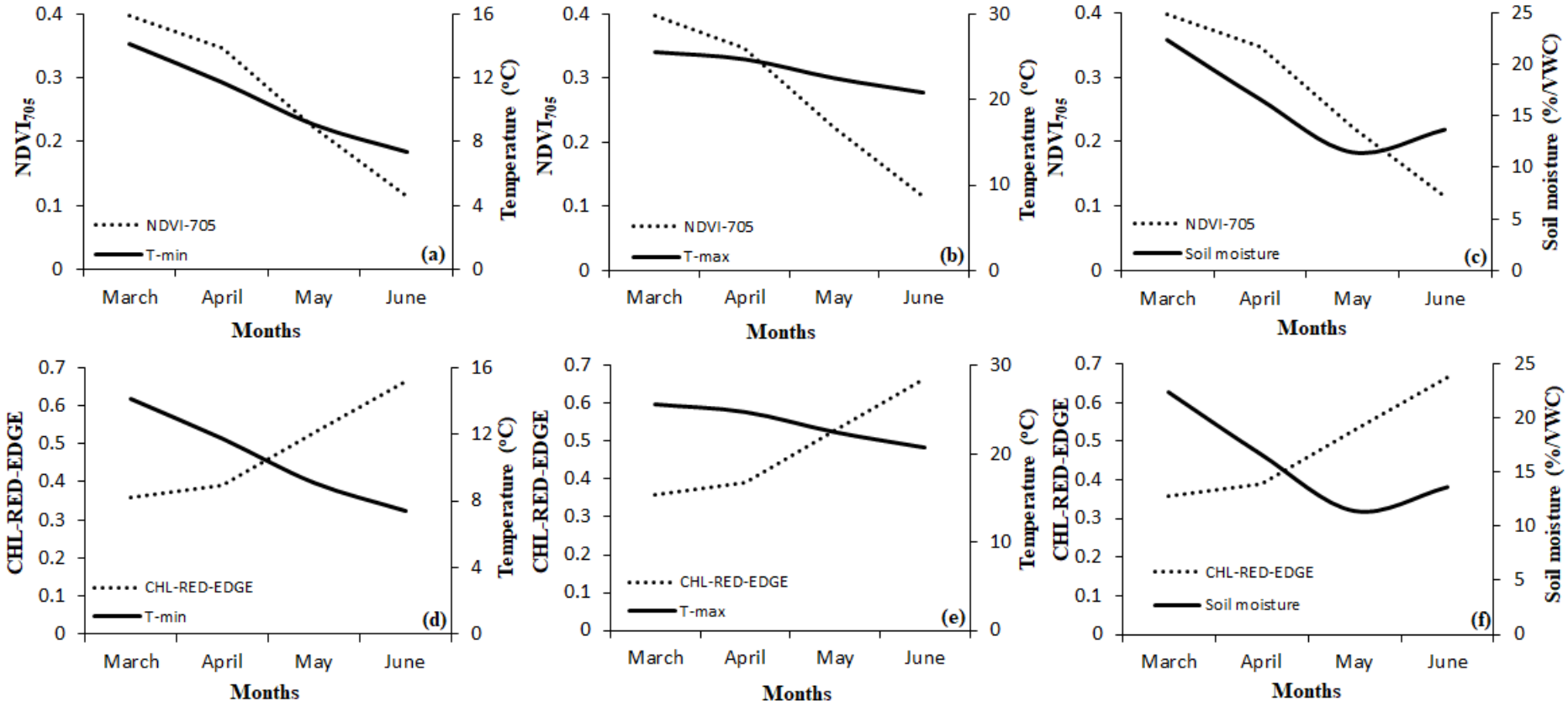

Figure 5.3 The responses of the (a-c) $NDVI_{705}$-based autumn grass senescence to (a) T_{min}, (b) T_{max} and (c) soil moisture together with that of the (d-f) CHL-RED-EDGE based autumn grass senescence to (d) T_{min}, (e) T_{max} and (f) soil moisture through time.

5.4 Discussion

This study demonstrated the value of the multi-temporal remotely acquired Sentinel 2 satellite data in explaining the occurrence of autumn senescence along climatic and topographic gradients in the subtropical sourveld grassland ecosystems. This has been a limitation in understanding the dynamics around the occurrence of autumn senescence as well as the subsequent impact on foraging resource quality and feed availability in these regions. Our findings indicated that the occurrence of autumn grass senescence in the present study area is controlled more by climatic drivers, particularly the soil moisture, T_{min}, and T_{max} than topographic factors. Although not pronounced in the current findings, the sensitivity of air temperature variables (i.e., T_{max} and T_{min}) in influencing the occurrence of autumn grass senescence in the area could be attributed to the reported extremities of these variables (Ndlovu *et al.* 2021). For instance, the observed consistent decline in air temperatures is believed to have promoted irregular frost events, as they are known to be a common phenomenon in the area during this period (Ismail *et al.* 2021), hence, grass senescence. These results concur with studies indicating that extreme temperature conditions affect the natural processes of photosynthetic enzymes, and, thereby, accelerating or delaying chlorophyll deterioration (Liu *et al.* 2018; Liu *et al.* 2016; Fracheboud *et al.* 2009), whereas water shortages are known to influence plant carboxylation reaction, hence, fast-tracking chlorophyll degradation and plant senescence (Tao *et al.* 2021; Tao *et al.* 2018; Sade *et al.* 2018; Munné-Bosch and Alegre 2004).

Although solar radiation and rainfall are known to be key climatic factors influencing plant phenology (Shoko *et al.* 2019), their impact was not significant in this study. However, these results should be discussed with caution, as the observed poor relationship between the remotely sensed autumn grass senescence and rainfall and solar radiation may not be universally constant, i.e., could be site-specific as a result of topographic and micro-climatic conditions. Specifically, the recorded poor correlation between the autumn grass senescence and rainfall in this study may possibly be a consequence of the high variability in rainfall during the same period (Ndlovu *et al.* 2021), which could destruct the uniformity in the phenology of the grass. Similarly, the poor relationship notable between autumn grass senescence and solar radiation could be justified by the relatively uniform topography of the study area, which was observed during field data collection. Meanwhile, our assumption is that meaningful characterization of the links between remotely sensed autumn grass senescence and the incoming solar radiation and topographic factors such as

slope, aspect, and elevation, requires heterogeneity in the landscape, which is possible in pronounced mountainous and valley areas. Shoko *et al.* (2019) also indicated that heterogeneity in topography promotes spatial distinction in vegetation phenology, regardless of the similarity in the age of the floral species. Our results further showed the effect of time lag between the occurrence of autumn grass senescence and the change in sensitive climatic factors, thereby suggesting that the chlorophyll breakdown is not concurrent with, but follows the triggering effect of the environmental cue. Evidently, the importance of understanding the response of autumn grass senescence to changes in climatic and topographic factors cannot be over-emphasized, particularly in countries like South Africa, considering the projected shifts in seasonal patterns (Van der Walt and Fitchett 2020), which may further alter the current dynamics in phenological stages like the autumn grassland senescence, leading to potential forage deficiencies, especially during dry seasons. With its ability to either shorten or extend the growing season of the floral species, hence, productivity (Gepstein *et al.* 2003), the understanding of the links between the autumn grass senescence and environmental factors may help to strengthen our projections on possible timing and duration of autumn grassland senescence, which will, in turn, improve our assessment of fodder bank capacities for quality forage provision. Whereas this highlights the essence of future research on this subject matter, the emphasis of such work should be aimed at heterogeneous terrains, while fully embracing the potential impact of frost activities in the analysis.

With regards to the performance of the RFR model, our results reinforce the evidence presented in previous studies that this model is robust when explaining ecological problems based on remotely acquired datasets (Royimani *et al.* 2019b; Mutanga *et al.* 2012). Again, although the findings in Figure 5.2 may give an impression that the topographic factors were among the important variables in April, May and June, a correct view is that these variables were only important in displaying the monthly relationship with the tested variables, which does not necessarily reflect the autumn grass senescence in the present case. According to our approach in this study, the autumn grassland senescence was explained based on the averaged performance of the month-to-month contributions of each variable and the variables that were consistently significant were identified as the environmental drivers of autumn grassland senescence.

5.6 Conclusion

The present study examined the relationship between remotely sensed autumn grass senescence and the climatic factors plus topography in the subtropical sourveld grasslands of the Midlands region, KwaZulu-Natal, South Africa. The study employed Sentinel 2 derivatives using the PLSR, MLR, CART, and RFR models and the RFR model emerged as the superior model. The results further showed that T_{min}, T_{max}, and soil moisture were the most influential factors in the occurrence of autumn grass senescence in the study site. However, the observable poor relationship between autumn grass senescence and the other climatic factors and topography is believed to be indicative of the micro-climatic conditions and the relative homogeneity in the topography. However, for a conclusive understanding of the overlaps between autumn grass senescence and the climatic factors and topography, we suggest further investigation, particularly focusing on areas with heterogeneous landscapes and taking into account the effect of frost occurrences in the analysis.

Chapter Six

6 Identifying the optimal waveband positions for mapping the autumn grassland senescence using the broadband multispectral remotely sensed dataset

The chapter is based on:

Royimani, L., Mutanga, O. & Odindi, J. Identifying the optimal waveband positions for mapping the autumn grassland senescence using the broadband multispectral remotely sensed dataset. (**Submitted to a Journal**).

Abstract

While remote sensing of grass senescence is addressed in the literature, knowledge of optimal waveband positions that are suitable for discriminating between senescent and non-senescent grass is still limited. Notably, detection of senescent grass is important for understanding the available forage in rangeland environments, and associated ecological implications. The free provision of remote sensing data from the modern broadband multispectral sensors with better spatial and spectral properties offers prospects for reliable and wall-to-wall monitoring of grassland senescence in rangeland `ecosystems. The current study tested the potential of the modern multispectral remote sensing dataset (i.e., Sentinel 2 and Landsat 8) in mapping the senescent grass, and to identify the optimal waveband positions that are suitable for discriminating between senescent and non-senescent grasses. Locational information for senescent and non-senescent grasses was acquired on the field and was used to train the classification process. A Random Forest classification approach was employed using the Landsat 8 and Sentinel 2 multispectral datasets to spectrally discern between senescent and non-senescent grasses. Our analysis yielded overall classification accuracies of 0.82 and 0.78 and kappa coefficients of 0.64 and 0.56 for Sentinel 2 and Landsat 8, respectively. Using the stepwise selection approach, the study further identified that the Red-Edge Position (REP), and the Visible green and red bands of the electromagnetic spectrum, were the optimal waveband positions for separating between senescent and non-senescent grass based on the broadband multispectral remote sensing. This study has demonstrated the value of the readily available broadband multispectral remote sensing data in mapping autumn grassland senescence, and this lays a foundation for effective operational scale monitoring of foraging resource conditions at the landscape scale, particularly during dry seasons.

Keywords: Broadband multispectral, optimal waveband positions, random forest, remote sensing, senescent grass.

6.1 Introduction

Grasslands are widely distributed and mostly situated in arid to semi-arid regions of the world, with an estimated areal coverage of about 40% globally (Wang *et al.* 2019), and 28% in southern Africa (Carbutt *et al.* 2011). Broadly, grassland ecosystems are valued for their socioeconomic and ecological importance. For instance, Wang *et al.* (2019) noted that grasslands account for approximately 30% of the global absorbed soil carbon, and, thus, making them one of the largest

carbon sinks. Equally, grasses are known for their integral role in the provision of wildlife habitat (Jones-Farrand *et al.* 2007), ecosystem energy exchange (Liu *et al.* 2019), and facilitation of soil development (Thompson and Kao-Kniffin 2019). In addition, grasslands provide the main source of free-ranging feed for the livestock and wildlife in the surrounding communities (Shoko and Mutanga 2017a; Nkonya *et al.* 2016), and, thereby, contributing to the national economies, food security, and poverty eradication, especially in developing regions (Herrero *et al.* 2013). Many studies (i.e., Meissner *et al.* 2013; Ramoelo *et al.* 2012; Knox *et al.* 2011) have further highlighted the importance of grass forage for livestock production, and linked to subsequent contributions to the Gross Domestic Products (GDPs) and food security. For instance, Havstad *et al.* (2007) reported that in the United States, grasslands have maintained a steady supply of forage production, which supports approximately 10% of the livestock production. Likewise, literature shows that about 250 million people in more than 100 nations are relying on rangeland resources like grasses for their livelihoods (Mansour *et al.* 2012). In this regard, the role of grasslands in ecological processes, economic growth, food security, and livelihood cannot be overlooked.

However, unlike other plants which are perennial in growth form, the growth and development of grasses are strongly influenced by seasonality, with most of them wilting during the dry winter season (Shoko *et al.* 2019). This process is formally known as natural or autumn senescence, and is described as the phenological stage by which plants, including grasses, degrade through time (Royimani *et al.* 2021). Research points out that autumn senescence is an agent through which grasses significantly lose their nutrients, and, thereby, affecting the condition and availability status of the subsequent forage (Woo *et al.* 2019; Kim *et al.* 2016; Cai *et al.* 2016). As a result, the remaining grasses at later stages of senescence are of low grazing value. Several chronological stages, which lead to this significant decline in quality and quantity of the grass during autumn senescence, have been detailed in the literature, and they broadly include; programmed cell death, which coincides with nutrient departure, coloration, and leaf fall (Mariën *et al.* 2019). Leaf fall in grasses is generally caused by the failure of dead leaf cells to hold onto the main grass plant. Fallen grass leaves, on the other hand, form part of the residual biomass (Royimani *et al.* 2021), and, thereby, reducing the amount of available standing above-ground biomass, thus, affecting the forage availability status. Given factors such as biological invasion (Royimani *et al.* 2019b) and climate change (Liu *et al.* 2019), which are reported to have serious negative implications on the growth and development of grasses, and, hence, forage productivity (Royimani *et al.* 2019b), there

is a need for accurate detection and mapping of senescent grass not only to understand forage reserves, but also to gain knowledge on associated ecological implications.

Monitoring of autumn grass senescence, through field surveys, has proved to be challenging, partly due to the extensive extent of the rangelands (Mariën *et al.* 2019). Also, conventional means for assessing grass senescence are often laborious, time-consuming, and costly (Laliberte *et al.* 2007), and, thus, limited to field- and plot-scale applications. Meanwhile, small-scale applications are usually not appropriate for wall-to-wall coverage, which is required for broad scale monitoring of rangeland resources. In contrast, earth observation technologies allow for non-destructive, cost-effective, repeated, and operational scale monitoring of grasslands even during the dry seasons (Shoko and Mutanga 2017b). Many studies have successfully discriminated senescent components of the vegetation from adjacent classes using remote sensing techniques (Berdugo *et al.* 2013; Di Bella *et al.* 2004; Boyer *et al.* 1988). For instance, Laliberte *et al.* (2007) estimated fractions of senescent grass cover from the green ones using a very high-resolution photographic image and object-based classification approach. Their findings yielded correlation coefficients of 0.88 and 0.95 for the senescent and green grass components, respectively. Similarly, Ren *et al.* (2017) investigated the start (green-up) and end (senescent) dates of the growing seasons in Mongolian grasslands using the Plant Senescence Reflectance Index (PSRI) derived from the Moderate Resolution Imaging Spectroradiometer (MODIS) dataset between 2000 and 2011. The performance of the PRSI was evaluated using the NDVI and it demonstrated a positive correlation ($p < 0.1$). Marsett *et al.* (2006), also estimated attributes (i.e., cover, height, and biomass) of senescent grasses in the region spreading between northern New Mexico and central Chihuahua to southeastern Arizona using the Soil Adjusted Total Vegetation Index (SATVI) and the raw Near Infrared (NIR) band of the Landsat 5 Thematic Mapper. Their results yielded coefficient of determination (R^2) values of 0.77, 0.85, and 0.80 and Nash Sutcliffe values of 0.77, 0.70, and 0.78 for biomass, height, and cover, respectively.

Despite the efforts made in previous studies, there is still a paucity in understanding the optimal waveband positions, especially using the broadband multispectral remote sensing datasets which are readily available, to accurately detect grassland senescence at the landscape scale. Advancements in remote sensing sensor technology, which have seen the launch of modern broadband multispectral instruments like the Landsat 8 and Sentinel 2, offer greater prospects for

closing this research gap. These broadband multispectral sensors are increasingly becoming a reliable source of readily available quality data for rangeland resource management at operational scales. Besides the broad swath-width (185 and 290 km, for Landsat 8 and Sentinel 2, respectively), these sensors offer special capabilities for land cover monitoring purposes than their predecessors such as the Landsat 7 Enhanced Thematic Mapper Plus (ETM+) and Sentinel 1. For instance, the Landsat 8 offers increased spectral bands compared to the Landsat 7 (Shoko and Mutanga 2017a), while the Sentinel 2 bands are more strategically positioned for land cover monitoring than the backscatter bands of the Sentinel 1 (Meneghini 2019). Moreover, the Sentinel 2 multispectral instrument provides refined spatial resolution (i.e., 10 to 20 m) vegetation related data and it also covers the Red Edge Position (REP) of the spectrum (Sibanda *et al.* 2017a), which is critical for explaining subtle changes in plant pigments during senescence (Clark *et al.* 1995a). Also, given their robust and advanced character (Royimani *et al.* 2019a), the non-parametric image classifiers like the Random Forest can help to achieve the maximum detection of senescent grass in rangelands. Taking the advantage of these benefits, the current study tested the potential of the modern multispectral datasets (i.e., Sentinel 2 and Landsat 8) in mapping senescent grass, and identified the optimal waveband positions for discriminating between senescent and non-senescent grasses based on the broadband multispectral remote sensing sensors, with medium spatial resolution in the midlands region of KwaZulu-Natal, South Africa.

6.2 Methods and materials

6.2.1 Field data collection

Locational information for the senescent and non-senescent grasses were acquired at Vulindlela communal rangelands (Figure 1.1) between the 21 and 26 of June 2021 using a Trimble Global Position System (GPS) receiver with a 0.5 m accuracy. A total of 160 (i.e., 80 for senescent and 80 for non-senescent) 30 m by 30 m plots were delineated using a purposive sampling approach (Royimani *et al.* 2019b), and their centre GPS points were collected. The 30 m by 30 m plots were established within homogenous patches of either senescent or non-senescent grasses to minimize the effect of possible geolocation mismatch with both the Sentinel 2 and Landsat 8 satellite sensors. These plots were created in 150 m apart to avoid possible overlaps and autocorrelations. The total number of collected points for each class is presented in table 6.1.

Table 6.1 Summary of the field collected data for each class.

Class name	No. of points
Senescent grass	80
Non-senescent grass	80
Total	160

6.2.2 Broadband multispectral remotely sensed data acquisition

A scene of the Landsat 8 and Sentinel 2, corresponding to the date of the 20th and 30th June 2021 respectively, were downloaded from the Google Earth Engine (GEE) to investigate the optimal waveband positions for classifying the senescent grass based on the broadband multispectral dataset. The descriptions, waveband positions, and the spatial resolutions of the two satellite images used are presented in table 6.2. In GEE, the Landsat 8 and Sentinel 2 surface reflectance images are available under the two respective files: "ee.ImageCollection("LANDSAT/LC08/C02/T1_L2")" and "ee.ImageCollection("COPERNICUS/S2_SR")". On download, these images are provided to the Level 2 type of processing, which caters for orthorectification and atmospheric corrections. In addition, further processing parameters were implemented to remove cloud cover and to convert the image digital numbers (DNs) to reflectance values before the actual image download.

Table 6.2 Description of waveband positions and resolutions for the Landsat 8 and Sentinel 2 spectral bands used in the current study.

Band No.	Band description	Bandwidth (µm)	Resolution (m)	Band description	Central wavelength (µm)	Resolution (m)
	Landsat 8			Sentinel 2		
Band 1	Coastal	0.43 – 0.45	30	–	–	–
Band 2	Blue	0.45 – 0.51	30	Blue	0.490	10
Band 3	Green	0.53 – 0.59	30	Green	0.560	10
Band 4	Red	0.63 – 0.67	30	Red	0.665	10
Band 5	NIR	0.85 – 0.88	30	RE1	0.705	20
Band 6	SWIR 1	1.57 – 1.65	30	RE2	0.740	20
Band 7	SWIR 2	2.11 – 2.29	30	RE3	0.783	20
Band 8	–	–	–	NIR	0.842	10
Band 8A	–	–	–	RE4	0.865	20
Band 11	–	–	–	SWIR 1	1.610	20
Band 12	–	–	–	SWIR 2	2.190	20

6.2.3 Classification algorithm and identification of optimal wavebands

The collected GPS points for the classes were used to retrieve corresponding Sentinel 2 and Landsat 8 spectral reflectance values in ArcGIS version 10.6. Before image classification, the extracted Landsat 8 and Sentinel 2 spectral data were randomly split into 70% and 30% for training and testing, respectively. Next, the Random Forest classification technique was employed in R version 4.0.5 to classify the senescent grass from the non-senescent one. The Random Forest is an ensemble machine learning algorithm that employs the bagging (bootstrap) approach to build multiple decision trees from a given set of predictors and it averages the outcome (Mutanga *et al.* 2012). With the bootstrap aggregation function in place, the Random Forest is able to reduce the variance error arising from the decision trees, thus, improving the classification accuracy (Odebiri *et al.* 2020). Variable importance ranking was performed to establish the spectral bands that yielded superior discrimination between the classes investigated. To identify the optimal

waveband positions for discerning senescent grass from non-senescent one, we employed the stepwise selection approach. In operation, the stepwise selection approach incorporates the capabilities of both the backward and forward feature selection and it indicates the variables (bands) that were added and those removed from the model for superior separation between the investigated classes (Silhavy *et al.* 2017; Olusegun *et al.* 2015; Wagner and Shimshak 2007).

6.2.4 Accuracy assessment

To evaluate the accuracy of the Random Forest classification model in discriminating between senescent and non-senescent grasses using the Landsat 8 and Sentinel 2 multispectral data, the confusion matrix otherwise known as a contingency table, was derived. We further calculated the user's, producer's, and overall classification accuracies, as well as the kappa statistic from the confusion matrix. The variable importance ranking for the best spectral bands in classifying the senescent grass from its co-occurring non-senescent grass was assessed based on Mean Decrease Accuracy. On the other hand, the performance of the established stepwise selection procedure was assessed based on the R-square with high R-square values representing the most sensitive bands and vice versa.

6.3 Results

6.3.1 Landsat 8 and Sentinel 2 classification performance

Given in Table 6.3 are the user's, producer's, and overall classification accuracy assessment results, as well as the kappa coefficient values obtained, when discriminating between the senescent and non-senescent grasses using the Landsat 8 and Sentinel 2 broadband multispectral imagery. The Sentinel 2 yielded higher overall classification accuracy (0.82) and kappa statistic (0.64) compared to the Landsat 8 (0.78 and 0.56, respectively).

Table 6.3 Classification accuracies from the Landsat 8 and Sentinel 2 images.

Class	**UA**	**PA**	**OA**	**Kappa**	**UA**	**PA**	**OA**	**Kappa**
	Sentinel 2				Landsat 8			
Senescent grass	0.84	0.76	0.82	0.64	0.74	0.81	0.78	0.56
Non-senescent grass	0.81	0.88			0.82	0.75		

Footnotes: UA = User's accuracy, PA = producer's accuracy, and OA = overall accuracy.

Figure 6.1 illustrates the performance of the individual bands of the two broadband multispectral remote sensing sensors (i.e., Landsat 8 and Sentinel 2) used in this study in separating between the senescent and non-senescent grass. Band 4 followed by band 5, in order of importance, were the most important variables in both sensors when discriminating between senescent and non-senescent grass. Band 4 in both sensors corresponds to the Visible red region of the electromagnetic, while band 5 in the Landsat 8 corresponds to the Near Infrared NIR and the Red-Edge in Sentinel 2. Landsat 8's bands 1, 7, and 3 were among the superior bands, while bands 2, 3, 8A and, 12 of the Sentinel 2 contributed to the significant bands in separating between senescent and non-senescent grasses.

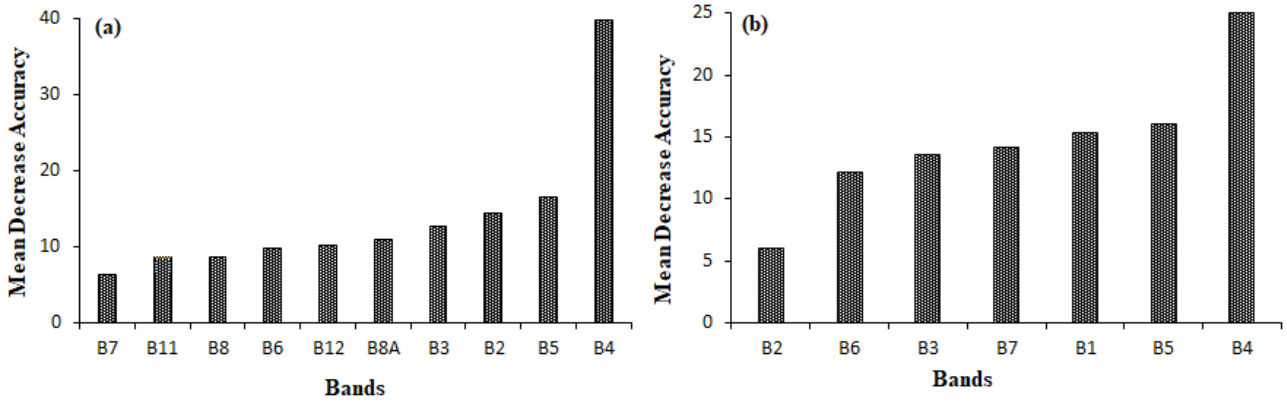

Figure 6.1 Important variables as ranked by the Random Forest model for separating between senescent and non-senescent grass using the (a) Sentinel 2 and (b) Landsat 8.

6.3.2 Spectral sensitive regions of the spectrum for discriminating between senescent and non-senescent grasses

Figure 6.2 presents the mean spectral profiles of senescent and non-senescent grass based on (a) Sentinel 2 and (b) Landsat 8 multispectral datasets. According to Sentinel 2, it can be noted that the mean spectra of senescent grass were distinctive from that of non-senescent grass around the Visible, REP and, the NIR regions of the electromagnetic spectrum. On the other hand, the Landsat 8 suggests that senescent grass is spectrally distinguishable from that of non-senescent grass in the Visible green to the NIR regions of the spectrum. The results (Figure 6.2), further showed that there were high levels of overlaps between the Landsat 8-based spectra of senescent and non-

senescent grass across the various regions of the electromagnetic spectrum. Also, it could be seen that the spectral reflectance values of senescent grass were generally higher than that of non-senescent grass in all the regions of spectral distinction.

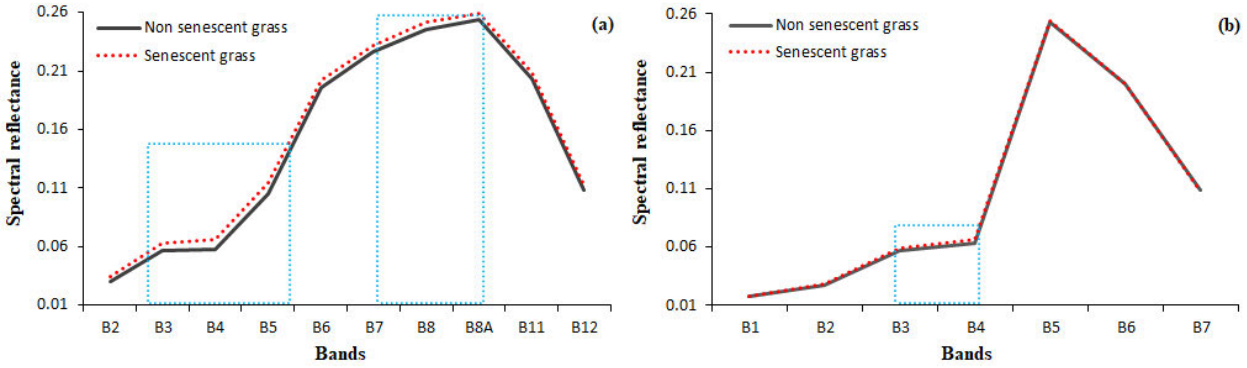

Figure 6.2 Mean spectral reflectance values for the senescent (dotted red) and non-senescent (solid black) grass from the (a) Sentinel 2 and (b) Landsat 8 multispectral datasets. The dotted blue boxes show areas with distinctive spectral variations.

6.3.3 Optimal wavebands for mapping senescent grass

Based on the results of the stepwise selection procedure, the Sentinel 2's REP (i.e., B 5 and 8A) provided the most suitable region of the spectrum for optimal mapping of senescent grass (Figure 6.3(a)). The figure (Figure 6.3(a)), further shows that the Sentinel 2's NIR band was sensitive for discriminating between senescent and non-senescent grasses. Also, the Visible green and red bands of both the Landsat 8 and Sentinel 2 sensors appeared to be amongst the most important wavebands for mapping grassland senescence.

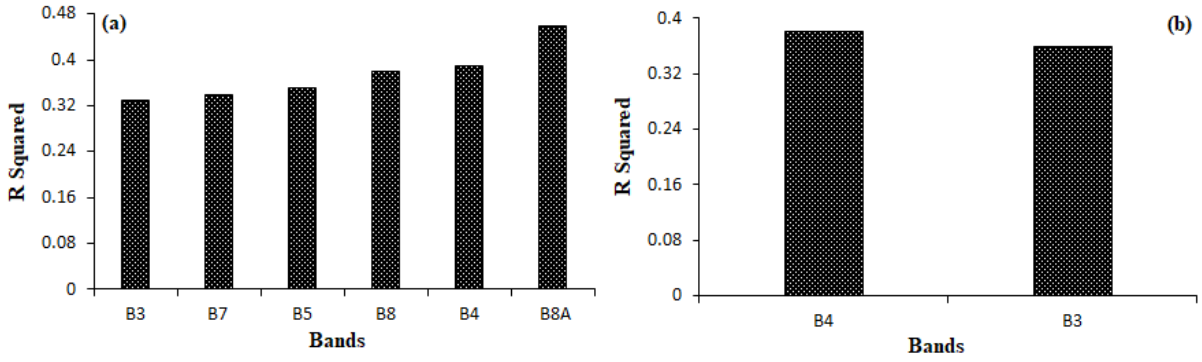

Figure 6.3 Significant bands for classifying senescent from non-senescent grass based on the (a) Sentinel 2 and (b) Landsat 8 multispectral sensors.

6.4 Discussion

The purpose of this study was twofold; firstly, to assess the potential of the modern multispectral remote sensing sensors (i.e., Sentinel 2 and Landsat 8) in mapping grass senescence, and, secondly, to determine the optimal waveband positions for discriminating between senescent and non-senescent grasses based on the broadband multispectral remote sensing instruments with averaged resolutions. Modern multispectral remote sensing sensors are valuable in detecting autumn grassland senescence. For instance, the Sentinel 2 yielded an overall classification accuracy of 0.82 and kappa coefficient of 0.64, while the Landsat 8 obtained 0.78 and 0.56 for overall classification accuracy and kappa, respectively. The difference in the classification accuracies obtained between these two sensors could be accounted for by the variation in the number of spectral bands and the spatial properties jointly with the coverage of the REP by the Sentinel 2 sensor. With increased spectral bands, finer spatial resolution, and the coverage of the REP, the Sentinel 2 is better positioned to acquire more meaningful information, hence, the superior classification accuracies. These results attest to the finding by Shoko and Mutanga (2017a), who indicated that the Sentinel 2 yields superior classification outputs relative to Landsat 8. However, based on Matongera *et al.* (2017), the magnitude of difference in the obtainable classification accuracies between these two sensors is generally within the acceptable range (9%), and, thereby highlighting the fact that they can be used concurrently in mapping autumn grassland senescence.

In addition, the results of this study indicated that, although not clearly distinctive, the Sentinel 2's-based spectral profile of senescent grass was higher than that of non-senescent grass across the regions of the electromagnetic spectrum. Specifically, when using the Sentinel 2 multispectral

dataset, optimal separation between the spectra of senescent and non-senescent grass was achievable around the Visible green and red as well as the REP and the NIR regions of the spectrum. This could be attributed to the strategic positioning of the Sentinel 2 spectral bands (Frampton *et al.* 2013), which caters for the swift changes in the biochemical and biophysical properties of the plants during senescence (Baranoski and Rokne 2005; Gitelson and Merzlyak 1994). On the other hand, the Landsat 8-based spectral reflectance of senescent and non-senescent grass displayed high level of overlap in all the other regions except the Visible green and red bands. The identification of the Visible red band as one of the key regions in this study is in agreement with previous studies that reported that the Visible red region of the electromagnetic spectrum is highly sensitive to the dry properties of the vegetation (Wu *et al.* 2021; Jacques *et al.* 2014; Roberts *et al.* 1993). For instance, Dube *et al.* (2021) reported that the red band of the Landsat 8 was among the most important variables when classifying grass during the dry winter seasons. However, the performance of the NIR in separating between senescent and non-senescent grass was not superior based on the Landsat 8, and this could be attributed to the averaged spatial properties (i.e., 30 m) of the sensor as opposed to the finer spatial resolution (i.e., 10 m) of the Sentinel 2. However, the Visible green and red bands of the modern multispectral remote sensing do allow for meaningful classification of senescent and non-senescent grasslands. Equally, the REP proved to be among the sensitive regions of the electromagnetic spectrum for assessing autumn grassland senescence. Gitelson and Merzlyak (1996) and Gitelson *et al.* (1996), also discovered that the REP is important for explaining subtle changes in vegetation during senescence. Clear identification of these suitable waveband positions across the various regions of the electromagnetic spectrum is illustrated in figure 6.4.

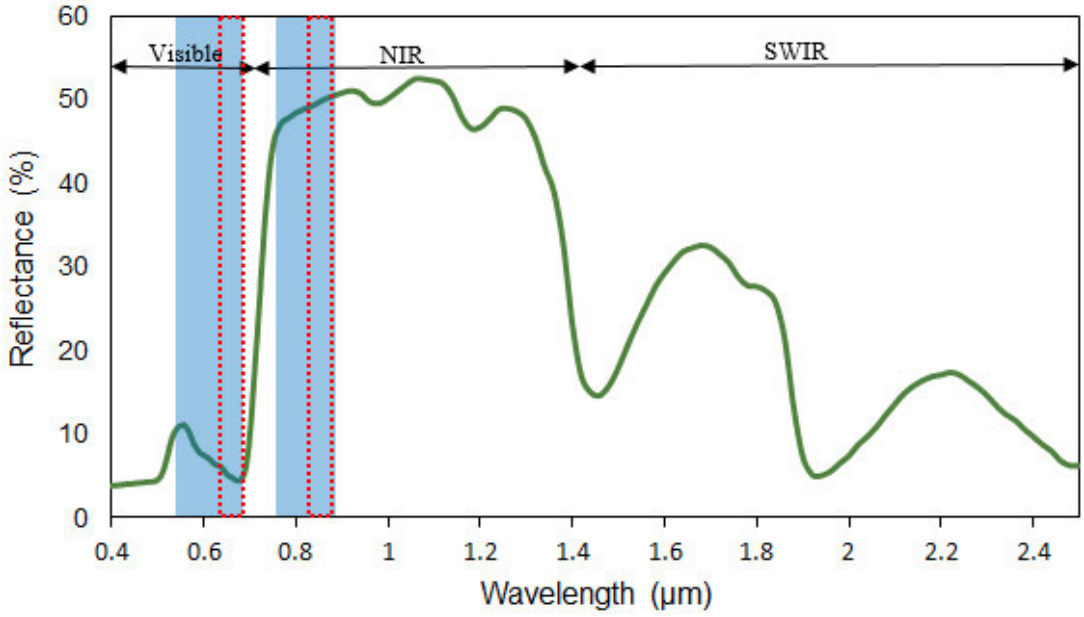

Figure 6.4 Typical spectral reflectance of the vegetation showing the sensitive waveband positions for discriminating between senescent and non-senescent grasses based on the broadband multispectral remote sensing dataset. The blue highlighted corresponds to the Sentinel 2 while the red dotted boxes indicates the Landsat 8 sensitive bands.

However, based on the results presented in this study, it should be noted that successful detection of autumn grassland senescence using remote sensing is not only a function of the spectral and spatial properties of the chosen sensor, but rather depended on the patch sizes of the senescent grass. For instance, the success of remote sensing sensors with bigger pixel sizes like the Landsat 8 (i.e., 30 m) in mapping autumn grassland senescence also relies on the availability of large senescent grass patches. This explains the reason why the bands of the Sentinel 2 including the NIR generally performed better than the Landsat 8 because of the finer spatial resolution (i.e., 10 m), which detected patches otherwise masked due to mixed-pixel problems in Landsat 8. Overall, these results have clearly demonstrated the contributions of the modern broadband multispectral remote sensing dataset in characterizing grass senescence. Given the benefits provided by these sensors, which include the large swath-width, free provision, and the improved spectral, spatial, temporal, and radiometric properties, among others, reliable assessment of rangeland resources can be guaranteed, even during the dry winter seasons when the quality and quantity of the forage is at minimum.

6.5 Conclusion

The present study has investigated the potential of the modern multispectral remote sensing dataset (i.e., Landsat 8 and Sentinel 2) in mapping autumn grassland senescence, as well as determining the optimal waveband positions for discriminating between senescent and non-senescent grass using the broadband multispectral remote sensing sensors. Using the robust non-parametric Random Forest classification approach, the study has shown that senescent grass can be separated from the non-senescent grass based on the Landsat 8 and Sentinel 2 multispectral remote sensing datasets with adequate accuracies. Again, the results of this study have indicated that the Visible green and red jointly with the REP and the NIR were the most suitable wavebands for mapping senescent grass based on Sentinel 2, while the Visible green and red were recognized as the most important wavebands based on the Landsat 8. The study has generally confirmed the value of the modern broadband multispectral remote sensing dataset with improve resolutions in characterizing senescent grass from adjacent non-senescent grass. These results are important for reliable monitoring of rangeland resources such as grasses even during the dry winter seasons when the quality and quantity of the forage has significantly declined because of senescence.

Chapter Seven

7 Remote sensing of grassland autumn senescence for foraging resource quality and quantity: a synthesis, conclusion and recommendations for future

7.1 Introduction

Precise detection of autumn grassland senescence is necessary, not only for the understanding of the associated impact on foraging resource quality and quantity, but also to gain insight on potential implications for fodder banks, particularly during dry seasons. Besides their ecological importance, grasslands are also valued for their provision of the livestock and wildlife feed (Meissner *et al.* 2013; Ramoelo *et al.* 2012; Knox *et al.* 2011). However, during senescence, the quality and quantity of the grass deteriorates (Das and Chaturvedi 2005), and, thereby, affecting the conditions and availability status of the subsequent forage. Although previous studies have indicated that grass leaves may senesce individually (Royimani *et al.* 2022), the impact of such senescing leaves is insignificant from a forage quality and quantity perspective due to its disjointed nature of occurrence as opposed to the uniform senescence of the entire grass plant in totality across the landscape. Consequently, research on grass senescence particularly with an intention to gain knowledge on associated impact on forage quality and quantity has been focused on the autumn grassland senescence which is relatively uniform across the landscape. The autumn grass senescence can be described as the seasonal wilting of the grass due to aging and the conditions associated with the autumn season (Mariën *et al.* 2019). Furthermore, the impact of autumn grass senescence on foraging resources is believed to be prevalent in sourveld than in sweetveld due to the inability of sourveld grass species to constantly hold nutrients during senescence (Zacharias 1995). This may present a greater risk of forage deficiencies, hence, livestock starvation. Also, with issues related to resource constrains for adoption of forage enhancement measures (e.g., fertilizer application and irrigation systems), which often delay senescence, the implications of autumn grassland senescence are expected to prevail in communal compared to commercial rangelands. One major socio-ecological benefit of autumn grassland senescence is its contribution to erosion reduction through shedding of leaves (Ackerly 1999; Kok *et al.* 1990). Therefore, studying the dynamics around the occurrence of autumn grassland senescence is critical for objective knowledge on the fodder banks as well as projections of potential forage shortages for the livestock and wildlife.

Data collection techniques for plant senescence assessment have by far relied on ground-based methods like field surveys and visual scoring of leaf coloration and fall and these are highly criticized for their limitation to small scale applications, associated cost and labour required, along with subjectivity (Anderegg *et al.* 2020; Mariën *et al.* 2019; Michelson *et al*. 2018). By contrast, with their "birds eye view" and repeated coverage in data acquisition (Sibanda *et al.* 2016), remote sensing offers plausible opportunities to explore dynamics around the occurrence of autumn grassland senescence in a timely, spatially and temporally explicit manner across the landscape. In addition, previous studies have embraced the use of plant chlorophyll – which is detectable through remote sensing means – as reliable proxy for monitoring vegetation senescence (Mariën *et al.* 2019). In light of the above given background, there is a need to consider the modern generation multispectral remote sensing datasets, including Sentinel 2 and Landsat 8, with improved spatial, spectral and temporal resolutions, jointly with broader areal and temporal coverages, in developing effective techniques to assess the dynamics around the occurrence of autumn grassland senescence. The importance of understanding the autumn grassland senescence, it's onset and environmental drivers as well as the associated impact on forage quality and quantity include the contribution to the knowledge on fodder bank capacities as well as the potential times of forage deficits. Such information is required to aid effective planning and decision-making by farmers, while equally forming a basis for policy formulation and development by government with regards to the availability status of free-ranging quality forage in the rangelands. Therefore, the objectives of this study were:

1. To provide a detailed overview on the progress of remote sensing applications in characterizing grass senescence and the possible challenges and opportunities.
2. To quantify the amount of decline in nGongoni (*Aristida junciformis*) grass quality and quantity owing to senescence using *in-situ* and Sentinel-2 data. Also, to assess forage availability status at pre-senescent and senescent stages based on the Dry Matter content (DM) of the grass.
3. To characterize the onset of autumn senescence in mesic subtropical sourveld grasslands using remotely sensed data.

4. To evaluate the correlation between remotely sensed autumn grass senescence and the climatic factors plus topography.
5. To test the potential of the modern multispectral remote sensing dataset (i.e., Sentinel 2 and Landsat) in mapping grass senescence, and to identify the optimal waveband positions that are suitable for discriminating between senescent and non-senescent grasses.

7.2 Exploration of remote sensing techniques and associated plant properties for detection of autumn senescence

Considering the increasing demand for meat and dairy products, as a result of population expansion (Kaliji *et al*., 2019) as well as the role of the livestock as a livelihood mechanism (Shoko *et al.* 2019), investigating the possible techniques for meaningful assessment of autumn grassland senescence in a spatially and temporally explicit manner at the landscape scale is an important undertaking. The significance of this study (chapter 2) was to provide a detailed overview on the progress of remote sensing applications in characterizing grass senescence and to highlight the associated challenges and opportunities. The findings indicated that effective characterization of plant senescence through remote sensing means is a function of monitoring the changes in key biochemical and biophysical properties of the floral species as indicators and these include, among others, biomass, chlorophyll content, leaf coloration and fall as well as LAI. Also, in contrast to the highly priced and small area coverage quality data of the high spatial and hyperspectral remote sensing instruments (Royimani *et al.* 2019a), the study indicated that the modern generation multispectral sensors like Sentinel 2 and Landsat 8 with better spatial, spectral, radiometric and temporal properties can benefit the detection of autumn grassland senescence. For instance, the Sentinel 2's 5-day revisit time is adequate to timely monitor changes in the chlorophyll content of the grass while the fine (10 m) spatial resolution and the REP are able to explain subtle changes in the concentration and distribution of pigments in the grass. In addition, the study noted that the advent of time-series algorithms such as the piecewise linear regression model with a breakpoint together with advanced and sophisticated models such as Random Forest is advantageous for ongoing and accurate characterization of autumn grassland senescence.

7.3 Quantifying the decrease in foraging resource quality and quantify due to senescence using Sentinel 2 and *in-situ* data

In order to understand the impact of grass senescence on foraging resource quality and quantity, this study (chapter 3) examined the amount of decrease in nGongoni (*Aristida junciformis*) grass quality and quantity due to senescence using *in-situ* and Sentinel 2 and the Random Forest Regression. This was attainable through estimating the quality and quantity of the grass at pre-senescence and senescence phenological stages and further assessed forage availability status at pre-senescence and senescence stages based on the Dry Matter content (DM) of the grass. The results demonstrated reasonable levels of accuracy in assessing pre-senescent and senescent grass quality and quantity. For instance, the Random Forest yielded R^2's of 91.3 and 96.6% as well as RMSEs of 2.12 and 0.55 µg Chl/cm^2 when explaining grass quality during pre-senescent and senescent stages, respectively. Again, the model obtained R^2's of 70.9 and 94.2% together with RMSEs of 0.34 and 0.02 kg/m^2 when predicting grass quantity at pre-senescent and senescent stages, respectively. The results further showed that optimal predictions of grass quality and quantity, both, at pre-senescent and senescent stages were achieved with the Red-Edge and its associated indices jointly with the Near Infrared (NIR) and red band derivatives. Furthermore, the findings exhibited a significant decrease in both quality (17.2 µg Chl/cm^2) and quantity (0.89 kg/m^2) of the nGongoni grass due to senescence. A total of 68.5 and 78.2 %/m^2 DM content was reported for the pre-senescent and the senescent nGongoni grasses.

7.4 Characterization of autumn senescence onset in sourveld grassland ecosystems based on remote sensing dataset

Given the reported remarkable decline in foraging resource quality and quantity following senescence (chapter 3), chapter 4 attempted to define the start date of autumn grassland senescence using remote sensing techniques and the piecewise linear regression model with a breakpoint. Using ten monthly vegetation indices derived from Sentinel 2, the study characterized the onset of autumn senescence in mesic subtropical sourveld grasslands. This was necessary to ascertain the duration of poor forage quality or the potential lifespan through which the provision of quality forage can be sustained in the rangeland. The findings suggested that the CHL-RED-EDGE and the $NDVI_{705}$ were the best proxies for characterizing the autumn grass senescence. When fitted in a piecewise linear regression model the $NDVI_{705}$ predicted that the grass in the study area starts senescing on day number ± 98 of the year (R^2 = 0.97, RMSE = 0.024) while the CHL-RED-EDGE

suggested day number ± 106 of the year (R^2 = 0.96, RMSE = 0.052). When averaging the two predicted dates, the findings indicated that the actual onset of autumn grassland senescence is on day number ± 102 of the year.

7.5 Evaluating the influence of climate and topography on autumn grassland senescence

Changes in climatic conditions and topography are among the primary drivers of the reported alterations and modifications in the physiology and phenology of the floral species (Shoko *et al.* 2019). Similarly, the use of climatic and topographic information can benefit the projection efforts of the occurrence of autumn grassland senescence. This is the case precisely because extreme weather events can lead to earlier or later senescence than normal, while higher altitudes often favour early grass senescence (Liu *et al.* 2016). Therefore, this study (chapter 5) examined the spatial correlation between remotely sensed autumn grass senescence *vis-a-vis* the climatic and topographic variables in the subtropical grasslands. Sentinel 2's $NDVI_{705}$ and CHL-RED-EDGE, as best proxies for explaining autumn grassland senescence in this area (chapter 4), were tested for sensitivity against climatic and topographic factors using the PLSR, the MLR, the CART and the RFR models. Specifically, the tested climatic factors were; T_{min}, T_{max}, rainfall, soil moisture, and solar radiation, while topographic features were; slope, elevation and aspect. The RFR outperformed all the other models. With regards to the environmental cues of autumn grassland senescence, the study showed that T_{max}, (p = 0.000 and 0.005 for the $NDVI_{705}$ and the CHL-RED-EDGE), T_{min} (p = 0.021 and 0.041 for the $NDVI_{705}$ and the CHL-RED-EDGE) and soil moisture (p = 0.031 and 0.040 for the $NDVI_{705}$ and the CHL-RED-EDGE) were the most influential autumn grass senescence drivers, whereas none of the topographic features displayed sensitivity. The study further noted that the poor influence exhibited by topography on autumn grassland senescence was site-specific due to issues related to the homogeneity of the landscape.

7.6 Testing the potential of the modern multispectral remote sensing in mapping grassland senescence and identifying the associated optimal wavebands for spectrally discriminating between senescent and non-senescent grasses

Although previous studies have demonstrated the contribution of remote sensing methods in assessing plant senescence (Anderegg *et al.* 2020; Mariën *et al.* 2019; Michelson *et al*. 2018), some key questions still remained unanswered. One of the questions relate to understanding suitable spatial and spectral windows, based on the readily available broadband multispectral dataset, for

optimal detection of autumn grassland senescence. Hence the current study (chapter 6) tested the potential of the modern multispectral remote sensing dataset (i.e., Sentinel 2 and Landsat 8) in mapping grass senescence and, in identifying optimal waveband positions that are suitable for discriminating between senescent and non-senescent grasses. In achieving this, the study employed the Random Forest classification algorithm. The findings indicated that overall classification accuracies of 0.82 and 0.78 and kappa coefficients of 0.64 and 0.56 were obtainable for Sentinel 2 and Landsat 8, respectively. Using the stepwise selection approach, the study further identified that the REP and the Visible green and red bands of the electromagnetic spectrum were the optimal waveband positions for separating between senescent and non-senescent grasses based on the broadband multispectral remote sensing, while the suitable spatial resolution depends on the patch size of the senescent grass.

7.7 Conclusion

Autumn grassland senescence is one of the key drivers of forage quality and quantity in rangeland ecosystems and remote sensing has played an instrumental role in providing a primary source of reliable quality data for this undertaking. The current study has, therefore, assessed the impact of autumn grass senescence on forage quality and quantity in subtropical sourveld grasslands of the Midlands communal rangelands, KwaZulu-Natal, South Africa, using the new generation broadband multispectral remote sensing instruments. Considering the projected shifts in climatic conditions in southern African, this was necessary in order to understand the impact of autumn grassland senescence not only on foraging resource quality but also on the fodder bank capacities. The findings of this study have demonstrated the role of the freely available modern multispectral remote sensing dataset with improved spectral, spatial, temporal and radiometric resolutions in optimally characterizing the dynamics around the autumn grassland senescence with reasonable accuracies. Specifically, the visible red, NIR and the REP as well as the $NDVI_{705}$ and CHL-RED-EDGE were generally identified as the most influential bands and indices for meaningful detection of autumn grassland ecosystem. Based on the results of this work, the following conclusions were drawn from each chapter (chapter 3 to 6):

1. The quality and quantity of foraging resources decreased by about 17.2 µg Chl/cm^2 and 0.89 kg/m^2, respectively, because of senescence.

2. The onset of autumn grassland senescence in the study area is on day number ± 102 of the year, which occurs in the month of April.
3. The occurrence of autumn grassland senescence in the study area is primarily controlled by macro-climatic conditions (i.e., T_{min}, T_{max}, and soil moisture) than topography.
4. The modern broadband multispectral remote sensing sensors with improved sensing properties are beneficial for effective monitoring of autumn grassland senescence, particularly the Visible green and red bands jointly with the REP. Moreover, the required spatial resolution for mapping autumn grassland senescence depends on the patch size of the senescent grass.

These results are critical as far as the availability and management efforts of free-ranging quality forage are concerned, particularly to ensure reliable livestock production systems among the small-holder farmers, who are often vulnerable due to challenges emanating from, among others, climate change, poor rangeland management methods and resource constraints. With this knowledge, the planning and decision-making of the farmers pertaining to grazing patterns and livestock numbers to be sustained in a particular veld can be significantly improved. In government and associated agencies, this information will help to support policy development with regards to sustainable utilization of foraging resources as the main source of free-ranging feed to the livestock, a key livelihood mechanism and a source of household wealth for many families.

7.8 Recommendations and the future

The findings of this study underline the relevance of the readily available broadband multispectral remotely sensed dataset in monitoring the dynamics of autumn grassland senescence. This is an important undertaking considering the impact of autumn senescence on foraging resources. However, in order to fully understand the potential impact of autumn grassland senescence in foraging resources including the livestock production system at the landscape scale, the following recommendations should be considered in future studies.

- Considering the success of Sentinel 2 in assessing dynamics around the autumn grass senescence coupled with the recent launch of Sentinel 3, which has a swath-width of 1270 km, these would enable the development of hybrid and fusion techniques for meaningful subcontinental detection of autumn grassland senescence, a task required for appropriate monitoring of foraging resources at the rangeland scale.

- The livestock numbers and grazing systems play a pivotal role in the availability status of foraging resources in rangeland environments. Therefore, future research should be on grazing systems used to assess possible irregularities between stocking densities, grazing systems and potential periods of forage deficiency, especially during dry seasons.
- The current study has revealed that only a handful of remote sensing studies has been conducted on grassland autumn senescence, however the majority are either based on snapshot or done during a single season. Taking the advantage of the free available high-temporal resolution Sentinel series data, future research should be focused on long-term understanding of the dynamics of autumn grass senescence.

Reference:

Abdel-Rahman, E. M., Mutanga, O., Adam, E. & Ismail, R. 2014. Detecting Sirex noctilio grey-attacked and lightning-struck pine trees using airborne hyperspectral data, random forest and support vector machines classifiers. *ISPRS Journal of Photogrammetry and Remote Sensing,* 88**,** 48-59.

Ackerly, D. 1999. Self-shading, carbon gain and leaf dynamics: a test of alternative optimality models. *Oecologia,* 119(3)**,** 300-310.

Adam, E., Mutanga, O. & Rugege, D. 2010. Multispectral and hyperspectral remote sensing for identification and mapping of wetland vegetation: a review. *Wetlands Ecology and Management,* 18(3)**,** 281-296.

Adamsen, F., Pinter, P. J., Barnes, E. M., LaMorte, R. L., Wall, G. W., Leavitt, S. W. & Kimball, B. A. 1999. Measuring wheat senescence with a digital camera. *Crop Science,* 39(3)**,** 719-724.

Adelabu, S. & Dube, T. 2015. Employing ground and satellite-based QuickBird data and random forest to discriminate five tree species in a Southern African Woodland. *Geocarto International,* 30(4)**,** 457-471.

Adjorlolo, C., Mutanga, O., Cho, M. & Ismail, R. 2012. Challenges and opportunities in the use of remote sensing for C3 and C4 grass species discrimination and mapping. *African Journal of Range & Forage Science,* 29(2)**,** 47-61.

Anderegg, J., Yu, K., Aasen, H., Walter, A., Liebisch, F. & Hund, A. 2020. Spectral vegetation indices to track senescence dynamics in diverse wheat germplasm. *Frontiers in plant science,* 10**,** 1749.

Archibald, S. & Scholes, R. 2007. Leaf green-up in a semi-arid African savanna-separating tree and grass responses to environmental cues. *Journal of Vegetation Science,* 18(4)**,** 583-594.

Asner, G. P., Townsend, A. R., Bustamante, M. M., Nardoto, G. B. & Olander, L. P. 2004. Pasture degradation in the central Amazon: linking changes in carbon and nutrient cycling with remote sensing. *Global Change Biology,* 10(5)**,** 844-862.

Asrar, G., Kanemasu, E. T., Miller, G. P. & Weiser, R. 1986a. Light interception and leaf area estimates from measurements of grass canopy reflectance. *IEEE Transactions on Geoscience and Remote Sensing,* (1)**,** 76-82.

Asrar, G., Weiser, R., Johnson, D., Kanemasu, E. & Killeen, J. 1986b. Distinguishing among tallgrass prairie cover types from measurements of multispectral reflectance. *Remote Sensing of Environment,* 19(2)**,** 159-169.

Ayantunde, A. A., Asse, R., Said, M. Y. & Fall, A. 2014. Transhumant pastoralism, sustainable management of natural resources and endemic ruminant livestock in the sub-humid zone of West Africa. *Environment, development and sustainability,* 16(5)**,** 1097-1117.

Baranoski, G. & Rokne, J. 2005. A practical approach for estimating the red edge position of plant leaf reflectance. *International Journal of Remote Sensing,* 26(3)**,** 503-521.

Bartlett, D. S., Whiting, G. J. & Hartman, J. M. 1989. Use of vegetation indices to estimate indices to estimate intercepted solar radiation and net carbon dioxide exchange of a grass canopy. *Remote Sensing of Environment,* 30(2)**,** 115-128.

Ben-Dor, E., Inbar, Y. & Chen, Y. 1997. The reflectance spectra of organic matter in the visible near-infrared and short wave infrared region (400–2500 nm) during a controlled decomposition process. *Remote Sensing of Environment,* 61(1)**,** 1-15.

Bennett, J., Ainslie, A. & Davis, J. 2010. Fenced in: Common property struggles in the management of communal rangelands in central Eastern Cape Province, South Africa. *Land Use Policy,* 27(2)**,** 340-350.

Berdugo, C. A., Mahlein, A.-K., Steiner, U., Dehne, H.-W. & Oerke, E.-C. 2013. Sensors and imaging techniques for the assessment of the delay of wheat senescence induced by fungicides. *Functional Plant Biology,* 40(7)**,** 677-689.

Bertin, R.I., 2008. Plant phenology and distribution in relation to recent climate change. *The Journal of the Torrey Botanical Society*, *135*(1), pp.126-146.

Blackburn, G. A. 1998. Quantifying chlorophylls and caroteniods at leaf and canopy scales: An evaluation of some hyperspectral approaches. *Remote sensing of environment,* 66(3)**,** 273-285.

Bork, E. W., West, N. E. & Price, K. P. 1999. Calibration of broad-and narrow-band spectral variables for rangeland cover component quantification. *International Journal of Remote Sensing,* 20(18)**,** 3641-3662.

Boyer, M., Miller, J., Belanger, M., Hare, E. & Wu, J. 1988. Senescence and spectral reflectance in leaves of northern pin oak (Quercus palustris Muenchh.). *Remote Sensing of Environment,* 25(1)**,** 71-87.

Bradley, B. A. 2014. Remote detection of invasive plants: a review of spectral, textural and phenological approaches. *Biological invasions,* 16(7)**,** 1411-1425.

Bremer, D. J., Lee, H., Su, K. & Keeley, S. J. 2011. Relationships between NDVI and visual quality in cool-season turfgrass: II. Factors affecting NDVI and its component reflectances. *Crop Science,* 51(5)**,** 2219-2227.

Brown, S. & Shrestha, B. 2000. Market-driven land-use dynamics in the middle mountains of Nepal. *Journal of Environmental Management,* 59(3)**,** 217-225.

Buchanan-Wollaston, V., Earl, S., Harrison, E., Mathas, E., Navabpour, S., Page, T. & Pink, D. 2003. The molecular analysis of leaf senescence–a genomics approach. *Plant biotechnology journal,* 1(1)**,** 3-22.

Butterfield, H. & Malmström, C. 2009. The effects of phenology on indirect measures of aboveground biomass in annual grasses. *International Journal of Remote Sensing,* 30(12)**,** 3133-3146.

Cai, J., Okamoto, M., Atieno, J., Sutton, T., Li, Y. & Miklavcic, S. J. 2016. Quantifying the onset and progression of plant senescence by color image analysis for high throughput applications. *PLoS One,* 11(6)**,** e0157102.

Carbutt, C., Tau, M., Stephens, A. & Escott, B. 2011. The conservation status of temperate grasslands in southern Africa. *Grassroots,* 11(1)**,** 17-23.

Castro, K. & Sanchez-Azofeifa, G. 2008. Changes in spectral properties, chlorophyll content and internal mesophyll structure of senescing Populus balsamifera and Populus tremuloides leaves. *Sensors,* 8(1)**,** 51-69.

Ceccato, P., Flasse, S., Tarantola, S., Jacquemoud, S. & Grégoire, J.-M. 2001. Detecting vegetation leaf water content using reflectance in the optical domain. *Remote sensing of environment,* 77(1)**,** 22-33.

Chaerle, L. & Van Der Straeten, D. 2000. Imaging techniques and the early detection of plant stress. *Trends in plant science,* 5(11)**,** 495-501.

Chan, J. C.-W. & Paelinckx, D. 2008. Evaluation of Random Forest and Adaboost tree-based ensemble classification and spectral band selection for ecotope mapping using airborne hyperspectral imagery. *Remote Sensing of Environment,* 112(6)**,** 2999-3011.

Chemura, A., Mutanga, O. & Odindi, J. Year: Published. Modelling Leaf Chlorophyll Content in Coffee (Coffea Arabica) Plantations Using Sentinel 2 Msi Data. *IGARSS 2018-2018 IEEE International Geoscience and Remote Sensing Symposium*. IEEE, 8228-8231.

Clark, R. N., King, T. V., Ager, C. & Swayze, G. A. Year: Published. Initial vegetation species and senescence/stress indicator mapping in the San Luis Valley, Colorado using imaging spectrometer data. *Summitville Forum'95*. Colorado Geological Survey Special Publication Denver, CO, 64-69.

Clark, R. N., King, T. V., Ager, C. & Swayze, G. A. 1995b. Initial vegetation species and senescience/stress indicator mapping in the San Luis Valley, Colorado using imaging spectrometer data.

Cole, B., McMorrow, J. & Evans, M. 2014. Spectral monitoring of moorland plant phenology to identify a temporal window for hyperspectral remote sensing of peatland. *ISPRS journal of photogrammetry and remote sensing,* 90**,** 49-58.

Corbane, C., Raclot, D., Jacob, F., Albergel, J. & Andrieux, P. 2008. Remote sensing of soil surface characteristics from a multiscale classification approach. *Catena,* 75(3)**,** 308-318.

Cousins, B. 1999. Invisible capital: The contribution of communal rangelands to rural livelihoods in South Africa. *Development Southern Africa,* 16(2)**,** 299-318.

Curran, P. 1980. Multispectral remote sensing of vegetation amount. *Progress in physical geography,* 4(3)**,** 315-341.

Darbes, L.A., Van Rooyen, H., Hosegood, V., Ngubane, T., Johnson, M.O., Fritz, K., & Mcgrath, N. 2014. Uthando Lwethu ("our love"): A Protocol for a Couples-Based Intervention to Increase Testing for HIV: A Randomised Controlled Trial in rural KwaZulu-Natal, South Africa. *BioMed Central*, 15 (64), pp 1-15. Available from: http://www.trialsjournal.com/content/15/1/64.

Das, D. & Chaturvedi, O. 2005. Structure and function of Populus deltoides agroforestry systems in eastern India: 2. Nutrient dynamics. *Agroforestry systems,* 65(3)**,** 223-230.

Dash, J., Curran, P., Tallis, M., Llewellyn, G., Taylor, G. & Snoeij, P. 2010. Validating the MERIS Terrestrial Chlorophyll Index (MTCI) with ground chlorophyll content data at MERIS spatial resolution. *International Journal of Remote Sensing,* 31(20)**,** 5513-5532.

Day, F. P. 1983. Effects of flooding on leaf litter decomposition in microcosms. *Oecologia,* 56(2-3)**,** 180-184.

De Waal, H. 1990. Animal production from native pasture (veld) in the Free State Region-a perspective of the grazing ruminant. *South African Journal of Animal Science,* 20(1)**,** 1-9.

Dertinger, U., Schaz, U. & Schulze, E. D. 2003. Age-dependence of the antioxidative system in tobacco with enhanced glutathione reductase activity or senescence-induced production of cytokinins. *Physiologia Plantarum,* 119(1)**,** 19-29.

Di Bella, C. M., Paruelo, J. M., Becerra, J., Bacour, C. & Baret, F. 2004. Effect of senescent leaves on NDVI-based estimates of f APAR: Experimental and modelling evidences. *International Journal of Remote Sensing,* 25(23)**,** 5415-5427.

Dong, T., Meng, J., Shang, J., Liu, J. & Wu, B. 2015. Evaluation of chlorophyll-related vegetation indices using simulated Sentinel-2 data for estimation of crop fraction of absorbed photosynthetically active radiation. *IEEE Journal of Selected Topics in Applied Earth Observations and Remote Sensing,* 8(8)**,** 4049-4059.

Dube, T. & Mutanga, O. 2016. The impact of integrating WorldView-2 sensor and environmental variables in estimating plantation forest species aboveground biomass and carbon stocks in uMgeni Catchment, South Africa. *ISPRS Journal of Photogrammetry and Remote Sensing,* 119**,** 415-425.

Dube, T., Onisimo, M. & Riyad, I. 2016. Quantifying aboveground biomass in African environments: A review of the trade-offs between sensor estimation accuracy and costs. *Tropical Ecology,* 57(3)**,** 393-405.

Dube, T., Shoko, C. & Gara, T. W. 2021. Remote sensing of aboveground grass biomass between protected and non-protected areas in savannah rangelands. *African Journal of Ecology*.

Egeru, A., Wasonga, O., Gabiri, G., MacOpiyo, L., Mburu, J. & Mwanjalolo Majaliwa, J. G. 2019. Land cover and soil properties influence on forage quantity in a semiarid region in East Africa. *Applied and Environmental Soil Science,* 2019.

Ellery, W., Scholes, R. & Scholes, M. 1995. The distribution of sweetveld and sourveld in South Africa's grassland biome in relation to environmental factors. *African Journal of Range & Forage Science,* 12(1)**,** 38-45.

Elvidge, C. D. 1990. Visible and near infrared reflectance characteristics of dry plant materials. *Remote Sensing,* 11(10)**,** 1775-1795.

Fataftah, N., Edlund, E., Lihavainen, J., Bag, P., Björkén, L., Näsholm, T. & Jansson, S. 2021. Nitrate fertilization may delay autumn leaf senescence, while amino acid treatments do not. *bioRxiv*.

Forsyth, G., Kruger, F. & Le Maitre, D. 2010. National veldfire risk assessment: Analysis of exposure of social, economic and environmental assets to veldfire hazards in South Africa. *National Resources and the Environment CSIR, Fred Kruger Consulting cc*.

Fracheboud, Y., Luquez, V., Bjorken, L., Sjodin, A., Tuominen, H. & Jansson, S. 2009. The control of autumn senescence in European aspen. *Plant physiology,* 149(4)**,** 1982-1991.

Frampton, W. J., Dash, J., Watmough, G. & Milton, E. J. 2013. Evaluating the capabilities of Sentinel-2 for quantitative estimation of biophysical variables in vegetation. *ISPRS journal of photogrammetry and remote sensing,* 82**,** 83-92.

Fuhlendorf, S. D. & Engle, D. M. 2001. Restoring heterogeneity on rangelands: ecosystem management based on evolutionary grazing patterns: we propose a paradigm that enhances heterogeneity instead of homogeneity to promote biological diversity and wildlife habitat on rangelands grazed by livestock. *BioScience,* 51(8)**,** 625-632.

Fynn, R., Morris, C., Ward, D. & Kirkman, K. 2011. Trait–environment relations for dominant grasses in South African mesic grassland support a general leaf economic model. *Journal of Vegetation Science,* 22(3)**,** 528-540.

Gao, Y. & Li, D. 2015. Assessing leaf senescence in tall fescue (Festuca arundinacea Schreb.) under salinity stress using leaf spectrum. *Eur J Hortic Sci,* 80(4)**,** 170-176.

Gepstein, S., Sabehi, G., Carp, M. J., Hajouj, T., Nesher, M. F. O., Yariv, I., Dor, C. & Bassani, M. 2003. Large-scale identification of leaf senescence-associated genes. *The Plant Journal,* 36(5)**,** 629-642.

Gitelson, A. & Merzlyak, M. N. 1994. Spectral reflectance changes associated with autumn senescence of Aesculus hippocastanum L. and Acer platanoides L. leaves. Spectral features and relation to chlorophyll estimation. *Journal of plant physiology,* 143(3)**,** 286-292.

Gitelson, A. A. & Merzlyak, M. N. 1996. Signature analysis of leaf reflectance spectra: algorithm development for remote sensing of chlorophyll. *Journal of plant physiology,* 148(3-4)**,** 494-500.

Gitelson, A. A., Merzlyak, M. N. & Lichtenthaler, H. K. 1996. Detection of red edge position and chlorophyll content by reflectance measurements near 700 nm. *Journal of plant physiology,* 148(3-4)**,** 501-508.

Gómez-Giráldez, P. J., Pérez-Palazón, M. J., Polo, M. J. & González-Dugo, M. P. 2020. Monitoring Grass Phenology and Hydrological Dynamics of an Oak–Grass Savanna Ecosystem Using Sentinel-2 and Terrestrial Photography. *Remote Sensing,* 12(4)**,** 600.

Goodchild, M., Kühn, K. & Jenkins, M. 2014. Delta-T Devices.

Govender, V. & Qwabe, B.R., 2022. Local Economic Development and Rural Women in A Development Paradigm: A Perspective of Vulindlela in Kwazulu-Natal, South Africa. *Journal of Southwest Jiaotong University*, *57*(5).

Gregersen, P., Holm, P. & Krupinska, K. 2008. Leaf senescence and nutrient remobilisation in barley and wheat. *Plant Biology,* 10**,** 37-49.

Guerini Filho, M., Kuplich, T. M. & Quadros, F. L. D. 2020. Estimating natural grassland biomass by vegetation indices using Sentinel 2 remote sensing data. *International Journal of Remote Sensing,* 41(8)**,** 2861-2876.

Guo, Y., Cai, Z. & Gan, S. 2004. Transcriptome of Arabidopsis leaf senescence. *Plant, cell & environment,* 27(5)**,** 521-549.

Guo, Y. & Gan, S.-S. 2014. Translational researches on leaf senescence for enhancing plant productivity and quality. *Journal of Experimental Botany,* 65(14)**,** 3901-3913.

Hardy, M., Meissner, H. & O'Reagain, P. 1997. Forage intake and free-ranging ruminants: A tropical perspective. *Proc. Int. Grassl. Congrees 18th, Winnepeg, and Saskatoon, Canada. Assoc. Manage. Centre, Calgary, AB, Canada. pp***,** 45-52.

Havstad, K. M., Peters, D. P., Skaggs, R., Brown, J., Bestelmeyer, B., Fredrickson, E., Herrick, J. & Wright, J. 2007. Ecological services to and from rangelands of the United States. *Ecological Economics,* 64(2)**,** 261-268.

Hemminga, M., Marba, N. & Stapel, J. 1999. Leaf nutrient resorption, leaf lifespan and the retention of nutrients in seagrass systems. *Aquatic Botany,* 65(1-4)**,** 141-158.

Herrero, M., Grace, D., Njuki, J., Johnson, N., Enahoro, D., Silvestri, S. & Rufino, M. C. 2013. The roles of livestock in developing countries. *animal,* 7(s1)**,** 3-18.

Heumann, B. W., Seaquist, J., Eklundh, L. & Jönsson, P. 2007. AVHRR derived phenological change in the Sahel and Soudan, Africa, 1982–2005. *Remote Sensing of Environment,* 108(4)**,** 385-392.

Hunt Jr, E. R., Daughtry, C. S. & Li, L. 2016. Feasibility of estimating leaf water content using spectral indices from WorldView-3's near-infrared and shortwave infrared bands. *International Journal of Remote Sensing,* 37(2)**,** 388-402.

Isikhungusethu Environmental Services (Pty) Ltd. 2016. *Vulindlela Local Area Plan Spatial Framework report*. Available from: Isikhungusethu Environmental Services (Pty) Ltd. [Access from: http://www.msunduzi.gov.za/site/search/downloadencode/vulindlela%20LAP.pdf; 26 February 2016].

Ismail, R., Crous, J., Sale, G., Morris, A. R. & Peerbhay, K. Y. 2021. Developing a satellite-based frost risk model for the Southern African commercial forestry landscape. *Southern Forests: a Journal of Forest Science,* 83(1)**,** 10-18.

Jacques, D. C., Kergoat, L., Hiernaux, P., Mougin, E. & Defourny, P. 2014. Monitoring dry vegetation masses in semi-arid areas with MODIS SWIR bands. *Remote sensing of environment,* 153**,** 40-49.

Jones-Farrand, D. T., Burger Jr, L. W., Johnson, D. H. & Ryan, M. R. 2007. Grassland establishment for wildlife conservation. *USGS Northern Prairie Wildlife Research Center***,** 202.

Kaliji, S.A., Mojaverian, S.M., Amirnejad, H. & Canavari, M. 2019. Factors affecting consumers' dairy products preferences. *AGRIS on-line Papers in Economics and Informatics,* 11(2), pp.3-11.

Karlson, M. & Ostwald, M. 2016. Remote sensing of vegetation in the Sudano-Sahelian zone: A literature review from 1975 to 2014. *Journal of Arid Environments,* 124**,** 257-269.

Kiguli, L., Palmer, A. & Avis, A. 1999. A description of rangeland on commercial and communal land, Peddie district, South Africa. *African journal of range and forage science,* 16(2-3)**,** 89-95.

Kim, J., Woo, H. R. & Nam, H. G. 2016. Toward systems understanding of leaf senescence: an integrated multi-omics perspective on leaf senescence research. *Molecular plant,* 9(6)**,** 813-825.

Knox, N. M., Skidmore, A. K., Prins, H. H., Asner, G. P., van der Werff, H. M., de Boer, W. F., van der Waal, C., de Knegt, H. J., Kohi, E. M. & Slotow, R. 2011. Dry season mapping of savanna forage quality, using the hyperspectral Carnegie Airborne Observatory sensor. *Remote sensing of environment,* 115(6)**,** 1478-1488.

Kok, C., Van der Velde, G. & Landsbergen, K. 1990. Production, nutrient dynamics and initial decomposition of floating leaves of Nymphaea alba L. and Nuphar lutea (L.) Sm.(Nymphaeaceae) in alkaline and acid waters. *Biogeochemistry,* 11(3)**,** 235-250.

Kuenzer, C., Klein, I., Ullmann, T., Foufoula Georgiou, E., Baumhauer, R. & Dech, S. 2015. Remote sensing of river delta inundation: Exploiting the potential of coarse spatial resolution, temporally-dense MODIS time series. *Remote Sensing*, *7*(7), pp.8516-8542.

Kumar, L., Skidmore, A. K. & Knowles, E. 1997. Modelling topographic variation in solar radiation in a GIS environment. *International journal of geographical information science,* 11(5)**,** 475-497.

Laliberte, A., Rango, A., Herrick, J., Fredrickson, E. L. & Burkett, L. 2007. An object-based image analysis approach for determining fractional cover of senescent and green vegetation with digital plot photography. *Journal of Arid Environments,* 69(1)**,** 1-14.

Lang, W., Chen, X., Liang, L., Ren, S. & Qian, S. 2019. Geographic and Climatic Attributions of Autumn Land Surface Phenology Spatial Patterns in the Temperate Deciduous Broadleaf Forest of China. *Remote Sensing,* 11(13)**,** 1546.

Lim, P. O., Kim, H. J. & Gil Nam, H. 2007. Leaf senescence. *Annu. Rev. Plant Biol.,* 58**,** 115-136.

Lim, P. O. & Nam, H. G. 2007. Aging and senescence of the leaf organ. *Journal of Plant Biology,* 50(3)**,** 291-300.

Little, I. T., Hockey, P. A. & Jansen, R. 2015. Impacts of fire and grazing management on South Africa's moist highland grasslands: A case study of the Steenkampsberg Plateau, Mpumalanga, South Africa. *Bothalia-African Biodiversity & Conservation,* 45(1)**,** 1-15.

Liu, G., Chen, X., Zhang, Q., Lang, W. & Delpierre, N. 2018. Antagonistic effects of growing season and autumn temperatures on the timing of leaf coloration in winter deciduous trees. *Global Change Biology,* 24(8)**,** 3537-3545.

Liu, J., Yang, X., Liu, H. L. & Qiao, Z. Year: Published. Algorithms and applications in grass growth monitoring. *Abstract and Applied Analysis*. Hindawi.

Liu, Q., Fu, Y. H., Zeng, Z., Huang, M., Li, X. & Piao, S. 2016. Temperature, precipitation, and insolation effects on autumn vegetation phenology in temperate China. *Global change biology,* 22(2)**,** 644-655.

Liu, Y., Zhang, Z., Tong, L., Khalifa, M., Wang, Q., Gang, C., Wang, Z., Li, J. & Sun, Z. 2019. Assessing the effects of climate variation and human activities on grassland degradation and restoration across the globe. *Ecological Indicators,* 106**,** 105504.

Lohman, K. N., Gan, S., John, M. C. & Amasino, R. M. 1994. Molecular analysis of natural leaf senescence in Arabidopsis thaliana. *Physiologia Plantarum,* 92(2)**,** 322-328.

Makanza, R., Zaman-Allah, M., Cairns, J. E., Magorokosho, C., Tarekegne, A., Olsen, M. & Prasanna, B. M. 2018. High-throughput phenotyping of canopy cover and senescence in maize field trials using aerial digital canopy imaging. *Remote Sensing,* 10(2)**,** 330.

Mansour, K., Mutanga, O., Everson, T. & Adam, E. 2012. Discriminating indicator grass species for rangeland degradation assessment using hyperspectral data resampled to AISA Eagle resolution. *ISPRS Journal of Photogrammetry and Remote Sensing,* 70**,** 56-65.

Mariën, B., Balzarolo, M., Dox, I., Leys, S., Lorène, M. J., Geron, C., Portillo-Estrada, M., AbdElgawad, H., Asard, H. & Campioli, M. 2019. Detecting the onset of autumn leaf senescence in deciduous forest trees of the temperate zone. *New Phytologist,* 224(1)**,** 166-176.

Mariën, B., Dox, I., De Boeck, H. J., Willems, P., Leys, S., Papadimitriou, D. & Campioli, M. 2021. Does drought advance the onset of autumn leaf senescence in temperate deciduous forest trees? *Biogeosciences,* 18(11)**,** 3309-3330.

Marsett, R. C., Qi, J., Heilman, P., Biedenbender, S. H., Watson, M. C., Amer, S., Weltz, M., Goodrich, D. & Marsett, R. 2006. Remote sensing for grassland management in the arid southwest. *Rangeland Ecology & Management,* 59(5)**,** 530-540.

Matongera, T. N., Mutanga, O., Dube, T. & Lottering, R. T. 2018. Detection and mapping of bracken fern weeds using multispectral remotely sensed data: a review of progress and challenges. *Geocarto International,* 33(3)**,** 209-224.

Matongera, T. N., Mutanga, O., Dube, T. & Sibanda, M. 2017. Detection and mapping the spatial distribution of bracken fern weeds using the Landsat 8 OLI new generation sensor. *International journal of applied earth observation and geoinformation,* 57**,** 93-103.

McKean, J., Buechel, S. & Gaydos, L. 1991. Remote sensing and landslide hazard assessment. *Photogrammetric engineering and remote sensing,* 57(9)**,** 1185-1193.

Meissner, H., Scholtz, M. & Palmer, A. 2013. Sustainability of the South African livestock sector towards 2050 Part 1: Worth and impact of the sector. *South African Journal of Animal Science,* 43(3)**,** 282-297.

Meneghini, A. 2019. An Evaluation of Sentinel-1 and Sentinel-2 for Land Cover Classification.

Merzlyak, M. N., Gitelson, A. A., Chivkunova, O. B. & Rakitin, V. Y. 1999. Non-destructive optical detection of pigment changes during leaf senescence and fruit ripening. *Physiologia plantarum,* 106(1)**,** 135-141.

Michelson, I. H., Ingvarsson, P. K., Robinson, K. M., Edlund, E., Eriksson, M. E., Nilsson, O. & Jansson, S. 2018. Autumn senescence in aspen is not triggered by day length. *Physiologia Plantarum,* 162(1)**,** 123-134.

Molle, G., Decandia, M., Giovanetti, V., Cabiddu, A., Fois, N. & Sitzia, M. 2009. Responses to condensed tannins of flowering sulla (Hedysarum coronarium L.) grazed by dairy sheep: Part 1: Effects on feeding behaviour, intake, diet digestibility and performance. *Livestock Science,* 123(2-3)**,** 138-146.

Moore, C. E., Brown, T., Keenan, T. F., Duursma, R. A., Van Dijk, A. I., Beringer, J., Culvenor, D., Evans, B., Huete, A. & Hutley, L. B. 2016. Reviews and syntheses: Australian vegetation phenology: new insights from satellite remote sensing and digital repeat photography. *Biogeosciences,* 13(17)**,** 5085-5102.

Morley, P. J., Jump, A. S., West, M. D. & Donoghue, D. N. 2020. Spectral response of chlorophyll content during leaf senescence in European beech trees. *Environmental Research Communications,* 2(7)**,** 071002.

Mucina, L., Rutherford, M. C. & Powrie, L. W. 2006. Vegetation Atlas of South Africa, Lesotho and Swaziland. *The Vegetation of South Africa, Lesotho and Swaziland'.(Eds L. Mucina and MC Rutherford.) pp***,** 748-789.

Munné-Bosch, S. & Alegre, L. 2004. Die and let live: leaf senescence contributes to plant survival under drought stress. *Functional Plant Biology,* 31(3)**,** 203-216.

Mutanga, O., Adam, E. & Cho, M. A. 2012. High density biomass estimation for wetland vegetation using WorldView-2 imagery and random forest regression algorithm. *International Journal of Applied Earth Observation and Geoinformation,* 18**,** 399-406.

Mutanga, O. & Shoko, C. Year: Published. Monitoring the Spatio-Temporal Variations of C3/C4 Grass Species Using Multispectral Satellite Data. *IGARSS 2018-2018 IEEE International Geoscience and Remote Sensing Symposium*. IEEE, 8988-8991.

Mutanga, O. & Skidmore, A. K. 2004. Narrow band vegetation indices overcome the saturation problem in biomass estimation. *International journal of remote sensing,* 25(19)**,** 3999-4014.

Mutanga, O., Skidmore, A. K. & Van Wieren, S. 2003. Discriminating tropical grass (Cenchrus ciliaris) canopies grown under different nitrogen treatments using spectroradiometry. *ISPRS Journal of Photogrammetry and Remote Sensing,* 57(4)**,** 263-272.

Nagler, P., Daughtry, C. & Goward, S. 2000. Plant litter and soil reflectance. *Remote Sensing of Environment,* 71(2)**,** 207-215.

Ndlovu, M., Clulow, A. D., Savage, M. J., Nhamo, L., Magidi, J. & Mabhaudhi, T. 2021. An assessment of the impacts of climate variability and change in KwaZulu-Natal Province, South Africa. *Atmosphere,* 12(4)**,** 427.

Niroula, A., Khatri, S., Timilsina, R., Khadka, D., Khadka, A. & Ojha, P. 2019. Profile of chlorophylls and carotenoids of wheat (Triticum aestivum L.) and barley (Hordeum vulgare L.) microgreens. *Journal of food science and technology,* 56(5)**,** 2758-2763.

Nkonya, E., Mirzabaev, A. & Von Braun, J. 2016. *Economics of land degradation and improvement–A global assessment for sustainable development*, Springer Nature.

O'Connor, R. C., Taylor, J. H. & Nippert, J. B. 2020. Browsing and fire decreases dominance of a resprouting shrub in woody encroached grassland. *Ecology,* 101(2)**,** e02935.

Oba, G. 2012. Harnessing pastoralists' indigenous knowledge for rangeland management: three African case studies. *Pastoralism: Research, Policy and Practice,* 2(1)**,** 1-25.

Odebiri, O., Mutanga, O., Odindi, J., Peerbhay, K. & Dovey, S. 2020. Predicting soil organic carbon stocks under commercial forest plantations in KwaZulu-Natal province, South Africa using remotely sensed data. *GIScience & remote sensing,* 57(4)**,** 450-463.

Odindi, J., Adam, E., Ngubane, Z., Mutanga, O. & Slotow, R. 2014. Comparison between WorldView-2 and SPOT-5 images in mapping the bracken fern using the random forest algorithm. *Journal of Applied Remote Sensing,* 8(1)**,** 083527-083527.

Odindi, J. & Kakembo, V. 2011. The hydrological response of Pteronia incana-invaded areas in the Eastern Cape Province, South Africa. *Ecohydrology,* 4(6)**,** 832-840.

Odindi, J., Mutanga, O., Rouget, M. & Hlanguza, N. 2016. Mapping alien and indigenous vegetation in the KwaZulu-Natal Sandstone Sourveld using remotely sensed data. *Bothalia-African Biodiversity & Conservation,* 46(2)**,** 1-9.

Olusegun, A. M., Dikko, H. G. & Gulumbe, S. U. 2015. Identifying the limitation of stepwise selection for variable selection in regression analysis. *American Journal of Theoretical and Applied Statistics,* 4(5)**,** 414-419.

Oudtshoorn, F. v. 1999. *Guide to grasses of southern Africa*, Briza publications.

Partridge, L. & Barton, N. H. 1996. On measuring the rate of ageing. *Proceedings of the Royal Society of London. Series B: Biological Sciences,* 263(1375)**,** 1365-1371.

Peddie, G. 1995. Vigour of sourveld in response to cattle and sheep grazing. *Bulletin of the Grassland Society of Southern Africa*.

Peñuelas, J. & Filella, I. 1998. Visible and near-infrared reflectance techniques for diagnosing plant physiological status. *Trends in plant science,* 3(4)**,** 151-156.

Pickup, G. 1996. Estimating the effects of land degradation and rainfall variation on productivity in rangelands: an approach using remote sensing and models of grazing and herbage dynamics. *Journal of Applied Ecology***,** 819-832.

Purdy, S. J., Cunniff, J., Maddison, A. L., Jones, L. E., Barraclough, T., Castle, M., Davey, C. L., Jones, C. M., Shield, I. & Gallagher, J. 2015. Seasonal carbohydrate dynamics and climatic regulation of senescence in the perennial grass, Miscanthus. *BioEnergy Research,* 8(1)**,** 28-41.

Qi, J., Marsett, R., Heilman, P., Bieden-bender, S., Moran, S., Goodrich, D. & Weltz, M. 2002. RANGES improves satellite-based information and land cover assessments in southwest United States. *Eos, Transactions American Geophysical Union,* 83(51)**,** 601-606.

Rabumbulu, M. & Badenhorst, M. 2017. Land degradation in the West-Central Free State: human-induced or climate variability, the perceptions of Abrahamskraal–Boshof district farmers. *South African Geographical Journal,* 99(3)**,** 217-234.

Ramoelo, A. & Cho, M. A. 2014. Dry season biomass estimation as an indicator of rangeland quantity using multi-scale remote sensing data.

Ramoelo, A., Cho, M. A., Mathieu, R., Madonsela, S., Van De Kerchove, R., Kaszta, Z. & Wolff, E. 2015. Monitoring grass nutrients and biomass as indicators of rangeland quality and quantity using random forest modelling and WorldView-2 data. *International Journal of Applied Earth Observation and Geoinformation,* 43**,** 43-54.

Ramoelo, A., Skidmore, A. K., Cho, M. A., Schlerf, M., Mathieu, R. & Heitkönig, I. M. 2012. Regional estimation of savanna grass nitrogen using the red-edge band of the spaceborne RapidEye sensor. *International Journal of Applied Earth Observation and Geoinformation,* 19**,** 151-162.

Rawnsley, R., Donaghy, D., Fulkerson, W. & Lane, P. 2002. Changes in the physiology and feed quality of cocksfoot (Dactylis glomerata L.) during regrowth. *Grass and forage science,* 57(3)**,** 203-211.

Ren, S., Chen, X. & An, S. 2017. Assessing plant senescence reflectance index-retrieved vegetation phenology and its spatiotemporal response to climate change in the Inner Mongolian Grassland. *International journal of biometeorology,* 61(4)**,** 601-612.

Renier, C., Waldner, F., Jacques, D. C., Babah Ebbe, M. A., Cressman, K. & Defourny, P. 2015a. A dynamic vegetation senescence indicator for near-real-time desert locust habitat monitoring with MODIS. *Remote Sensing,* 7(6)**,** 7545-7570.

Renier, C., Waldner, F., Jacques, D. C., Ebbe, M. A. B., Cressman, K. & Defourny, P. 2015b. A dynamic vegetation senescence indicator for near-real-time desert locust habitat monitoring with MODIS. *Remote Sensing,* 7(6)**,** 7545-7570.

Roberts, D., Smith, M. & Adams, J. 1993. Green vegetation, nonphotosynthetic vegetation, and soils in AVIRIS data. *Remote Sensing of Environment,* 44(2-3)**,** 255-269.

Royimani, L., Mutanga, O. & Dube, T. 2021. Progress in remote sensing of plant senescence: a review on the challenges and opportunities. *IEEE Journal of Selected Topics in Applied Earth Observations and Remote Sensing*.

Royimani, L., Mutanga, O., Odindi, J., Dube, T. & Matongera, T. N. 2019a. Advancements in satellite remote sensing for mapping and monitoring of alien invasive plant species (AIPs). *Physics and Chemistry of the Earth, Parts A/B/C,* 112**,** 237-245.

Royimani, L., Mutanga, O., Odindi, J., Sibanda, M. & Chamane, S. 2022. Determining the onset of autumn grass senescence in subtropical sour-veld grasslands using remote sensing proxies and the breakpoint approach. *Ecological Informatics,* 69**,** 101651.

Royimani, L., Mutanga, O., Odindi, J. & Slotow, R. 2023. Multi-Temporal Assessment of Remotely Sensed Autumn Grass Senescence across Climatic and Topographic Gradients. *Land,* 12(1)**,** 183.

Royimani, L., Mutanga, O., Odindi, J., Zolo, K. S., Sibanda, M. & Dube, T. 2019b. Distribution of Parthenium hysterophoru L. with variation in rainfall using multi-year SPOT data and random forest classification. *Remote Sensing Applications: Society and Environment,* 13**,** 215-223.

Ruiz-Arias, J., Tovar-Pescador, J., Pozo-Vázquez, D. & Alsamamra, H. 2009. A comparative analysis of DEM-based models to estimate the solar radiation in mountainous terrain. *International Journal of Geographical Information Science,* 23(8)**,** 1049-1076.

Sade, N., del Mar Rubio-Wilhelmi, M., Umnajkitikorn, K. & Blumwald, E. 2018. Stress-induced senescence and plant tolerance to abiotic stress. *Journal of Experimental Botany,* 69(4)**,** 845-853.

Santos, M. J., Greenberg, J. A. & Ustin, S. L. 2010. Using hyperspectral remote sensing to detect and quantify southeastern pine senescence effects in red-cockaded woodpecker (Picoides borealis) habitat. *Remote Sensing of Environment,* 114(6)**,** 1242-1250.

Sarath, G., Baird, L. M. & Mitchell, R. B. 2014. Senescence, dormancy and tillering in perennial C4 grasses. *Plant Science,* 217**,** 140-151.

Scott-Shaw, C. & Escott, B. 2011. KwaZulu-Natal provincial pre-transformation vegetation type map–2011. *Unpublished GIS Coverage [kznveg05v2_1_11_wll. zip], Biodiversity Conservation Planning Division, Ezemvelo KZN Wildlife, PO Box,* 13053.

Selemani, I. S. 2014. Communal rangelands management and challenges underpinning pastoral mobility in Tanzania: a review. *Livestock Research for Rural Development,* 26(5).

Shah, S. H., Angel, Y., Houborg, R., Ali, S. & McCabe, M. F. 2019. A random forest machine learning approach for the retrieval of leaf chlorophyll content in wheat. *Remote Sensing,* 11(8)**,** 920.

Sharma, L. K., Bu, H., Denton, A. & Franzen, D. W. 2015. Active-optical sensors using red NDVI compared to red edge NDVI for prediction of corn grain yield in North Dakota, USA. *Sensors,* 15(11)**,** 27832-27853.

Shipley, B. & Vu, T. T. 2002. Dry matter content as a measure of dry matter concentration in plants and their parts. *New Phytologist,* 153(2)**,** 359-364.

Shoko, C. & Mutanga, O. 2017a. Examining the strength of the newly-launched Sentinel 2 MSI sensor in detecting and discriminating subtle differences between C3 and C4 grass species. *ISPRS Journal of Photogrammetry and Remote Sensing,* 129**,** 32-40.

Shoko, C. & Mutanga, O. 2017b. Seasonal discrimination of C3 and C4 grasses functional types: An evaluation of the prospects of varying spectral configurations of new generation sensors. *International journal of applied earth observation and geoinformation,* 62**,** 47-55.

Shoko, C., Mutanga, O. & Dube, T. 2019. Remotely sensed C3 and C4 grass species aboveground biomass variability in response to seasonal climate and topography. *African Journal of Ecology,* 57(4)**,** 477-489.

Shoko, C., Mutanga, O. & Dube, T. 2020. Optimal season for discriminating C3 and C4 grass functional types using multi-date Sentinel 2 data. *GIScience & Remote Sensing,* 57(1)**,** 127-139.

Shreve, B., Thiex, N. & Wolf, M. 2006. NFTA Method 2.1. 4—Dry matter by oven drying for 3 hr at 105C. *National Forage Testing Association, Lincoln, NE*.

Sibanda, M., Mutanga, O., Dube, T., S Vundla, T. & L Mafongoya, P. 2019. Estimating LAI and mapping canopy storage capacity for hydrological applications in wattle infested ecosystems using Sentinel-2 MSI derived red edge bands. *GIScience & remote sensing,* 56(1)**,** 68-86.

Sibanda, M., Mutanga, O. & Rouget, M. 2015. Examining the potential of Sentinel-2 MSI spectral resolution in quantifying above ground biomass across different fertilizer treatments. *ISPRS journal of photogrammetry and remote sensing,* 110**,** 55-65.

Sibanda, M., Mutanga, O. & Rouget, M. 2016. Comparing the spectral settings of the new generation broad and narrow band sensors in estimating biomass of native grasses grown under different management practices. *GIScience & Remote Sensing,* 53(5)**,** 614-633.

Sibanda, M., Mutanga, O. & Rouget, M. 2017a. Testing the capabilities of the new WorldView-3 space-borne sensor's red-edge spectral band in discriminating and mapping complex grassland management treatments. *International Journal of Remote Sensing,* 38(1)**,** 1-22.

Sibanda, M., Mutanga, O., Rouget, M. & Kumar, L. 2017b. Estimating biomass of native grass grown under complex management treatments using worldview-3 spectral derivatives. *Remote Sensing,* 9(1)**,** 55.

Sibanda, M., Onisimo, M., Dube, T. & Mabhaudhi, T. 2021. Quantitative assessment of grassland foliar moisture parameters as an inference on rangeland condition in the mesic rangelands of southern Africa. *International Journal of Remote Sensing,* 42(4)**,** 1474-1491.

Silhavy, R., Silhavy, P. & Prokopova, Z. 2017. Analysis and selection of a regression model for the Use Case Points method using a stepwise approach. *Journal of Systems and Software,* 125**,** 1-14.

Sims, D. A. & Gamon, J. A. 2002. Relationships between leaf pigment content and spectral reflectance across a wide range of species, leaf structures and developmental stages. *Remote sensing of environment,* 81(2-3)**,** 337-354.

Singh, L., Mutanga, O., Mafongoya, P. & Peerbhay, K. Y. 2018. Multispectral mapping of key grassland nutrients in KwaZulu-Natal, South Africa. *Journal of Spatial Science,* 63(1)**,** 155-172.

Skidmore, A. K., Ferwerda, J. G., Mutanga, O., Van Wieren, S. E., Peel, M., Grant, R. C., Prins, H. H., Balcik, F. B. & Venus, V. 2010. Forage quality of savannas—Simultaneously mapping foliar protein and polyphenols for trees and grass using hyperspectral imagery. *Remote sensing of environment,* 114(1)**,** 64-72.

Smart, C. M. 1994. Gene expression during leaf senescence. *New phytologist,* 126(3)**,** 419-448.

Sonobe, R., Hirono, Y. & Oi, A. 2020. Non-destructive detection of tea leaf chlorophyll content using hyperspectral reflectance and machine learning algorithms. *Plants,* 9(3)**,** 368.

Stichler, C. 2002. Grass growth and development. *Texas Cooperative Extension, Texas A&M University*.

Storey, J., Lacasse, J., Smilek, R., Zeiler, T., Scaramuzza, P., Rengarajan, R. & Choate, M. 2005. Image Impact of the Landsat 7 ETM+ Scan Line Corrector Failure.

Stylinski, C., Gamon, J. & Oechel, W. 2002. Seasonal patterns of reflectance indices, carotenoid pigments and photosynthesis of evergreen chaparral species. *Oecologia,* 131(3)**,** 366-374.

Sun, D., Wesche, K., Chen, D., Zhang, S., Wu, G., Du, G. & Comerford, N. 2011. Grazing depresses soil carbon storage through changing plant biomass and composition in a Tibetan alpine meadow. *Plant, Soil and Environment,* 57(6)**,** 271-278.

Tao, Z., Ge, Q., Wang, H. & Dai, J. 2021. The important role of soil moisture in controlling autumn phenology of herbaceous plants in the Inner Mongolian steppe. *Land Degradation & Development,* 32(13)**,** 3698-3710.

Tao, Z., Wang, H., Dai, J., Alatalo, J. & Ge, Q. 2018. Modeling spatiotemporal variations in leaf coloring date of three tree species across China. *Agricultural and Forest Meteorology,* 249**,** 310-318.

Teague, R., Provenza, F., Norton, B., Steffens, T., Barnes, M., Kothmann, M. & Roath, R. 2008. Benefits of multi-paddock grazing management on rangelands: limitations of experimental grazing research and knowledge gaps. *Grasslands: ecology, management and restoration. Hauppauge, NY, USA: Nova Science Publishers*, pp.41-80.

Thompson, G. L. & Kao-Kniffin, J. 2019. Urban grassland management implications for soil C and N dynamics: a microbial perspective. *Frontiers in Ecology and Evolution,* 7**,** 315.

Timothy, D., Onisimo, M. & Riyad, I. 2016. Quantifying aboveground biomass in African environments: A review of the trade-offs between sensor estimation accuracy and costs. *Tropical Ecology,* 57(3)**,** 393-405.

Tomé, A. & Miranda, P. 2004. Piecewise linear fitting and trend changing points of climate parameters. *Geophysical Research Letters*, 31(2).

Trigg, S. N., Curran, L. M. & McDonald, A. K. 2006. Utility of Landsat 7 satellite data for continued monitoring of forest cover change in protected areas in Southeast Asia. *Singapore Journal of Tropical Geography,* 27(1)**,** 49-66.

Van der Walt, A. J. & Fitchett, J. M. 2020. Statistical classification of South African seasonal divisions on the basis of daily temperature data. *South African Journal of Science,* 116(9-10)**,** 1-15.

Volaire, F., Norton, M.R. & Lelièvre, F. 2009. Summer drought survival strategies and sustainability of perennial temperate forage grasses in Mediterranean areas. *Crop Science*, 49(6), pp.2386-2392.

Wagner, J. M. & Shimshak, D. G. 2007. Stepwise selection of variables in data envelopment analysis: Procedures and managerial perspectives. *European journal of operational research,* 180(1)**,** 57-67.

Wang, Q., Yang, Y., Liu, Y., Tong, L., Zhang, Q.-p. & Li, J. 2019. Assessing the impacts of drought on grassland net primary production at the global scale. *Scientific reports,* 9(1)**,** 1-8.

Wiseman, R., Morris, C. & Granger, J. 2002. Effects of pre-planting treatments on the initial establishment success of indigenous grass seedlings planted into a degraded Aristida junciformis-dominated grassland. *South African journal of botany,* 68(3)**,** 362-369.

Woo, H. R., Kim, H. J., Lim, P. O. & Nam, H. G. 2019. Leaf senescence: Systems and dynamics aspects. *Annual review of plant biology,* 70**,** 347-376.

Wu, C., Wang, X., Wang, H., Ciais, P., Peñuelas, J., Myneni, R. B., Desai, A. R., Gough, C. M., Gonsamo, A. & Black, A. T. 2018. Contrasting responses of autumn-leaf senescence to daytime and night-time warming. *Nature Climate Change,* 8(12)**,** 1092-1096.

Wu, J., Kurosaki, Y., Gantsetseg, B., Ishizuka, M., Sekiyama, T. T., Buyantogtokh, B. & Liu, J. 2021. Estimation of dry vegetation cover and mass from MODIS data: Verification by roughness length and sand saltation threshold. *International Journal of Applied Earth Observation and Geoinformation,* 102**,** 102417.

Xu, D., Chen, B., Yan, R., Yan, Y., Sun, X., Xu, L. & Xin, X. 2019. Quantitative monitoring of grazing intensity in the temperate meadow steppe based on remote sensing data. *International Journal of Remote Sensing,* 40(5-6)**,** 2227-2242.

Yang, J. & Udvardi, M. 2018. Senescence and nitrogen use efficiency in perennial grasses for forage and biofuel production. *Journal of Experimental Botany,* 69(4)**,** 855-865.

Yu, X., Guo, Q., Chen, Q. & Guo, X. 2019. Discrimination of senescent vegetation cover from landsat-8 OLI imagery by spectral unmixing in the northern mixed grasslands. *Canadian Journal of Remote Sensing,* 45(2)**,** 192-208.

Zacharias, P. 1995. Blaze'n graze: Management of sourveld after the burn. *Bulletin of the Grassland Society of Southern Africa (South Africa)*.

Zhou, X., Zhu, X., Dong, Z. & Guo, W. 2016. Estimation of biomass in wheat using random forest regression algorithm and remote sensing data. *The Crop Journal,* 4(3)**,** 212-219.

ZHU, L.-f., YU, S.-m. & JIN, Q.-y. 2012. Effects of aerated irrigation on leaf senescence at late growth stage and grain yield of rice. *Rice Science*, 19(1)**,** 44-48.